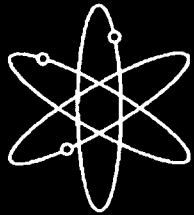
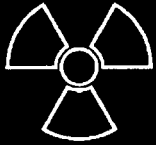
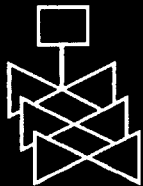


# **United States Nuclear Regulatory Commission Package Performance Study Test Protocols**



**Draft Report for Comment**



**U.S. Nuclear Regulatory Commission  
Office of Nuclear Regulatory Research  
Washington, DC 20555-0001**



## AVAILABILITY OF REFERENCE MATERIALS IN NRC PUBLICATIONS

### NRC Reference Material

As of November 1999, you may electronically access NUREG-series publications and other NRC records at NRC's Public Electronic Reading Room at <http://www.nrc.gov/reading-rm.html>. Publicly released records include, to name a few, NUREG-series publications; *Federal Register* notices; applicant, licensee, and vendor documents and correspondence; NRC correspondence and internal memoranda; bulletins and information notices; inspection and investigative reports; licensee event reports; and Commission papers and their attachments.

NRC publications in the NUREG series, NRC regulations, and *Title 10, Energy*, in the Code of *Federal Regulations* may also be purchased from one of these two sources.

1. The Superintendent of Documents  
U.S. Government Printing Office  
Mail Stop SSOP  
Washington, DC 20402-0001  
Internet: [bookstore.gpo.gov](http://bookstore.gpo.gov)  
Telephone: 202-512-1800  
Fax: 202-512-2250
2. The National Technical Information Service  
Springfield, VA 22161-0002  
[www.ntis.gov](http://www.ntis.gov)  
1-800-553-6847 or, locally, 703-605-6000

A single copy of each NRC draft report for comment is available free, to the extent of supply, upon written request as follows:

Address: Office of the Chief Information Officer,  
Reproduction and Distribution  
Services Section  
U.S. Nuclear Regulatory Commission  
Washington, DC 20555-0001  
E-mail: [DISTRIBUTION@nrc.gov](mailto:DISTRIBUTION@nrc.gov)  
Facsimile: 301-415-2289

Some publications in the NUREG series that are posted at NRC's Web site address <http://www.nrc.gov/reading-rm/doc-collections/nuregs> are updated periodically and may differ from the last printed version. Although references to material found on a Web site bear the date the material was accessed, the material available on the date cited may subsequently be removed from the site.

### Non-NRC Reference Material

Documents available from public and special technical libraries include all open literature items, such as books, journal articles, and transactions, *Federal Register* notices, Federal and State legislation, and congressional reports. Such documents as theses, dissertations, foreign reports and translations, and non-NRC conference proceedings may be purchased from their sponsoring organization.

Copies of industry codes and standards used in a substantive manner in the NRC regulatory process are maintained at—

The NRC Technical Library  
Two White Flint North  
11545 Rockville Pike  
Rockville, MD 20852-2738

These standards are available in the library for reference use by the public. Codes and standards are usually copyrighted and may be purchased from the originating organization or, if they are American National Standards, from—

American National Standards Institute  
11 West 42<sup>nd</sup> Street  
New York, NY 10036-8002  
[www.ansi.org](http://www.ansi.org)  
212-642-4900

Legally binding regulatory requirements are stated only in laws; NRC regulations; licenses, including technical specifications; or orders, not in NUREG-series publications. The views expressed in contractor-prepared publications in this series are not necessarily those of the NRC.

The NUREG series comprises (1) technical and administrative reports and books prepared by the staff (NUREG-XXXX) or agency contractors (NUREG/CR-XXXX), (2) proceedings of conferences (NUREG/CP-XXXX), (3) reports resulting from international agreements (NUREG/IA-XXXX), (4) brochures (NUREG/BR-XXXX), and (5) compilations of legal decisions and orders of the Commission and Atomic and Safety Licensing Boards and of Directors' decisions under Section 2.206 of NRC's regulations (NUREG-0750).

**United States Nuclear  
Regulatory Commission  
Package Performance  
Study Test Protocols**

**Draft Report for Comment**

---

---

Manuscript Completed: February 2003  
Date Published: February 2003

**Division of Engineering Technology  
Office of Nuclear Regulatory Research  
U.S. Nuclear Regulatory Commission  
Washington, DC 20555-0001**



## COMMENTS ON DRAFT REPORT

Any interested party may submit comments on this report for consideration by the NRC staff. Comments may be accompanied by additional relevant information or supporting data. Please specify the report number, Draft NUREG-1768, in your comments, and send them by May 30, 2003, to the following address:

Chief, Rules Review and Directives  
U.S. Nuclear Regulatory Commission  
Mail Stop T-6-D-59  
Washington, DC 20555-0001

You may also provide comments at the NRC Web site:

<http://www.nrc.gov/public-involve/doc-comment/form.html>.  
For any questions about the material in this report, please contact:

Dr. Andrew J. Murphy, Jr.  
Mail Stop T-10-D-20  
U.S. Nuclear Regulatory Commission  
Washington, DC 20555-0001  
Phone: 301-415-6011  
Fax: 301-415-5074  
E-mail: [ajm1@nrc.gov](mailto:ajm1@nrc.gov)

## ABSTRACT

This test protocols report presents the NRC staff's preliminary plans for an experimental phase of the Package Performance Study (PPS), which is examining the response of transportation casks to extreme transportation accident conditions. The staff proposes to conduct tests of full-scale rail and full-scale truck casks including a high-speed impact with an unyielding surface followed by an extreme fire test. The NRC has a contract in place with Sandia National Laboratories (SNL) to conduct the impact and fire tests and to carry out a series of analyses to support the test program. These tests support the PPS objectives of enhancing public confidence in the inherent safety of spent nuclear fuel cask design, validating the capability of the cask models and analysis codes to accurately capture cask and fuel response to extreme mechanical and thermal environments, and providing data to refine dose risk estimates.

The objective of publishing this report is to continue the process of enhanced public involvement in the development of this program and to satisfy a specific commitment the NRC made to make these preliminary test plans available and to request comments on them. The following is a list of specific issues about which the staff is specifically soliciting comments. These include:

- the types and number of cask designs that should be tested,
- the speed and orientation used in the impact tests,
- the method used to conduct the impact tests, dropped from a tower as proposed in this report or propelled along a horizontal track (e.g., on a rocket-sled track),
- the reasonableness of the proposed range of speeds (96 to 144 kph [60 to 90 mph]) given that the frequency with which a rail cask might be expected to impact a hard rock surface at these speed is  $10^{-6}$  to  $10^{-8}$  per year,
- the appropriateness of the impact speed of 120 kph [75 mph] proposed by the NRC staff for the rail cask collision test and the appropriate speed for the truck cask collision test,
- the scale of the casks to be tested ( e.g., full-sized casks or partial scale),
- the duration and size of the cask fire test,
- the position of the cask relative to the fire,
- the number and type(s) of fuel assemblies included in the casks, and
- the ability of the proposed tests to yield risk insights consistent with NRC's risk-informed regulatory initiatives.

## Table of Contents

ABSTRACT .....	iii
EXECUTIVE SUMMARY .....	ix
Package Performance Study .....	ix
Test Protocols .....	x
Public Comments .....	xii
ACKNOWLEDGEMENTS .....	xv
1.0 INTRODUCTION .....	1
1.1 Background .....	2
1.2 Package Performance Study Overview .....	4
1.3 Casks Examined by These Test Protocols .....	5
2.0 IMPACT TEST PROTOCOL .....	7
2.1 Background .....	7
2.2 Objectives .....	7
2.3 Tasks .....	8
2.4 Finite Element Analyses .....	12
2.4.1 Description of HI-STAR 100 Cask and Impact Limiter [obtained from the <i>HI-STAR Safety Analysis Report</i> (Holtec, 2000)] .....	13
2.4.2 Finite Element Model I .....	14
2.4.3 Model 1 PRONTO-3D Finite Element Results .....	18
2.4.4 Model 2 Finite Element Model with Improved Impact Limiter .....	28
2.4.5 Description of GA-4 truck cask [obtained from the <i>GA-4 Legal Weight Truck Spent Fuel Shipping Cask Safety Analysis Report for Packaging</i> (General Atomics, 1998)] .....	35
2.4.6 Finite element model .....	37
2.4.7 GA-4 PRONTO-3D Finite Element Results .....	39
2.5 Limitations of Analyses .....	47
2.6 Structural Panel Recommendations .....	48
2.7 Impact Test Protocol .....	48
3.0 FIRE TESTS .....	52
3.1 Background .....	52
3.2 Method .....	53
3.3 Computer Simulations .....	54
3.3.1 Simulation of Fires .....	54
3.3.2 Simulation of Packaging .....	55
3.3.3 Simulation of Fuel Bundles and Basket .....	55
3.4 Preliminary Analyses .....	55
3.4.1 Case 1: Rail Cask 1.3 Meters Above the Fuel Pool Surface, No Wind .....	57
3.4.2 Case 2: Rail Cask 0.3 Meters Above the Fuel Pool Surface, No Wind .....	60
3.4.3 Case 3: Rail Cask 3.3 Meters Above the Fuel Pool Surface, No Wind .....	62
3.4.4 Truck Cask One Meter Above the Fuel Pool Surface, No Wind Condition .....	64
3.5 Fire Instrumentation .....	67
3.5.1 Types of Fire Instrumentation .....	67
3.6 Fire Tests Protocol .....	69
3.7 Thermal Expert Panel Recommendations .....	71
4.0 SUMMARY OF TEST PROTOCOLS .....	72
5.0 REFERENCES .....	74
APPENDIX A: Frequency of Accidents and Metrics for PPS Test Parameters .....	A-1
APPENDIX B: Peer Review Panel Members .....	B-1

## List of Figures

<u>Figure</u>	<u>Title</u>	<u>Page</u>
Figure 1.	Schematic drawing of HI-STAR cask body.....	13
Figure 2.	Schematic drawing of the HI-STAR impact limiter.....	14
Figure 3.	Finite element model of HI-STAR cask.....	15
Figure 4.	Closure region.....	16
Figure 5.	Finite element model of closure lid bolt.....	17
Figure 6.	Cask loading orientations.....	19
Figure 7.	Cask assembly after a 96 kph [60 mph] CG-over-corner impact onto a rigid surface.....	19
Figure 8.	Details of the damage depicted in Figure 7.....	20
Figure 9.	Kinetic energy versus time for a 96 kph [60 mph] CG-over-corner impact.....	21
Figure 10.	Nominal acceleration of a cask subject to a 96 kph [60 mph] CG-over-corner impact.....	21
Figure 11.	Equivalent plastic strain in closure lid bolts for 96 kph [60 mph] CG-over-corner impact.....	22
Figure 12.	Closure lid gap in seal area for 96 kph [60 mph] CG-over-corner impact.....	23
Figure 13.	End-on 96 kph [60 mph] impact onto a rigid surface.....	24
Figure 14.	Kinetic energy versus time for a 96 kph [60 mph] end-on impact onto a rigid surface.....	24
Figure 15.	Acceleration versus time for a 96 kph [60 mph] end-on impact onto a rigid surface.....	25
Figure 16.	Side-on 96 kph [60 mph] impact onto a rigid surface.....	26
Figure 17.	Kinetic energy versus time for a 96 kph [60 mph] side-on impact onto a rigid surface.....	27
Figure 18.	Acceleration versus time for a 96 kph [60 mph] side-on impact onto a rigid surface.....	27
Figure 19.	Illustrates the three major components of the detailed impact limiter: encapsulating shell, energy absorbing material, and the steel substructure.....	28
Figure 20.	HI-STAR impact limiter after 60 mph CG-over-corner impact onto a rigid target.....	30
Figure 21.	Detail of the damage depicted in Figure 20.....	31
Figure 22.	HI-STAR cask assembly after 96 kph [60 mph] CG-over-corner impact onto a rigid target, with foam material removed to show inner structure of impact limiter.....	31
Figure 23.	Plot of cask kinetic energy versus time for the HI-STAR cask at an impact velocity of 96 kph [60 mph] onto a rigid surface.....	32
Figure 24.	Plot of the cask acceleration versus time for the HI-STAR cask at an impact velocity of 96 kph [60 mph] onto a rigid surface.....	32
Figure 25.	HI-STAR impact limiter assembly after 120 kph [75 mph] CG-over-corner impact onto a rigid target.....	33
Figure 26.	HI-STAR impact limiter assembly after 120 kph [75 mph] CG-over-corner impact onto a rigid target, with honeycomb material removed to show inner structure of the impact limiter.....	33
Figure 27.	Equivalent Plastic Strain in cask for the CG-over-corner orientation after a 120 kph [75 mph] impact onto a rigid target.....	34
Figure 28.	Plot of cask kinetic energy versus time for the HI-STAR cask at an impact velocity of 120 kph [75 mph] onto a rigid surface.....	34
Figure 29.	Plot of the cask acceleration versus time for the HI-STAR cask at an impact velocity of 120 kph [75 mph] onto a rigid surface.....	35
Figure 30.	Schematic drawing of GA-4 cask body.....	36
Figure 31.	Back-breaker cask orientation.....	37
Figure 32.	Finite element model of GA-4 cask.....	37
Figure 33.	GA-4 cask impact orientations.....	38
Figure 34.	GA-4 cask after 96 kph [60 mph] back-breaker impact.....	39
Figure 35.	Section view of the GA-4 Cask after a 96 kph [60 mph] back-breaker impact.....	39
Figure 36.	Kinetic Energy vs. time for a 96 kph [60 mph] GA-4 cask back-breaker impact.....	40
Figure 37.	Acceleration vs time for a 96 kph [60 mph] GA-4 cask back-breaker impact.....	40

Figure 38. Section view of the GA-4 Cask after a 96 kph [60 mph] back-break impact showing equivalent plastic strain in containment boundary. ....	41
Figure 39. Section view of the GA-4 Cask after a 96 kph [60 mph] back-break impact showing equivalent plastic strain in the depleted uranium. ....	42
Figure 40. Depleted Uranium segment modeled as three separate pieces to simulate the effect of fracturing. ....	42
Figure 41. GA-4 cask after 96 kph [60] mph back-breaker impact, modeled with fractured DU segments. ....	43
Figure 42. Section view of GA-4 cask through the plane of impact, after 96 kph [60 mph] back-breaker impact, modeled with fractured DU segments. ....	43
Figure 43. Kinetic Energy vs. time for a 96 kph [60 mph] GA-4 cask back-breaker impact with fractured DU segments. ....	44
Figure 44. Acceleration vs time for a 96 kph [60 mph] GA-4 cask back-breaker impact with fractured DU segments. ....	44
Figure 45. Section view of the GA-4 Cask after a 96 kph [60 mph] back-break impact showing equivalent plastic strain in containment boundary, modeled with fractured DU segments. ....	45
Figure 46. GA-4 cask after a 120 kph [75 mph] back-breaker impact, modeled with fractured DU segments. ....	45
Figure 47. Kinetic Energy vs. time for a 120 kph [75 mph] GA-4 cask back-breaker impact with fractured DU segments. ....	46
Figure 48. Acceleration vs. time for a 120 kph [75 mph] GA-4 cask back-breaker impact with fractured DU segments. ....	46
Figure 49. Section view of the GA-4 Cask after a 120 kph [75 mph] back-break impact showing equivalent plastic strain in containment boundary, modeled with fractured DU segments. ....	47
Figure 50. Finite element model of the Holtec HI-STAR 100 rail cask. ....	56
Figure 51. Finite element model of the GA-4 truck cask. ....	56
Figure 52. CAFE results for Case 1 (1.3 m above fuel pool surface). ....	58
Figure 53. Temperature History for Case 1 (1.3 m above fuel pool surface). ....	59
Figure 54. CAFE results for Case 2 (0.3 m above fuel pool surface). ....	60
Figure 55. Temperature History for Case 2 (0.3 m above fuel pool surface). ....	61
Figure 56. CAFE results for Case 3 (3.3 m above fuel pool surface). ....	62
Figure 57. Temperature History for Case 3 (3.3 m above fuel pool surface). ....	63
Figure 58. CAFE results for the truck cask (1 m above fuel pool surface). ....	65
Figure 59. Temperature History for the Truck Cask (1 m above fuel pool surface). ....	66

## List of Tables

<u>Table</u>	<u>Title</u>	<u>Page</u>
Table 1.	HI-STAR impact limiter honeycomb materials strength and directionality. ....	14
Table 2.	Foam parameter values. ....	18
Table 3.	Cask body constitutive model parameters. ....	18
Table 4.	Foam parameter values for detailed impact limiter. ....	28

## **EXECUTIVE SUMMARY**

The U.S. Nuclear Regulatory Commission (NRC) believes that current regulations and programs for transporting spent nuclear fuel (SNF) result in a high degree of safety. The agency bases this belief largely upon the staff's confidence in the shipping casks the NRC certifies. Ongoing confirmatory research regarding transportation safety further supports the agency's belief.

Under the current regulations, the NRC requires that SNF casks must be designed and constructed to survive a sequence of tests designed to simulate postulated accidents. These tests include a 9-meter [30 foot] drop onto an unyielding surface and a 30-minute fully engulfing fire. NRC regulations permit certification through testing, analysis, comparison to similar certified designs, or various combinations of these methods. Typically, the agency has certified SNF casks using a combination of analyses and testing of scale models or cask components. Previous NRC risk studies have estimated that the agency's certification standards encompass well over 99% of possible transportation accidents.

NRC certification of SNF casks has contributed to an excellent safety record for transporting spent fuel. Further, the characteristics of both fuel and cask systems continue to evolve, and the testing and analytical techniques used in certification applications continue to improve. However, the near-term possibility of a significant increase in the number of spent fuel shipments has focused public attention on the safety of SNF transportation. Despite the excellent record achieved to date and general improvements in cask design and analysis, some stakeholders have voiced concerns regarding transportation safety and the lack of full-scale testing of SNF casks.

The NRC believes the safety protection provided by the current transportation regulatory system is well established. NRC's primary role in transportation of spent fuel is certification of the casks used for transport. The NRC ensures that shipping casks are robust by regulating their design and construction, by independently confirming the ability of designs to meet the regulations and accident conditions through modeling and analyses, and by overseeing that licensees properly build, use, and maintain the casks. NRC's confidence in casks that it certifies is also supported by ongoing transportation safety research and by the outstanding safety record compiled using NRC-certified casks. Currently, NRC has certified several transportation cask designs that could be used to transport spent fuel, and additional designs are under review.

### **Package Performance Study**

Because of stakeholder concerns and a desire to further validate the computer models used to evaluate the safety of cask transportation, the NRC initiated in 1999 a program known as the Package Performance Study (PPS). Under this ongoing program, the NRC staff is examining the adequacy of the analytical methods and data that are used to estimate the response of transportation casks to those improbable, extreme accidents that might cause radioactive materials to be released to the environment. However, the PPS is not intended to involve the development of new standards for transportation casks.

The NRC staff identified the tasks that are described in this report through two series of public meetings and associated comment periods, during which the staff solicited and discussed the various concerns of citizens, members of the nuclear industry, and governmental organizations. The staff with contractor support subsequently rated and summarized those concerns in the "Spent Nuclear Fuel Transportation Package Performance Study Issues Report," NUREG/CR-6768, June 2002, which Sandia National Laboratories (SNL) prepared for the NRC. Specifically, on the basis of its review of the public record from both the public meetings and written comments, the NRC staff concluded that the following four tasks would address the primary concerns raised by stakeholders:

- (1) Use recent accident data to reanalysis the truck and rail accident speed and fire duration statistics developed by the Modal Study (Fischer et. al., 1987).
- (2) Perform high-speed collision tests on full-scale rail and truck casks<sup>1</sup> and compare the test results to pretest damage predictions developed by computer models.
- (3) Expose full-scale rail and truck casks to fully engulfing, long-duration fires and compare the measured cask temperatures to pretest temperature predictions developed by computer models.
- (4) Conduct laboratory tests to examine rod failure, pellet fracturing, and the release of particles from the failed rods, and use the test results to determine the response to extreme impacts of fuel pellets, fuel rods, and fuel rods containing fuel pellets.

This report addresses Tasks 2 and 3, listed above. It does not address the reanalysis of rail and truck accident statistics published in the Modal Study because that reanalysis does not involve conducting any tests or experiments. Similarly this report does not discuss the NRC's plans regarding laboratory tests to determine the response of spent fuel pellets and rods to extreme accident conditions because those test are proceeding on a different schedule from the impact and thermal tests being conducted under the PPS.

## **Test Protocols**

This report summarizes the field tests that the NRC proposes to perform under the PPS, as well as the analyses performed to develop the test summaries. Throughout this report, these summaries are called "test protocols." Publication of these test protocols does not imply any commitment on the part of the NRC to conduct any of these tests, or to conduct any test exactly as described in this report.

### Collision Test Protocol

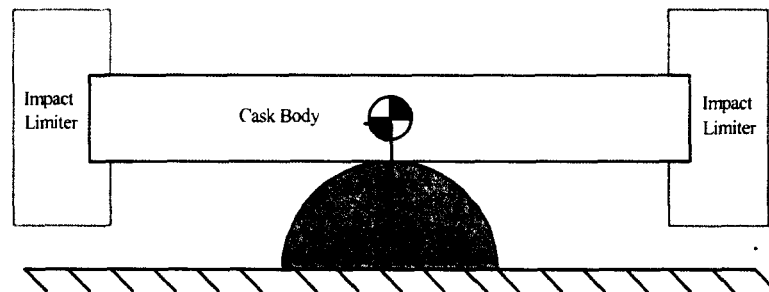
Within the context of the PPS, the NRC plans to conduct separate high-speed impact tests of a full-scale rail spent fuel cask and full-scale truck spent fuel cask using a drop impact as opposed to a horizontal impact test. The drop impact test was proposed after weighing such factors as test

---

<sup>1</sup> The "Spent Nuclear Fuel Transportation Package Performance Study Issues Report," NUREG/CR-6768, did not specify the type of transportation cask to be tested; subsequently, the NRC has proposed that the PPS test program should involve one rail cask design and one truck cask design

objectives, costs, local environmental and logistical concerns, and modeling issues. The staff will then compare the results of these tests to detailed pre-test damage predictions developed by computer models. (The computer model analyses conducted in the process of developing the preliminary design of the impact test are described in this report.) The staff proposes the following tasks for the collision test protocol:

- Subject a full-scale rail cask to an extreme impact onto a flat, unyielding surface (The staff proposes an unyielding surface because (1) the proposed impact test is intended to evaluate cask performance and an unyielding surface causes all of the cask kinetic energy to be spent deforming the cask, and (2) an unyielding surface simplifies the analysis by deforming only the cask and not the target.)
- Equip the lid end of the test cask with an impact limiter; ensure the cask contains a fuel canister, if the test cask design uses canisters, with one real fuel assembly containing surrogate fuel, and sufficient dummy assemblies to fill the canister or cask.
- Structure the test to deliver the impact onto the lid end of the cask that is equipped with the impact limiter.
- Orient the cask so the impact is on the corner or edge of the lid.
- Subject a full-scale truck cask to an extreme “back-breaker” impact<sup>2</sup> onto one of the internal flat sides of the cask, midway between the impact limiters onto a rigid semi-cylinder, as shown in the following illustration.



- Ensure that the cask contains one real fuel assembly and sufficient dummy assemblies to fill the cask.
- Test cask performance on impact with an unyielding surface at an impact speed of 96 to 144 kph [60 to 90 mph] (based on preliminary analysis of the computer model).

#### Proposed Speed for Rail Impact Test

The NRC staff with contractor support obtained preliminary impact analyses to support the development of the test protocols. These analyses spanned the range of impact speeds from 96 to 144 kph [60 to 90 mph]; this report presents the results of these analyses for impact speeds of 96 and 120 kph [60 and 75 mph]. The NRC staff reviewed these SNL analyses and developed three criteria for proposing test parameters for the PPS impact and thermal tests. The NRC staff

---

<sup>2</sup> A back-breaker impact is one in which the cask strikes the target between the impact limiters in a sideways orientation. The impact target is similar to a bridge column or abutment.

conducted a trial application of these criteria to determine the speed for the rail cask impact. (Appendix A to this report fully describes the three criteria and the trial application.) The NRC staff optimized the benefits of the three criteria, i.e., (1) enhancing public confidence, (2) validating the computer models, and (3) ensuring realism in the probability of the occurrence of the test parameters. On the basis of that optimization, the NRC staff proposes the impact speed of 120 kph [75 mph].

### Fire Test Protocol

Within the context of the PPS, the NRC plans to conduct separate fire tests of a full-scale rail cask and a full-scale truck cask. For these thermal tests, PPS will use a fully engulfing, optically dense fire, which completely surrounds the test specimen and obscures visibility of the test specimen through the flames. In each test, the fire will burn for more than the half-hour duration of the thermal certification test. The NRC staff will compare the measured temperature history of the cask at various points to the detailed pretest predictions developed by computer models. (Again, the computer model analyses conducted in the process of developing the preliminary design of the thermal test are described in this report.) The staff proposes the following tasks for the fire test protocol:

- Subject a full-scale rail cask to a fully engulfing, optically dense fire for a duration of more than a half hour.
- Subject a full-scale truck cask to a fully engulfing, optically dense fire for a duration of more than a half hour.

### **Public Comments**

The NRC is publishing and distributing this report to solicit public comments regarding the proposed SNF cask performance test protocols, while they are still at a conceptual level as reflected in this report. In addition to continuing the interactions in developing the scope of the PPS, this review at the conceptual level is being conducted because detailed planning and procurement for a specific series of tests will be resource intensive. The NRC anticipates that the public comments could result in worthwhile changes to the underlying test approaches and plans. The agency is particularly interested in stakeholders' views on the following eleven issues

- How many casks and what types of cask designs should be used in the tests?
- At what scale should the cask impact tests be conducted (e.g., full-scale or a partial-scale)?
- Should the impact tests be conducted as drops from a tower, as proposed in this report, or along a horizontal track using a rocket sled?
- What should the impact speed and orientation be for the rail cask impact test?
- Is 96 to 144 kph [60 to 90 mph] a reasonable speed range for the rail cask impact test given that the frequency for a rail cask impacting a hard rock surface within this speed range is  $10^{-6}$  to  $10^{-8}$  per year?
- Is the 120 kph [75 mph] rail cask impact speed proposed by the NRC staff appropriate?
- What should the impact speed be for the back breaker truck cask impact test?
- What should be the duration and size of the cask fire tests?

- What should be the cask position relative to the fire?
- How many and what types (real or surrogate, PWR or BWR) of fuel assemblies should be in the casks during the tests?
- Will the proposed tests be able to yield risk insights consistent with NRC's risk-informed regulatory initiatives?

After receiving and considering all stakeholder comments on the test protocols, the NRC staff will develop detailed test plans and procedures for each of the PPS testing programs, again making use of SNL's expertise. The NRC will make these detailed plans, procedures, and tests available to the public before finalizing and conducting the planned tests. Thus, the finalized detailed plans will reflect public comments on these test protocols, constraints imposed by NRC's programmatic priorities, and the available funding to support these tests.

## **ACKNOWLEDGEMENTS**

The NRC staff acknowledges the considerable assistance in the development of this report from the staff from the Transportation Risk and Packaging Dept. of Sandia National Laboratories, in particular to: Ken Sorenson, Douglas Ammerman, Carlos Lopez, Robert. Kalan, Jorman Koski, and Jeremy Sprung

Andrew Murphy, RES, and Robert Lewis, NMSS, prepared the Executive Summary and Appendix A.

## 1.0 INTRODUCTION

Spent nuclear fuel may only be transported in packages that have received a certificate of compliance from the NRC. To receive a certificate of compliance, spent fuel casks must be able to survive without any loss of containment:

- a drop of 9 meters onto an unyielding surface,
- exposure to a 30 minute fully engulfing 800°C pool fire,
- a puncture test consisting of a 1 meter drop onto a 15 cm diameter mild steel bar, and
- immersion in 0.9 meters of water.

These certification requirements must be performed in sequence in the most damaging orientation. After this testing, leak rate, shielding, and subcriticality requirements apply.

The shipment of spent nuclear fuel (SNF) in casks certified by the Nuclear Regulatory Commission (NRC) has an excellent safety record. Further, the characteristics of both fuel and cask systems continue to evolve, and the testing and analytical techniques used in certification applications continue to improve. However, the near-term possibility of a significant increase in the number of spent fuel shipments has focused public attention on the safety of SNF transportation. Despite the excellent safety record achieved to date and general improvements in cask design and analysis, some stakeholders have voiced concerns regarding transportation safety and the lack of full-scale testing of SNF casks.

Because of stakeholder concerns and a desire to further validate the computer models used to evaluate the safety of cask transportation, the NRC initiated in 1999 a program known as the Package Performance Study (PPS). Under this ongoing program, the NRC staff is examining the adequacy of the analytical methods and data that are used to estimate the response of transportation casks to those improbable, extreme accidents that might cause radioactive materials to be released to the environment. However, the PPS is not intended to involve the development of new standards for transportation casks. Initiation of the PPS is wholly consistent with NRC's commitment to continually assess the regulations governing and safety of the transport of spent nuclear fuel. The tasks in the PPS represent a six -year work plan that the NRC has developed in a systematic and open way, to address spent fuel shipment issues that need further study.

This report was written to solicit comment and feedback from the technical transportation community, the regulated industry, interested public organizations, and concerned citizens regarding the field tests and laboratory tests proposed for the PPS. Panels of structural and thermal experts and the NRC's Advisory Committee on Nuclear Waste reviewed a preliminary draft of the report. The members of the structural and thermal review panels are given in Appendix B. The comments from these reviews have been incorporated into this report.

This report presents summary descriptions of the field tests proposed for the PPS and also of the analyses performed to define the tests. The field tests will subject a full-scale spent nuclear fuel rail transportation cask and a full-scale spent nuclear fuel truck transportation cask first to an extreme accident impact and then to an extreme accident fire. Throughout this report, the

summary descriptions are called test protocols. Because they are summary descriptions, these protocols are less detailed than the final full test plans that will be written next summer and fall.

Publication of these test protocols does not imply any commitment on the part of the NRC to conduct any of the tests, or to conduct any test as described in this report. When the detailed plans for PPS field tests are developed, they will reflect public comments on these test protocols, and constraints posed by the programmatic priorities of the NRC, including the funding available to support these tests.

## **1.1 Background**

In March 2000, the NRC published NUREG/CR-6672, *Reexamination of Spent Fuel Shipment Risk Estimates* (Sprung et al., 2000). NUREG/CR-6672 provides a current assessment of the risks associated with the transport of spent nuclear fuel. The methods and data used to perform the NUREG/CR-6672 study raised a number of technical issues about the performance of spent fuel packages during extreme accidents. The NRC initiated the PPS partly to address these issues and to address stakeholder concerns about the safety of spent fuel shipments. To ensure that the PPS would address stakeholder concerns and also the NUREG/CR-6672 issues, NRC held eight public meetings at which these concerns and were discussed. At each of these meetings, the discussions were transcribed. To facilitate discussion at these meetings of the technical issues related to the NUREG/CR-6672 methodology, prior to the meetings that report was placed on the PPS website and was also sent directly to interested individuals.

After the first four meetings were held, Sandia National Laboratories (SNL) collected and interpreted the concerns and issues raised at these meetings in an Issues Report (Sprung et al., 2002). The principal recommendations of this report reflected:

- the fact that concerned citizens found analysis an unconvincing way to demonstrate the response of a spent fuel cask to extreme collisions or fires; and the request by numerous concerned citizens that this response be examined by testing of a real spent fuel cask,
- the statement by many concerned citizens that accident statistics had to be reanalyzed using recent data, especially truck accident statistics, since for example interstate highway speed limits had increased substantially from 55 mph to 75 mph on many interstates, and
- the recommendation made by technical consultants to state and environmental organizations that the response of spent fuel to accident conditions be examined by experiments since there was almost no experimental data available from which to estimate this response.

A draft of the Issues Report was disseminated for public review and comment to assess the accuracy of SNL's interpretation of the issues and concerns. Then, four more public meetings were held to review the Issues Report and the issues it recommended for further study by the PPS. In general, feedback from the public was positive and supported the recommendations presented in the Issues Report. In particular, a common theme in both written and oral feedback was that the NRC should perform full-scale cask tests to confirm the accuracy of the thermal and structural analyses used to estimate cask response to the conditions posed by extreme collisions and fires.

The Issues Report recommended that the following four studies should be conducted:

1. Perform a high-speed collision test on a full-scale rail cask and compare the test results to pretest predictions of cask damage developed by three-dimensional finite element collision calculations.
2. Expose a full-scale rail cask to a fully engulfing, long-duration fuel fire and compare the measured temperatures to pretest predictions of the cask temperatures developed by three-dimensional finite element heat transport calculations.
3. Determine the response of fuel pellets, fuel rods, and fuel rods that contain fuel pellets to extreme impacts by performing laboratory tests that examine rod failure, pellet fracturing, and the release of particles from the failed rods.
4. Use recent accident data to reconstruct the truck accident and train accident event trees and accident speed and fire duration statistics that were published in the Modal Study (Fischer et al., 1987).

Because the third study is proceeding on a different schedule and the fourth study does not involve any testing, these test protocols describe only the field tests planned for the first two studies and not the laboratory tests that will examine the response of spent fuel pellets and rods to impact forces or the reexamination of accident statistics.

For impact testing, the NRC proposes to use a drop impact as opposed to a horizontal impact test. The drop impact test was proposed after weighing such factors as test objectives, costs, local environmental and logistical concerns, and modeling issues.

The collision and fire test conditions proposed in the protocols presented in this report were developed using the results of preliminary structural and thermal calculations. These calculations examined the cask geometry, its orientation and speed at impact during the collision test, its orientation and height above the ground for the pool fire tests, and the specifications for the cask internals (position in the cask and weight of real or surrogate fuel assemblies). Since these calculations form the basis for many of the recommended test conditions, the methods used to perform these calculations and the results of the calculations are presented for each protocol.

The remainder of this report is divided into the following three sections:

- Package Performance Study Overview
- Impact Test Protocols
- Fire Test Protocols

The Package Performance Study Overview sections of this report provide information that place the test protocol sections in perspective. To facilitate public review and comment on this protocols report, the NRC has placed this report on the PPS web site (<http://ttd.sandia.gov/nrc/modal.htm>) and will hold a series of public meetings at which the report will be summarized and discussed. Based on the review comments received from the technical community and public, the NRC will then decide how the PPS will proceed.

## 1.2 Package Performance Study Overview

The PPS has three objectives:

- Confirm finite element analyses as a valuable tool to accurately capture cask and fuel response to extreme mechanical and thermal environments.
- Demonstrate the inherent safety in spent fuel cask design – Public outreach is a significant element.
- Provide data to refine dose risk estimates to the public and workers by replacing conservative assumptions with empirical data and new or updated transport statistics.

To achieve these objectives, the PPS will perform the four studies identified in the issues report and presented in the previous section.

The following paragraphs provide brief descriptions of near-term PPS tasks and indicate their status or expected completion date:

- **Complete Test Protocols Report** **Completed**  
The Test Protocols report provides preliminary descriptions of: (1) the types of mechanical and thermal field tests and (2) the laboratory rod and pellet impact and thermal tests that are being considered for performance by the PPS. The report also describes the analyses conducted to delineate the proposed tests and any assumptions that underlie these analyses. The benefits that each test will provide are also discussed.
- **Review of Test Protocols by Expert Panels** **Completed**  
The Test Protocols report was reviewed by two expert panels, a structural panel and a thermal panel, and revised to reflect the comments of each panel.
- **Public Review and Comment on Protocols** **Winter-Spring 2003**  
Comments on the protocols will be solicited in a variety of ways. To solicit feedback, the protocols will be sent to individuals with a known interest in the PPS program, they will be posted to the PPS web site (<http://ttd.sandia.gov/nrc/modal.htm>); and they will be presented to the public and discussed at a series of public meetings.
- **Conduct 3D structural and thermal finite element analyses** **Spring-Fall 2003**  
After review and consideration of all the comments received about the test protocols, detailed three-dimensional finite element analyses will be performed to finalize cask orientation and impact speed for the mechanical test, and cask orientation and location relative to the pool for the pool fire test.
- **Detailed Test Plans** **Winter 2004**  
After reviewing the comments received from the public concerning the protocols, detailed test plans that reflect the comments received will be written for the field and laboratory tests.
- **Complete Test Procedures** **Summer 2004**

The final detailed test plans will be completed in the fall of 2004. These plans will fully describe the tests that will be conducted for the PPS. They will have taken into account all the public and technical review comments on the test protocols that were received. Upon completion of the detailed test plans, a review by the National Academy of Sciences will be commissioned.

### **1.3 Casks Examined by These Test Protocols**

These test protocols describe the analyses and tests of a full-scale Holtec HI-STAR 100 rail cask equipped with a MPC-24 canister and of a GA-4 truck cask, that are proposed for performance by the PPS. The HI-STAR 100 rail cask and the GA-4 truck cask were used to develop this test protocols report because they meet several cask selection criteria proposed for the PPS:

- Each cask design is currently certified by the NRC.
- Each cask design will likely be used to ship commercial spent nuclear fuel.
- Each cask design is like that of one of the four representative types of spent fuel casks examined in NUREG/CR-6672.

The use of the HI-STAR 100 rail cask and the GA-4 truck cask to develop the analyses and discussions presented in this Test Protocols report does not imply that these casks will be the cask actually selected by the NRC for use in the PPS tests. Final cask selection by NRC will reflect comments and critiques of this report made at public meetings and during technical reviews by the expert panels, and also the ability of each cask that might be used during the PPS to satisfy the selection criteria cited above.

## **2.0 IMPACT TEST PROTOCOL**

This test protocol outlines the methods that will be used to develop a basis for validating the finite element impact analyses performed to support NRC risk assessments and to address the impact testing concern described in the Issues Report. The main objectives of these tests are to demonstrate the inherent safety of the transportation casks certified by the NRC and to demonstrate that finite element analysis can accurately predict the response of casks to extreme impact events.

### **2.1 Background**

The most recent assessments of the response of spent fuel casks to structural assaults conducted for the NRC (the Modal Study and NUREG/CR-6672) have used finite element calculations to estimate the damage that might be caused by the impacts. NUREG/CR-6672 used the most detailed finite element models ever employed in a transportation risk assessment, but even these models used simplified representations of the generic casks (e.g., the cask penetrations were not modeled, and to reduce computational time, lid bolts were represented by square shapes). The size of cask seal failures was estimated from the opening and sliding displacements of the cask lid relative to the cask body.

The fraction of spent fuel rods that experienced cladding failure due to the impacts was estimated using data in SAND90-2406 (Sanders et al., 1992). Specifically, the strains in the spent fuel rod cladding in a Pressurized Water Reactor (PWR) or a Boiling Water Reactor (BWR) fuel assembly generated by extreme impacts were estimated by extrapolation of regulatory impact cladding strains and by comparison of these extrapolated strain values to the failure strain criterion published in SAND90-2406. Finally, the results of these unyielding surface calculations were extrapolated to real yielding surfaces by partitioning the absorption of the available impact energy between the real yielding surface and the cask, and assuming that the damage caused by transfer into the cask of a given amount of energy was independent of the characteristics of the impact surface once energy loss to that surface was properly accounted for.

The public review and comments on NUREG/CR-6672 (Sprung et al., 2000) raised questions about the ability of the simplified NUREG/CR-6672 cask models to capture the response to extreme impact events. The Issues Report generated as the first phase of the PPS study recognized this concern as valid, and recommended that more detailed finite element analyses and an actual full-scale cask impact test should be performed to determine the adequacy of the cask models used in NUREG/CR-6672.

### **2.2 Objectives**

High-speed impact tests of a full-scale rail spent fuel cask and of a full-scale truck spent fuel cask are proposed as part of the PPS. The results of these tests will be compared to detailed pretest predictions of these results developed by finite element analysis. Less detailed finite element analyses were performed to develop the preliminary design of the impact tests that are described in this report.

A full-scale rail cask will be subjected to a high-speed impact onto an unyielding (essentially rigid) target. The impact test to be conducted for the full-scale truck cask will involve a high-speed impact of the center part of the cask onto an unyielding semi-cylinder, such that the impact limiters of the cask are bypassed in the impact (a “back-breaker” impact). Finite element analyses will be used to design the tests and predict the cask’s response. After the tests, the measured responses will be compared to the finite element analysis predictions. These comparisons will serve as the basis for validating that finite element analyses can be used to predict the response of casks to impacts that are at or beyond the design basis.

The testing described in this protocol report is not intended to validate or confirm the process with which the NRC certifies spent fuel packages. In the certification process it is required that packages be subjected to the various hypothetical accident conditions in the orientation that causes the most damage. The orientation chosen for the PPS test may not be the most damaging orientation for all of the cask components. It will be chosen to best meet the objectives of the PPS program—to demonstrate the inherent safety of certified casks and to demonstrate that finite element analyses can accurately predict the release (or lack of release) of radioactive material from a spent fuel cask subjected to an extreme impact. Release of radioactive material is most likely to occur as the result of damage to the closure region of the cask, and for this reason, the impact orientation chosen will be the one that produces the greatest assault to this region. Another impact of concern is one that does not involve the impact limiters that are attached to the two ends of the cask. The “back-breaker” impact on the truck cask will address this issue.

In preparing this test protocols report, preliminary analyses were performed to define the impact angle and approximate impact speed of the cask. In addition to public comments, more detailed finite element analyses will be used to determine the impact speed. The rail cask examined by these preliminary analyses was the Holtec HI-STAR 100. The truck cask examined was the GA-4. NRC has not committed to using these casks for the actual tests and will not make a decision about the casks to be used in the tests until after comments are received on this report.

### **2.3 Tasks**

Many tasks must be performed to analyze and conduct a full-scale cask high-speed impact test. Developing a measure of success for the comparison of the analysis and test results is the most important because instrumentation for the test will depend on how this comparison is to be made.

The current plan for the test set-up is to test only the cask and not the cask plus its conveyance. During shipments the cask is transported on a rail car or a flat-bed trailer and during most collision accidents, the damage done to the conveyance will decrease the damage done to the cask. So testing of the cask without mounting it on a rail car or trailer will lead to conservative results because the cask will suffer more damage than it would if it were mounted on its conveyance. Because cask tie-downs are designed to fail in a way that does not compromise the cask, omitting the conveyance from the test cannot lead to a less severe environment for the cask. Other than this, the cask will be tested in as close to its as transported configuration as possible.

In this plan, an impact limiter will be used on the end of the rail cask being impacted; the cask will contain a spent fuel canister, and surrogate contents will be placed in the canister. For the reference design the canister contents are a welded Multi-Purpose Canister (MPC) with either 24

PWR assemblies or 68 BWR assemblies. The test configuration will use the PWR MPC-24 canister. Surrogates will be used for the 24 PWR assemblies that are normally contained within the MPC-24; 23 of these surrogates will be mass simulations constructed of a single square steel tube filled with appropriate material to achieve the correct weight. The other mock spent fuel assembly will be constructed in the same manner as a fresh fuel assembly, but with surrogate material replacing the uranium dioxide fuel.

The analyses in this plan do not show the impact limiters for the truck cask because they do not participate in a "back-breaker" impact. The actual test will likely be performed with the impact limiters in place to demonstrate that their attachment hardware does not fail during the test. The GA-4 cask has a capacity of 4 PWR assemblies. In the test, one assembly will be constructed in the same manner as a fresh fuel assembly using surrogate material instead of uranium dioxide. The other three assemblies will be mass simulations.

A high-speed impact test can be conducted in either of two manners: a rocket-sled test with the cask traveling horizontally to impact a vertical target, or a drop test with the cask falling vertically to impact a horizontal target. The advantage of a horizontal sled test is that most real accidents occur with a horizontal orientation. The disadvantages of a horizontal test orientation are: 1) it is much more difficult to construct an essentially rigid target with a vertical impact surface (as is required for a sled test) than one with a horizontal impact surface (as is required for a drop test); 2) a rocket sled pushing the mass of a rail cask has a very large safety standoff distance; 3) it is more difficult to collect the data from on-board instrumentation in a sled test; and 4) the difference between the planned and the actual impact velocity can be significant.

To elaborate on several of these considerations, the NRC staff examined several options available for conducting the high-speed full-scale cask impact test that is proposed for the Package Performance Study. During the initial planning and scoping phases of the PPS, the NRC staff envisioned that any testing for PPS would likely involve a horizontal crash test as opposed to a vertical drop test. As the PPS tests matured, it became apparent to the NRC staff that a drop test had advantages, considering such factors as the test objectives, costs, local environmental and logistical concerns, and modeling applications. The base-line case described in this protocols report is now free drop tests employing a new drop facility and unyielding target. For perspective, a new drop tower might be high enough to allow an 82.3 m [270 ft]. free drop of a 136,000 kg [300,000 lb] test unit and the unyielding target will weigh 1,360,000 kg [3,000,000 lbs].

Instead of using a free drop to achieve the desired impact velocity, it is possible to accelerate a test article on a horizontal sled track using rocket motors. To construct a new target for a horizontal impact would be more expensive than the current cost estimate for a new target for a vertical test. There is an existing sled track target, but extensive upgrades would be needed. Moreover, a rocket sled test is much less precise than a free drop test, and there is a relatively large uncertainty on the velocity achieved in the test (~10%). Sled tests are much more complicated than drop tests, and therefore there are more things that can go wrong. This results in a less-controlled experiment and a greater chance of not being able to predict the cask performance by modeling and analyses before the test. Also, a common problem is failure of the instrumentation leads, which results in loss of data from the test.

The existing drop target at the Sandia cable site was also considered. This target has been used extensively over the past 16 years, and has had to be reconditioned on several occasions. None of the tests have subjected the target to an impact by a package weighing over 13,600 kg [30,000 lbs]. The cable site is used for many types of tests other than radioactive material package tests. Some of these tests could not be conducted if a permanent drop tower were built over the existing target. The current testing schedule at the cable site would not allow this construction to begin until after 2005.

In light of the above, the NRC staff proposes a free drop test onto a newly constructed target. The staff acknowledges that some may prefer a horizontal crash test to a drop test from the standpoint of visual impressions. Therefore, NRC staff is especially interested in and explicitly seeking public comment on this issue during the public comment period.

To withstand the tremendous forces generated by a high-speed impact of a 118,000 kg [130-ton] cask, the target for this test will be a block of concrete (approximately 7.6 m [25 ft] thick, 12.2 m [40 ft] long, and 6.1 m [20 ft] wide) topped with a plate of steel. The target will weigh more than 1,360,000 kg [3,000,000 lb]. The steel plate is welded to a steel sub-structure imbedded in the concrete to distribute the impact load throughout the entire mass of concrete. For the truck cask impact a thick-walled steel semi-cylinder filled with concrete will be welded to the top of the steel plate that is the upper surface of the target for the rail cask impact.

There must be a way of measuring the response of the casks to the impacts. Discrepancies between the test results and analysis predictions can come from three sources: 1) test parameters that are different than the values that were assumed by the analysis (e.g., impact angle); 2) inaccuracies of the measured results from the test; and 3) inaccuracies in the finite element model (either the material constitutive behavior or the degree of discretization).

The very stiff structure of the HI-STAR 100 cask implies that the proposed impact velocity will only produce small deformations in cask structures (the impact speed chosen for the test will be such that some permanent deformation occurs in the cask structure). Conversely, because the impact limiter will be crushed to its capacity, deformation of the impact limiter will be very large. These large deformations of the impact limiter can be compared to the deformations predicted by pretest analysis. But the main concern for the impact test is how well the pretest analysis does in predicting the response of the cask body, not the impact limiter. Because deformations to the cask body will likely be small, accurate measurements ( $\pm 0.0254$  mm [ $\pm 0.001$  in].) are needed to compare with the results of the pretest finite element analysis. Measurements to this accuracy on a full-scale cask are difficult because the thermal expansion of cask structures caused by a change of a few degrees in temperature will produce changes in structure dimensions of this magnitude, leading to larger inaccuracy in the measured result. Loss of cask containment can be caused by very small deformations of the cask closure, which cause the cask body and the lid to separate. Displacement gages can be used to measure relative displacement between these two parts. Strain gage bolts (bolts that are the same as the closure bolt, but have a sensing element placed inside of them that measures their tension) can be used to measure the load in the closure bolts. Comparison between analytically predicted closure movement and bolt loads with the output of these gages can be made.

Accelerometers measure the acceleration at the mounting location on the cask as a function of time. In certification testing, an array of gages is generally used to determine the “rigid-body” response of the cask. Because these gages will detect the impacts of the individual surrogate fuel assemblies onto the canister and of the canister onto the cask body, interpretation of the accelerometer data will not be simple in the proposed test. Gages attached to the cask sidewall will be less affected by these internal impacts than gages placed on the cask lid. Gages on the lid will provide information about the timing and perhaps the magnitude of force from the impact of the MPC on the lid.

Comparison of test and analysis accelerations requires examining both the magnitude and the temporal variation of the accelerations. Several factors may cause the measured acceleration to differ from the predicted accelerations. For example, if the accelerometer can’t be mounted at the location assumed in the pretest analyses, the measured and predicted results could be significantly different, and even if mounted at the location assumed in the calculations, the way that the accelerometer is mounted can affect the measurement. This makes correlation between measured results and analysis somewhat imprecise. Generally, agreement of peak acceleration within 10% is considered very good and agreement within 20% is acceptable.

The primary concern for these impact tests is to demonstrate the ability of the cask system to maintain containment of its radioactive contents. The HI-STAR 100 has several barriers to prevent release of radioactive material. The innermost barrier is the spent fuel cladding (how to measure the effectiveness of this barrier is another topic that the Package Performance Study is investigating). The next barrier is the welded MPC (an MPC is not required in every certified cask). It is expected that the impact test will not diminish the effectiveness of this barrier. The final barrier is the cask. While no radioactive material will be used in this test, it is possible to assess the over-all performance of the cask by testing to see if it maintains pressure (because most fission products will be present as constituents of particles, failure to maintain pressure does not necessarily imply failure to contain radioactive material, since a small leak path may not allow a significant quantity of particles to escape from the cask). The pressure in the space between the cask body and the MPC can be monitored with pressure transducers during the test. Failure of the MPC, if it occurs, will likely occur at the weld joint that attaches the MPC lid to its body. The ability of finite element analysis to predict the response of this region can be monitored by attaching strain gages to the MPC body and/or the closure ring at the weld location. Post-test verification of the integrity of the MPC can be measured by performing a leak test on the closure. Modification of the MPC will be required to perform this test.

For the “back-breaker” impact of the GA-4 the deformations to the cask body will be larger than they are for the HI-STAR 100. This will allow meaningful comparisons to be obtained by dimensional inspection. In addition, there will be relatively large strains in areas of the cask that are not being impacted. Strain gages can be placed in these locations and the measured strains during the test can be compared to the finite element prediction. Another area of concern is separation of the DU shielding segments. The amount of separation in the test can be determined by radiography and compared with the amount predicted by the finite element analysis. Accelerations at the two ends of the cask and at the center can also be measured. The possibility of damage to the containment boundary is also of concern. A post-test leak test can determine if the package remains leak-tight following the impact, but the finite element calculations do not directly give leak rate. It is not anticipated that this test will result in damage to the closure

region of the cask because all of the deformation and energy absorption is distant from it. Therefore, any leakage after the test is likely to be the result of tearing in the wall of the cask or in one of the longitudinal welds. The strain levels in these components predicted by the finite element analysis calculations can serve as an indicator of possible tearing, but correlation will be difficult.

Based on the possible instrumentation to be used in the proposed test, a preliminary instrumentation suite is recommended in the impact test protocol section below. During the development of the detailed test plan, the final instrumentation suite will be determined.

While not absolutely necessary for comparing test and analysis results, this type of test should be well documented with photographic coverage. Pre-test and post-test activities will be documented with both video and still cameras. The test will be documented with real-time and high-speed video cameras and high-speed film cameras.

The finite element analyses discussed below are similar in level of detail to those conducted for NUREG/CR-6672 (Sprung et al., 2000). These analyses were used to determine the recommended impact orientation and approximate impact velocity for the tests. They do not include all of the details of the casks, and therefore cannot provide a precise prediction of the test results. A detailed pre-test finite element analysis will be performed to develop the final pre-test predictions of cask response to the test impacts. The finite element model for this analysis will contain all of the significant features of the impact limiter, cask, MPC, and surrogate contents. However, there are some features of a cask that are too small to include in the detailed finite element model (e.g., bolt threads, cell structure of honeycomb impact limiters, etc.). During the development of the detailed test plan, the consequences of omitting these features will be investigated. Depending on the results of this investigation, it may be necessary to perform component tests and analyses to determine the optimum way of treating these omitted features.

Initially, the detailed finite element analyses will be performed using the nominal material properties at the appropriate strain rate for the materials specified in the cask and impact limiter design drawings. During the fabrication of the actual test casks and impact limiters by the manufacturers, as-built material properties may be determined for some materials. If the actual material properties are significantly different from the nominal properties, it may be necessary to re-run the initial detailed pretest analyses using the actual properties.

## **2.4 Finite Element Analyses**

To determine the structural response of the HI-STAR and GA-4 casks to extreme impacts, finite element analyses are conducted of the cask impacting a rigid surface. For the HI-STAR cask this preliminary analysis is conducted using two different finite element models. In the first model, the cask is modeled using a homogenous, isotropic representation of the honeycomb impact limiter. Using this model the cask assembly is analyzed for three different impact orientations. In the second finite element model, a more detailed model of the impact limiter is constructed. The detailed impact limiter model includes three different strengths of honeycomb material (each modeled as homogeneous and isotropic) and the steel substructure of pipes and gussets inside the impact limiter. This model is analyzed for an impact onto a rigid surface in the center of gravity (CG)-over-corner orientation for two different velocities — 96 kph [60 mph] and 120 kph [75

mph]. This corresponds to drop heights of 36.57 m [120 ft] and 65 m [213 ft], respectively. For the GA-4 cask the preliminary analyses are modeled without impact limiters (the mass is added to the cask ends), so only a single model is used. The impacts were in a side-on orientation impacting a semi-cylindrical rigid target at speeds of 96 kph [60 mph] and 120 kph [75 mph].

The analyses were conducted using the Sandia non-linear transient dynamic finite element code PRONTO-3D. PRONTO-3D is a shock-wave propagation code developed specifically for impact analyses. It uses an explicit time integration algorithm for solving the equations of motion. User supplied inputs are the model geometry, boundary conditions, material constitutive behavior and properties, and the initial impact velocity.

#### 2.4.1 Description of HI-STAR 100 Cask and Impact Limiter [obtained from the *HI-STAR Safety Analysis Report* (Holtec, 2000)]

A schematic drawing of the HI-STAR 100 cask is presented in Figure 1. The cask is approximately 2.1 m [7 ft] in diameter and 5.18 m [17 ft] long. The cask body is 229 mm [9 inches] thick, constructed of multiple concentric shell layers. The shell layers are constructed in a manner that ensures a permanent state of interfacial pressure between adjacent layers. The cask body houses a 41,000 kg [90,000 lb], MPC canister, sealed with a 152.4 mm [6 in] thick closure lid. The closure lid is secured to the cask body with fifty-four 41.275 mm [1-5/8 in] closure bolts.

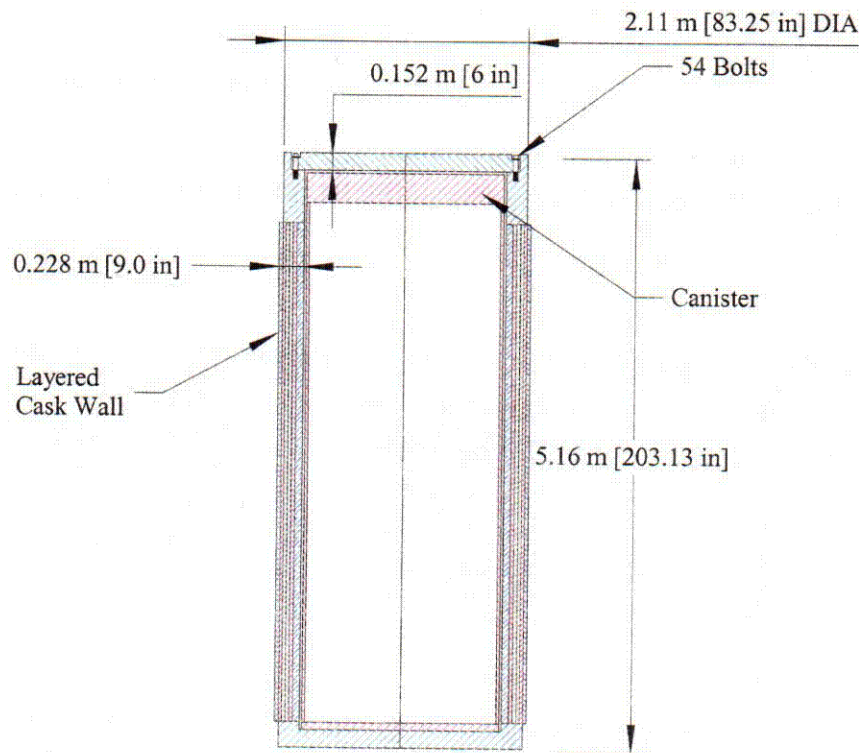
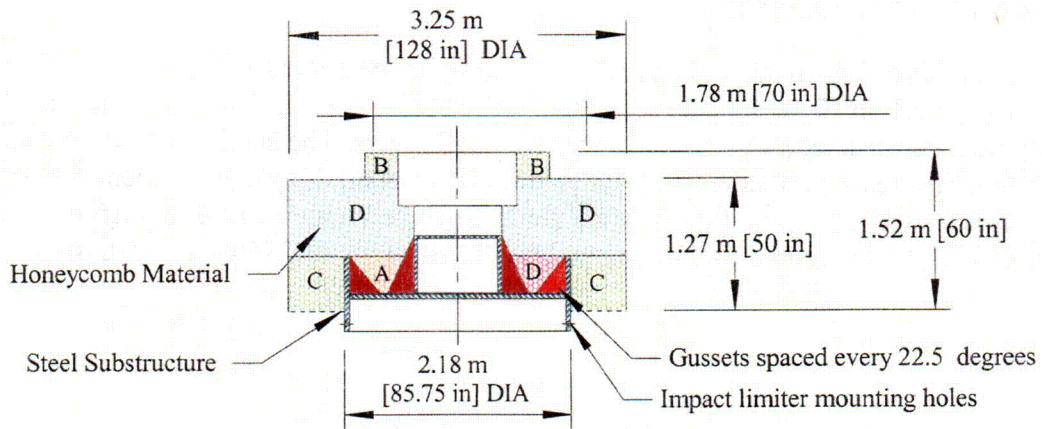


**Figure 1. Schematic drawing of HI-STAR cask body.**

The cask body is made from four different steels. The upper and lower flanges and the closure lid are constructed of alloy steel, ASTM A-350-LF3. The layered shells are constructed from carbon steel, ASTM A-516 Grade 70, with the inner layer using alloy steel, ASTM A-203E. The high-

strength bolts are made from a Ni-Cr alloy, ASTM B-637, and the canister is constructed using stainless steel, AISI 304.

The HI-STAR 100 impact limiter is shown schematically in Figure 2. The impact limiter is approximately 3.35 m [11 ft] in diameter and 1.52 m [5 ft] thick. Uni-axial and bi-axial aluminum honeycomb is used as the energy absorbing material. The material is segmented and four different crush strengths are used in the limiter; these values are given in Table 1. The impact limiter contains a steel substructure consisting of steel pipes, gussets, and plates. The steel substructure is used to constrain some of the honeycomb material and also to fasten the impact limiter to the cask body. The top impact limiter is fastened to the cask body using twenty 25.4 mm [1 in] diameter bolts. The impact limiter is encapsulated using a 3.175 mm [1/8 in] thick stainless steel plate.



Note: Honeycomb segments between the gussets alternate between type A and type D.

**Figure 2. Schematic drawing of the HI-STAR impact limiter.**

**Table 1. HI-STAR impact limiter honeycomb materials strength and directionality.**

Material	Honeycomb Crush Strength, Mpa (psi)	Honeycomb Directionality
A	4.8 (700)	Uni-directional
B	7.6 (1100)	Uni-directional
C	11.7 (1700)	Bi-directional
D	15.8 (2300)	Bi-directional

#### 2.4.2 Finite Element Model I

The initial finite element model developed for the HI-STAR cask is shown in Figure 3. The model consists of four components: the impact limiter, the cask, the canister, and the canister contents. The cask has two components: the cask body and the cask closure lid. The impact limiter has three components, an outer encasing shell (not shown in Figure 3), an energy absorbing aluminum honeycomb material, and a steel sub-plate. The full model contains 80,689 elements with a total of 92,266 nodal points. A plane of symmetry exists along the cylindrical

axis of the cask, which allows the cask to be modeled using only one half of the number of elements. This reduces the analysis time without affect the accuracy of the result.

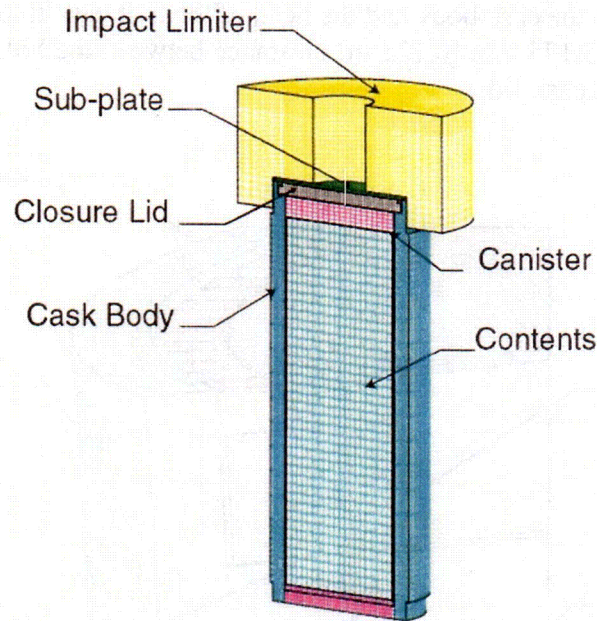


**Figure 3. Finite element model of HI-STAR cask.**

For these preliminary models, several simplifying assumptions are made. While the steel MPC is modeled, the fuel assemblies carried in the canister are treated as a homogenous crushable material. The crush strength of this material is chosen from the buckling strength of PWR fuel rods subjected to axial loading. The density of this material is adjusted so that the total weight of the cask is equal to the specified design weight. Modeling the fuel assemblies in this manner does not allow direct determination of the behavior of the fuel rods, but provides an assessment of the loads that these assemblies transmit through the canister to the cask. The layered shell structure of the central section of the HI-STAR cask body is modeled as a monolithic steel structure. This will have little effect on the total stiffness of the cask body. In addition, for an impact onto the lid end of the cask, the highest loads and deformations in the cask will occur in the lid and the cask top flange, which are both monolithic forged steel components.

The initial velocity vector of the cask is assumed to be perpendicular to the rigid surface. All of the interior contact surfaces in the model (between the contents and the canister, the canister and inner shell, the lid and the cask body, and the cask body and the impact limiter) are assumed to be frictionless. The contact between the cask and the rigid surface is also assumed to be frictionless. For most aspects of the problem neglecting friction is conservative, as there is no significant loss of impact energy because of frictional heating. Including friction at contact surfaces tends to cause the various parts of the model structure to behave more like a single component and thus the parts of the structure separate less easily.

The closure of the cask is explicitly modeled. A section of the closure lid area is presented in Figure 4. The lid is recessed into the upper flange of the cask and is held in place with 54 - 41.275

mm [1.625 in] diameter bolts (only 27 bolts are modeled in the model of half of the cask). There is a 6.35 mm [0.250 in] radial gap between the outer radius of the closure lid and the inside radius of the cask flange. The bolt model cross-section is square with square heads. The cross-sectional areas of the square bolt shank and head are the same as those of a corresponding round bolt. The bottom of the shank is rigidly attached to the cask body and the head of the bolt has “fixed contact” with the top surface of the lid. There is a 3.175 mm [0.125 in] clearance between the bolt shank surface and the surface of the bolt holes in the cask lid.

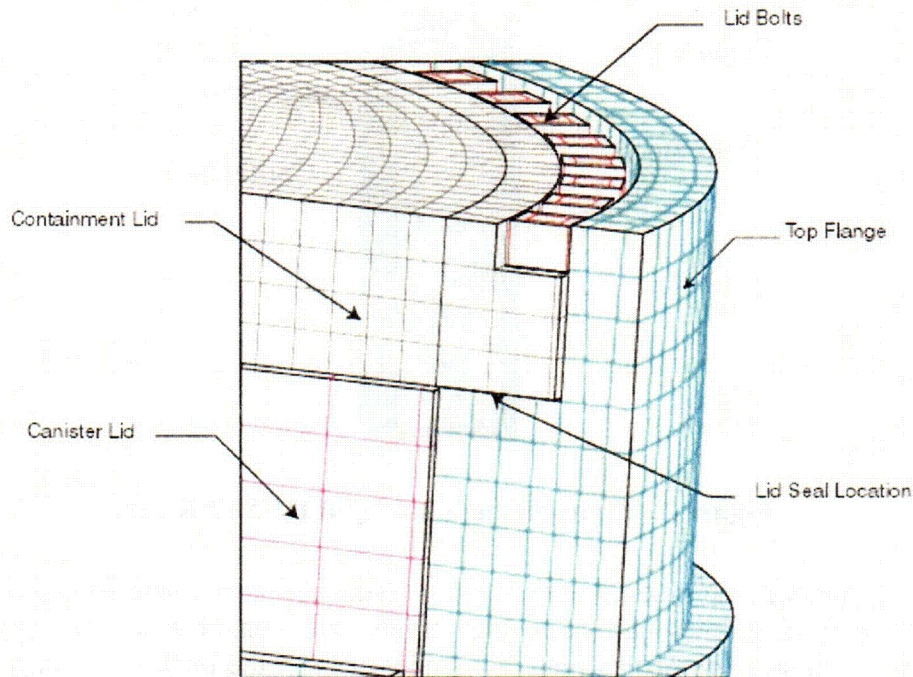


**Figure 4. Closure region.**

Figure 5 shows the finite element mesh of a closure bolt. The shank of the bolt has one element in its cross-section and four elements along the length. The head of the bolt has one element through the thickness and five elements in the cross-section. The inner element of these five elements has a cross-section identical to that of the bolt shank. This preliminary bolt model should properly capture both the shear and tensile loading in the bolt. However, its ability to model bending may be limited. A more detailed bolt model will be developed for the detailed analysis. The initial preload in the bolt caused by the initial tightening torque is neglected. Neglecting this preload is conservative because the preload must be overcome by loading of the cask lid by the impact of the canister onto the cask lid before there is any deformation to the bolts. This means that a lid with a preloaded closure will experience a smaller opening due to impact loads than a closure without a preload.

The closure lid seal is not included in the current model, but the deformation between the sealing surfaces of the cask body and lid are calculated to determine the formation and size of any gap that may develop as a result of impact loads. The gap between the cask body and closure lid is determined at 82 equally spaced locations around the half-model circumference of the closure lid at the center of the sealing surfaces. Summation of the trapezoidal areas that lie between each

adjacent pair of points minus the compliance of the cask seal provides an estimate of the leak path cross-sectional area produced by the cask impact.

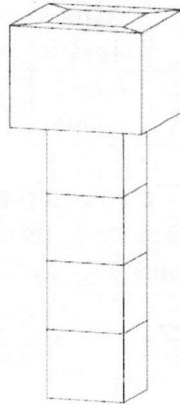


**Figure 5. Finite element model of closure lid bolt.**

In the first finite element model, the impact limiter is modeled as a single continuous mass of isotropic crushable material surrounded by an encapsulating 3.175 mm [1/8 in] thick stainless steel shell. The impact limiter is mounted on top of a 41.2 mm [1-5/8 in] thick sub-plate, which is bolted to the top of the cask flange. By design, there is a 6.35 mm [1/4 in] clearance between the impact limiter sub-plate and the top surface of the closure lid. To simplify the current model, the attachment bolts for the sub-plate are not modeled. Instead, the contacting surfaces of the plate and flange are connected. The bolts used to attach the impact limiter to the cask body are also not included in the model; inertial forces are relied upon to keep the impact limiter in place. The honeycomb material is modeled using a “new foam” material constitutive model developed by SNL. The constitutive model includes seven material parameters:

- $E$  - Young's Modulus  $E$
- $\nu$  - Poisson's Ratio
- $A$  - Foam crush strength
- $B$  - Hardening modulus
- $Poly$  - Bulk modulus of crushed foam
- $P$  - Internal air pressure
- $\phi$  - Volume fraction

Values of these parameters for the honeycomb material used in the analyses are given in Table 2. The value for the crush strength of the foam is picked as a nominal value to simulate the four different, uni-axial and bi-axial honeycomb crush strengths found in the HI-STAR limiter and the influence of the pipe and gusset structures. A value of 68.9 Gpa [10 million psi] is used for the bulk modulus of aluminum and volume fraction of 0.40 is a typical value for bi-axial honeycomb material. The value for Young's modulus is determined from test data and the hardening modulus is assumed to be small, but nonzero.

**Table 2. Foam parameter values.**

<b>E</b> <b>Mpa</b> <b>(psi)</b>	<b>v</b>	<b>A</b> <b>Mpa</b> <b>(psi)</b>	<b>B</b> <b>Mpa</b> <b>(psi)</b>	<b>Poly</b> <b>Gpa</b> <b>(psi)</b>	<b>P</b> <b>Mpa</b> <b>(psi)</b>	<b>φ</b>
67.1 (9740)	0	20.68 (3000)	0.689 (100)	68.9 (10e6)	0.101 (14.7)	0.40

The cask body was model as a monolithic steel structure. A power-law hardening constitutive model was used to model the material behavior. This model treats the material as elastic up to the limit of proportionality and captures the plasticity by the equation:

$$\sigma = \sigma_p + A \langle \varepsilon_p - \varepsilon_L \rangle^n .$$

Where  $\sigma_p$  is the stress at the limit of proportionality,  $A$  is the hardening constant,  $\varepsilon_p$  is the equivalent plastic strain,  $\varepsilon_L$  is the Luder's strain (the flat portion of the stress strain curve immediately after yielding for low-carbon steels),  $\langle \rangle$  indicates the Heavyside function where the expression enclosed in the brackets is unchanged when positive, and equal to zero when negative, and  $n$  is the hardening exponent.

The constitutive behavior of the canister is also modeled using a power-law equation. The high-strength bolts are modeled with a bi-linear elastic plastic material model. A summary of all of the parameters for the cask body materials is presented in Table 3.

**Table 3. Cask body constitutive model parameters.**

<b>Component</b>	<b>Material Model</b>	<b>E</b> <b>Gpa</b> <b>(ksi)</b>	<b>v</b>	$\sigma_y$ or $\sigma_p$ <b>Mpa</b> <b>(ksi)</b>	$A$ or $E_p$ <b>Mpa</b> <b>(ksi)</b>	<b>N</b>
Closure lid and canister	Power-law Hardening	193.1 (28,000)	0.27	0.186 (37)	1.33 (193)	0.748190
Cask flanges and side	Power-law Hardening	193.1 (28,000)	0.27	0.278 (40)	1.33 (193)	0.748190
Bolts	Elastic-plastic	206.8 (30,000)	0.30	0.724 (105)	0.206 (30)	

### 2.4.3 Model 1 PRONTO-3D Finite Element Results

PRONTO-3D analyses were conducted for the HI-STAR cask impacting a rigid target at 96 kph [60 mph] in three orientations: CG-over corner, end-on, and side-on. Figure 6 presents a schematic representation of the three orientations. For all three orientations, the impact limiter absorbed the majority of the energy.

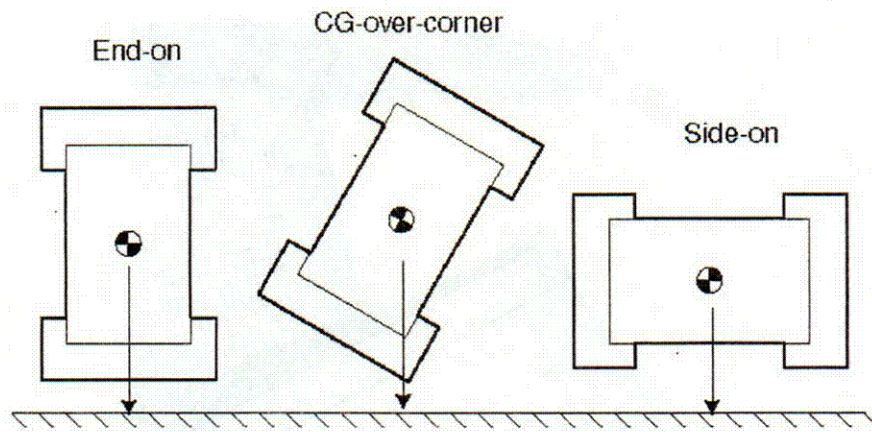


**Figure 6. Cask loading orientations.**

Center of Gravity-Over-Corner Impact

The results of the CG-over corner impact are shown in Figure 7 and Figure 8. To aid in viewing the analysis results, the figures are presented with the impacted side of the cask facing upward. For the CG-over-corner orientation, the impact limiter was crushed from an initial thickness of 1.05 m [41.375 in], to a minimum final thickness of approximately 0.45 m [18 in].

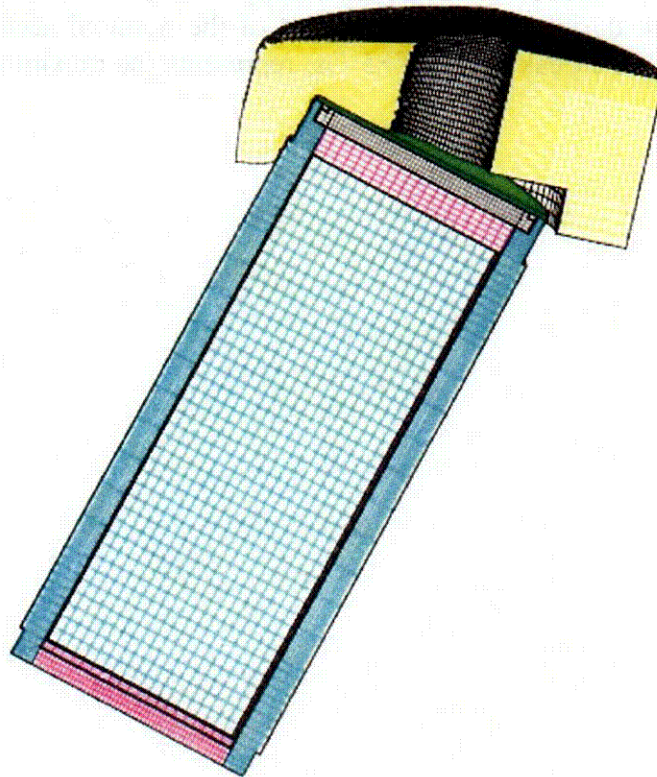


**Figure 7. Cask assembly after a 96 kph [60 mph] CG-over-corner impact onto a rigid surface.**

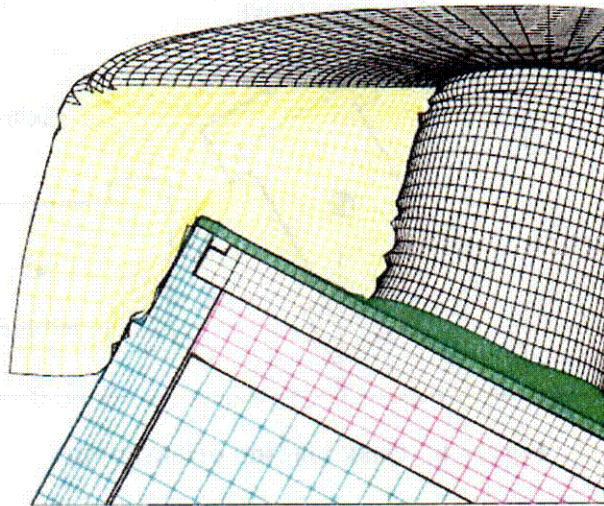


**Figure 8. Details of the damage depicted in Figure 7.**

Figure 9 presents a plot of the total cask kinetic energy vs. time for the CG-over-corner calculation. Using the kinetic energy, the velocity of the cask as a function of time may be calculated. The velocity function is then numerically differentiated to determine the nominal acceleration of the cask during the impact. A plot of the nominal acceleration versus time is presented in Figure 10. The peak value of 85 Gs, represents the maximum load experienced by the cask.

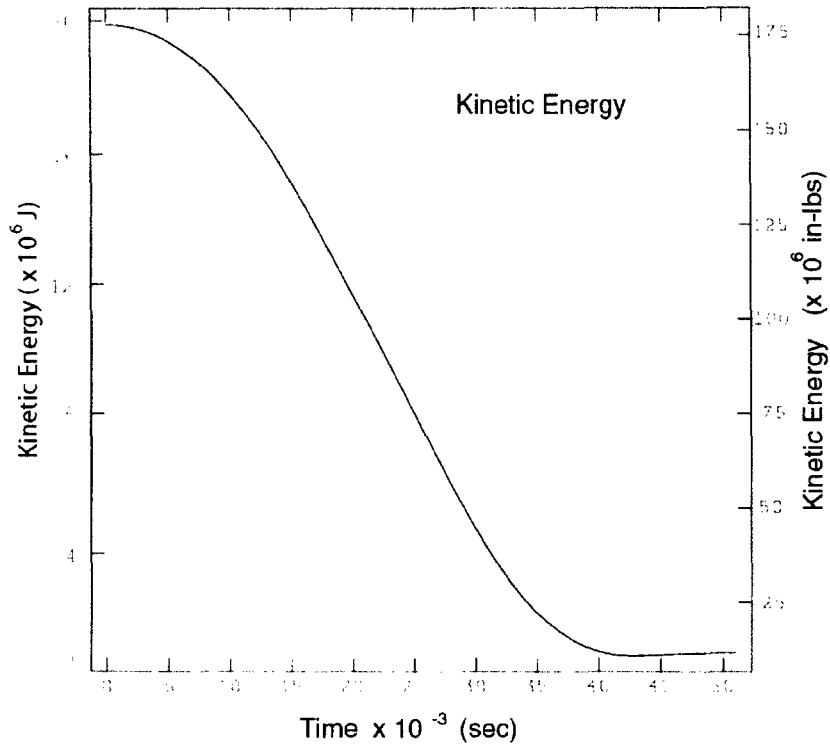


**Figure 9. Kinetic energy versus time for a 96 kph [60 mph] CG-over-corner impact.**

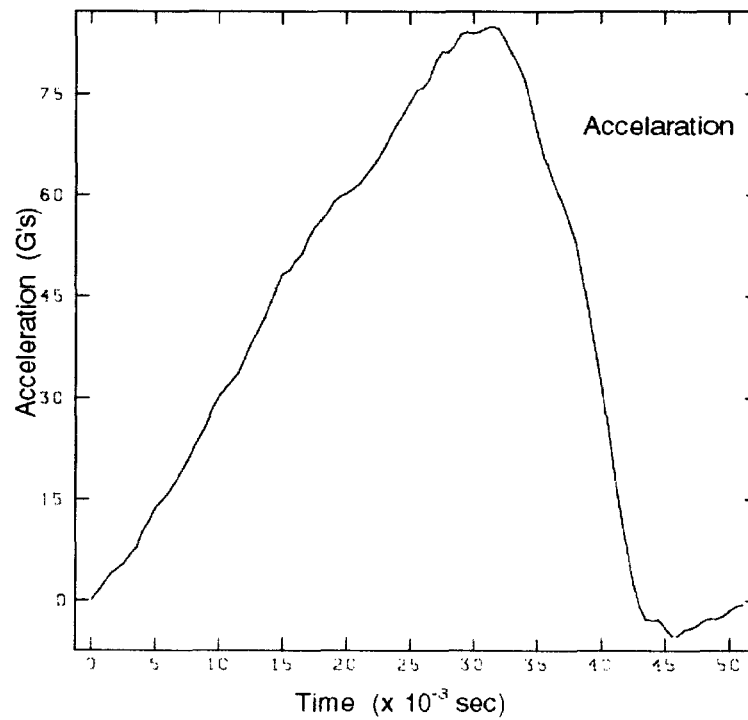


**Figure 10. Nominal acceleration of a cask subject to a 96 kph [60 mph] CG-over-corner impact.**

The response of the cask body to a 96 kph [60 mph] impact is primarily elastic. The most highly stressed cask components are the bolts used to secure the closure lid. Neither the cask body nor the bolts experience strains high enough to indicate material failure. Figure 11 depicts the equivalent plastic strain in the first four most highly stressed bolts. These bolts are located adjacent to the symmetry plane opposite the point of impact. As shown, only the first two bolts closest to the symmetry plane experience plastic deformation. A maximum plastic strain of 0.1% is found in the most highly stressed bolt. This plastic strain causes a gap to form between the closure lid and its mating flange surface. Figure 12 is a plot of this gap calculated at 82 points around the circumference of the model at the centerline of the sealing surface. In this figure, the zero angular location is on the symmetry plane opposite the impact point. Figure 12 shows that the largest calculated separation of the lid from its mating flange is 0.76 mm [0.030 in]. When calculating the leakage area caused by the impact, the seal compliance must be subtracted from the separation distances. These separation distances are also conservative because no bolt torque preload is included in the calculation. As noted above, bolt preload would reduce the gap because no bolt stretching would occur until the preload is relieved.



**Figure 11. Equivalent plastic strain in closure lid bolts for 96 kph [60 mph] CG-over-corner impact.**

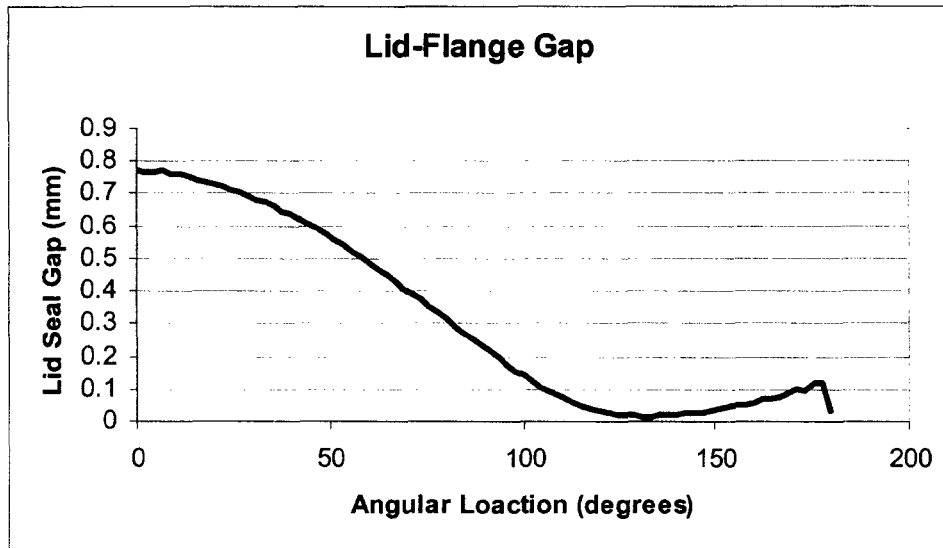
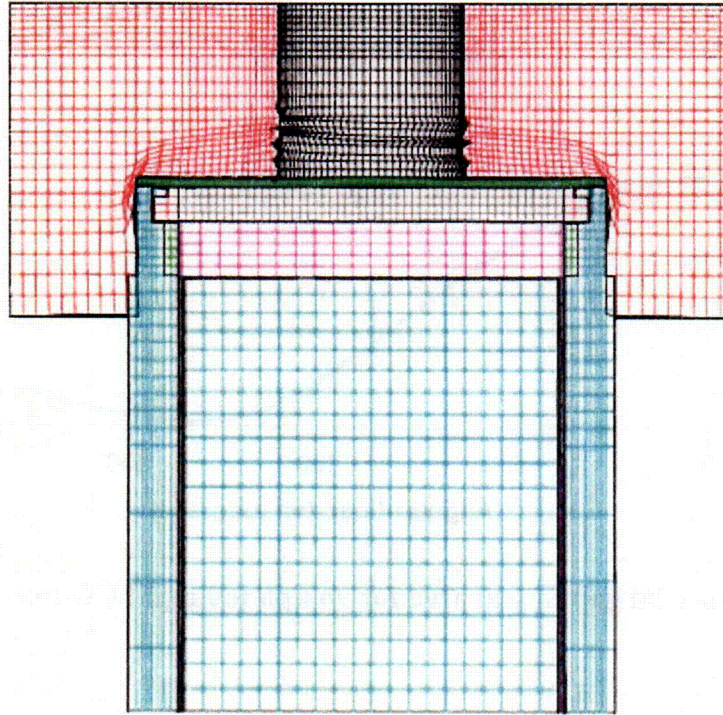


Figure 12. Closure lid gap in seal area for 96 kph [60 mph] CG-over-corner impact.

End-on Impact

The resulting deformation from the end impact calculation is presented in Figure 13. The kinetic energy and acceleration for this impact are plotted in Figure 14 and Figure 15, respectively. For this orientation, the maximum acceleration and loss of kinetic energy are larger than the CG-over-corner orientation results. However, in this orientation, the impact limiter actually helps support the closure lid. Immediately after impact, the sub-plate is deformed and the gap between the sub-plate and the closure lid is eliminated. Consequently, the impact limiter supports almost the entire surface of the closure lid, which reduces the load on the closure bolts. As a result, there is no plastic deformation in the closure bolts, no separation of the closure lid from its mating flange and the stresses in the cask body remain elastic. Clearly, this impact orientation causes much less deformation of the cask closure than the CG-over-corner orientation.



**Figure 13. End-on 96 kph [60 mph] impact onto a rigid surface.**

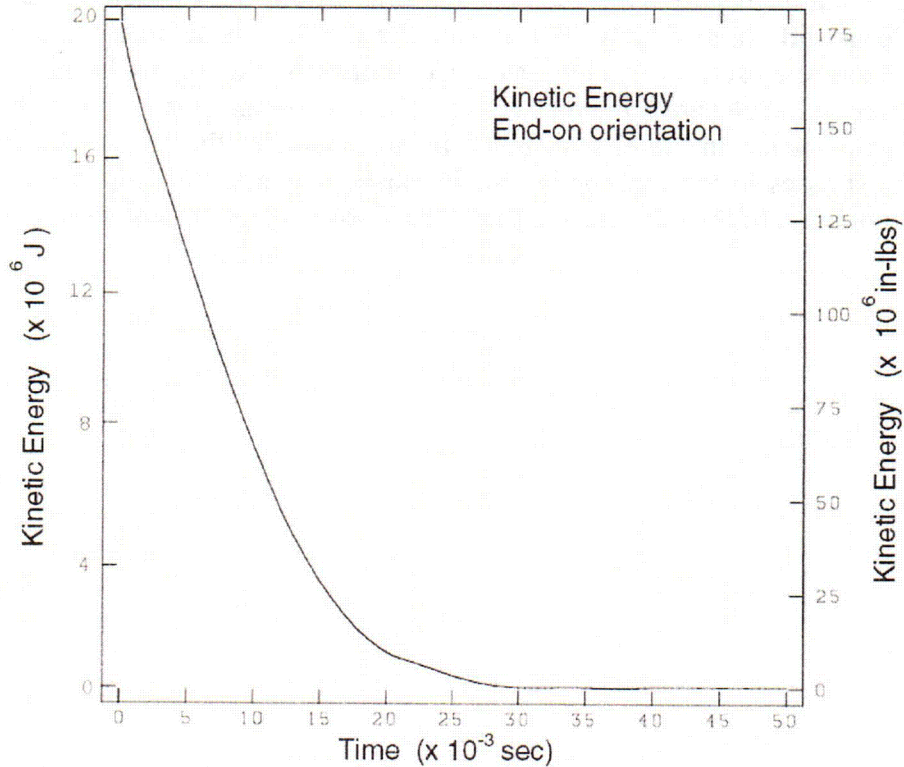


**Figure 14. Kinetic energy versus time for a 96 kph [60 mph] end-on impact onto a rigid surface.**

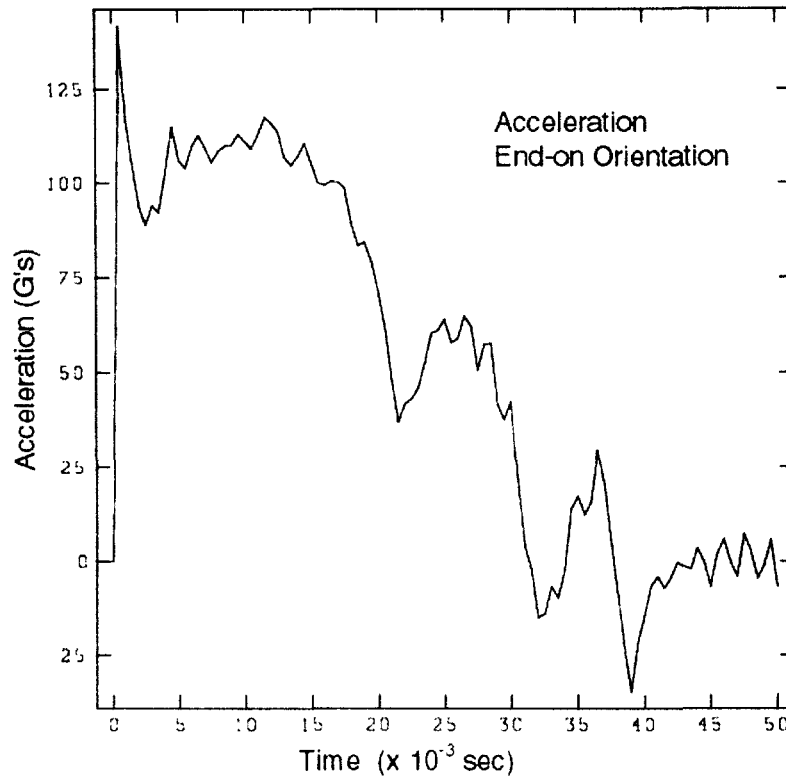


**Figure 15. Acceleration versus time for a 96 kph [60 mph] end-on impact onto a rigid surface.**

### Side-on Impact

For the third impact orientation, the side-on impact, the cask model had to be modified. First, a second impact limiter was added to the bottom of the cask and both impact limiter models were modified to include a structural pipe not modeled in the impact limiter depicted in Figure 1. As shown in Figure 16, this pipe fits over the outside of the cask and extends into the body of the energy absorbing honeycomb material. The pipe is used to fasten the impact limiter to the side of the cask and also to provide lateral support. In the model, the pipe is attached to the side of the cask using “tied contact surfaces.” Friction was also added between this pipe and the honeycomb material to prevent the impact limiter from sliding off of the pipe. The results of the side-on impact are presented in Figure 16.

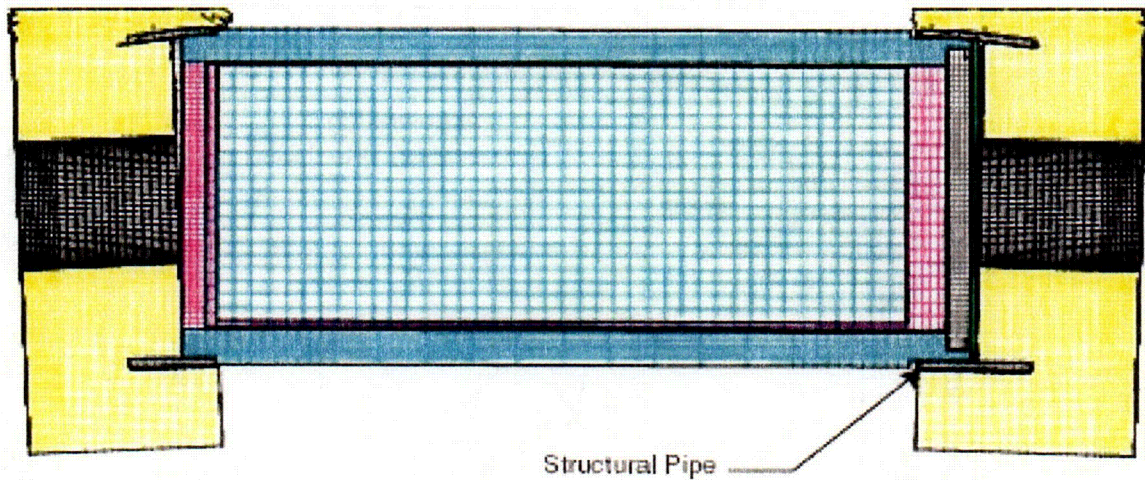


**Figure 16. Side-on 96 kph [60 mph] impact onto a rigid surface.**

A plot of the variation with time of impact kinetic energy is presented in Figure 17. The addition of the mass of the second impact limiter causes the initial cask kinetic energy to be slightly higher at the start of this analysis than it was for the CG-over-corner impact calculation, and the final kinetic energy is greater than zero due to rebounding of the cask from the rigid surface. The variation with time of the cask acceleration is given in Figure 18. A maximum acceleration of 135 Gs is reached after approximately 25 milliseconds. This is higher than the maximum acceleration calculated for the CG-over-corner impact. However, due to the cask orientation, most of the impact load is transmitted to the sidewall of the cask body. There is some very local plastic deformation in the cask lid flange where this flange contacts the impact limiter pipe that was modeled only for this impact orientation. However, neither the cask body nor the bolts experience strains high enough to indicate material failure. Three of the closure bolts in this area do exhibit some very small plastic shear deformations. However, the resulting gap between the closure lid and the cask flange is about ten times smaller than the gap calculated for the CG-over-corner impact. Addition of the bolt preload would eliminate this small gap. Thus, the results of this impact orientation are also less severe than the CG-over-corner orientation.

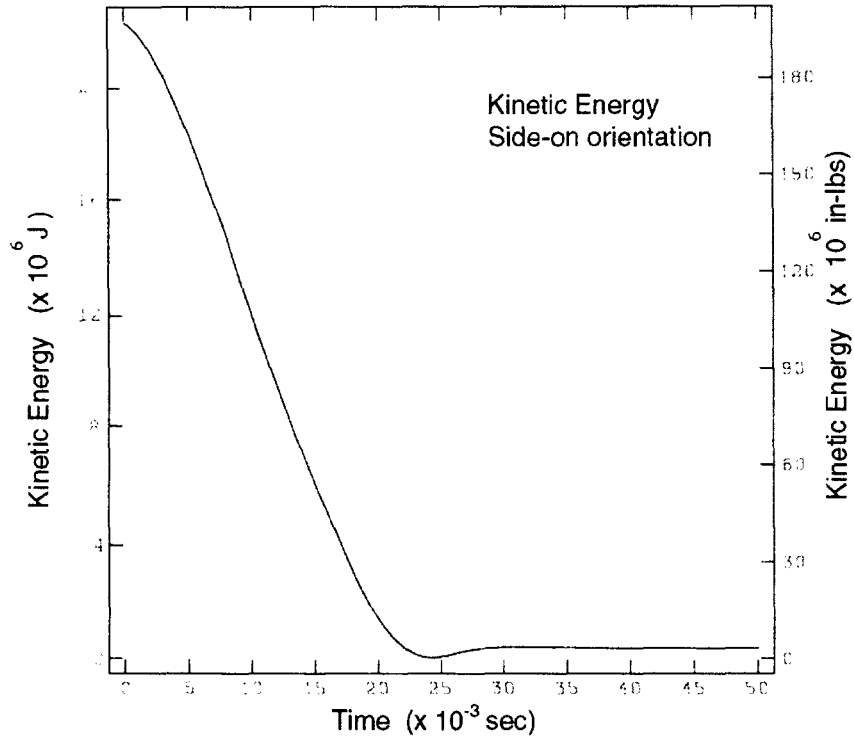


**Figure 17. Kinetic energy versus time for a 96 kph [60 mph] side-on impact onto a rigid surface.**

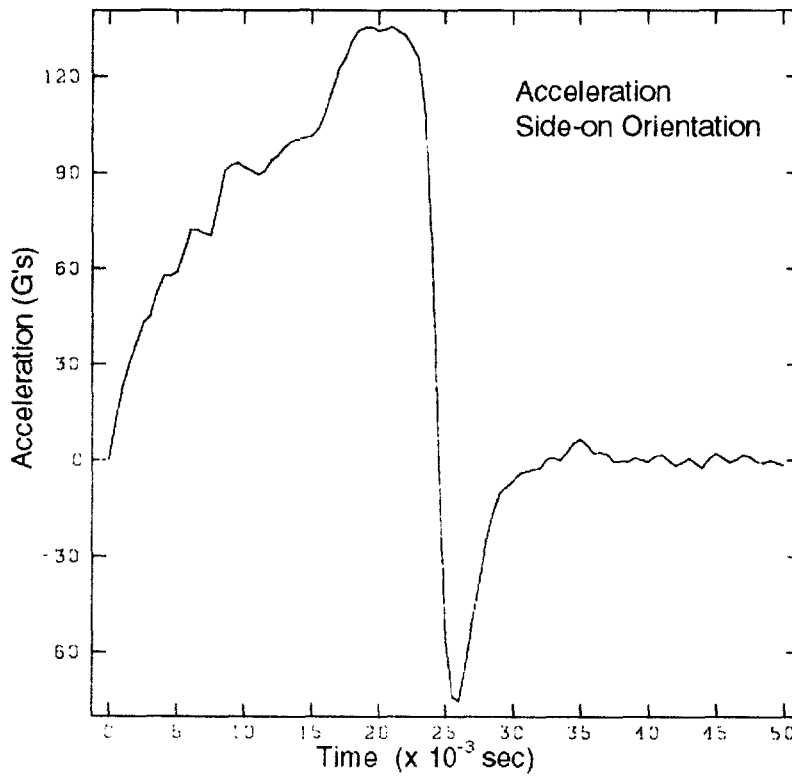


**Figure 18. Acceleration versus time for a 96 kph [60 mph] side-on impact onto a rigid surface.**

#### 2.4.4 Model 2 Finite Element Model with Improved Impact Limiter

To further refine the finite element model, a more detailed impact limited model was constructed and analyzed in the CG-over-corner orientation. The model of the impact limiter is shown in Figure 19. The impact limiter model consists of three major components: the encasing shell, an energy absorbing material, and a steel substructure.

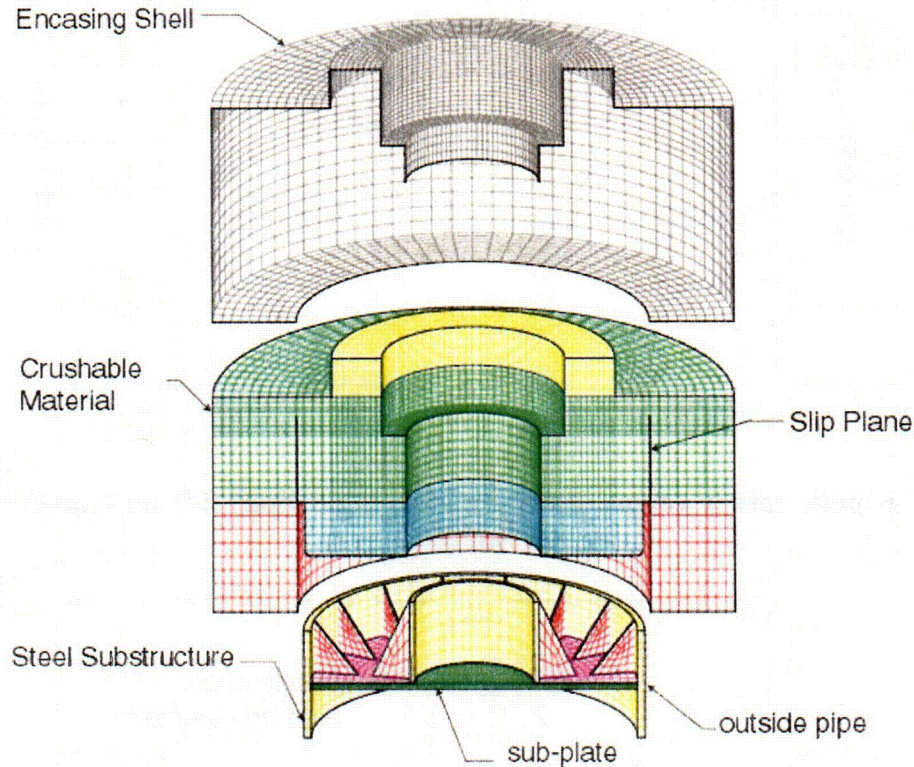


**Figure 19. Illustrates the three major components of the detailed impact limiter: encapsulating shell, energy absorbing material, and the steel substructure.**

Three different strengths of honeycomb material are used in the detailed impact limiter. The honeycomb material is modeled using the same new foam constitutive model discussed above. Values of the parameters for the three different honeycomb materials are given in Table 4.

**Table 4. Foam parameter values for detailed impact limiter.**

Foam Material	E MPa (psi)	$\nu$	A MPa (psi)	B Pa (psi)	Poly GPa (psi)	P Pa (psi)	$\phi$
1	67.16 (9740)	0	11.72 (1700)	6.896e5 (100)	68.95 (10e6)	1.01e5 (14.7)	0.40
2	67.16 (9740)	0	6.895 (1000)	6.895e5 (100)	68.95 (10e6)	1.01e5 (14.7)	0.20
3	67.16 (9740)	0	15.89 (2300)	6.895e5 (100)	68.95 (10e6)	1.01e5 (14.7)	0.40

The various honeycomb materials are modeled as one continuous structure. The contact between the honeycomb material and the steel substructure is assumed to be frictionless. Similarly, the contact between the steel substructure and the cask body is also frictionless.

The steel substructure is made up of structural pipes, gussets and a steel sub-plate. The outer 47.6 mm [1-7/8 in] thick pipe fits over the side of the cask and is used to secure the impact limiter to the cask body. The retaining bolts are not included in this analysis and there is a line-to-line fit between the pipe and the cask wall. The pipe/gusset weldments are connected as an assembly using a 3.175 mm [1/8 in] thick plate. The pipe and gusset assembly rests on top of a 41.3 mm [1-5/8 in] thick sub-plate. The sub-plate is bolted to the top of the cask. However, these bolts are not included in the current model. Instead, the sub-plate is attached to the cask using “contact surfaces.”

There are several modeling assumptions made to simplify the model and avoid numerical complications. These assumptions focus on eliminating large local shear deformation in the honeycomb material. The first modeling change was the addition of a slip plane to the model starting at the top outside diameter of the pipe and going up into the honeycomb material (see Figure 19). This slip plane allows the outside section of the honeycomb material to slide past the outside pipe without severely distorting the honeycomb material near the top surface of the pipe. The addition of the slip plane will have little impact on the total energy absorbed by the honeycomb.

In a similar fashion, the interaction between the honeycomb material and the pipe gussets may cause local deformations, which severely distort the honeycomb elements. To prevent this, the contact between the pipe gussets and the honeycomb is removed from the model. The honeycomb material in the area of the gussets is constructed as one continuous, uniform piece. This material and the gusset material occupy the same space, but do not interact. Similarly, this assumption should have little effect on the total energy being absorbed by the impact limiter.

Another area where local finite element distortion could affect the performance of the finite element model is the area between the top surface of the outside pipe and the rigid impact surface. The honeycomb material that is trapped between the top surface of the pipe and the rigid surface can become extremely deformed. This, large, local deformation is caused by the relatively small area of the pipe ripping through the relatively soft honeycomb material. In reality this would lead to some coining or stamping of the material, between the top of the pipe and the rigid surface. To prevent this large, local deformation from causing numerical problems in the finite element model, the upper section of the outer pipe is defined so that it does not have contact with the honeycomb material. The upper section of the pipe is allowed to pass through the honeycomb material and therefore eliminates any possible numerical problems. This is a realistic assumption since the upper section of the outside pipe will easily shear through the foam material. Ignoring the energy loss as a result of this shear stress is a conservative assumption.

A PRONTO3D analysis was conducted for the detailed model in the CG-over-corner orientation impacting at velocities of 96 kph [60 mph] and 120 kph [75 mph]. The results of the 96 kph [60 mph] impact are shown in Figure 20 and Figure 21. For this speed, the impact limiter absorbed a majority of the energy. Figure 22 shows the distortion in the steel substructure caused by contact of the outside pipe with the rigid surface. A plot of the kinetic energy with time is given in Figure 23 and a plot of the nominal acceleration versus time is presented in Figure 24. The peak

acceleration of 54 Gs shown in Figure 24, represents the maximum load experience by the cask. This acceleration level is below the design level for the closure lid bolts. In addition, the force of impact is transferred through the impact limiter and across the surface of the closure lid. The sub-plate is deformed and the closure lid is actually supported by the impact limiter and this reduces the force on the lid closure bolts. As a result, the lid closure bolts experience no plastic deformation.

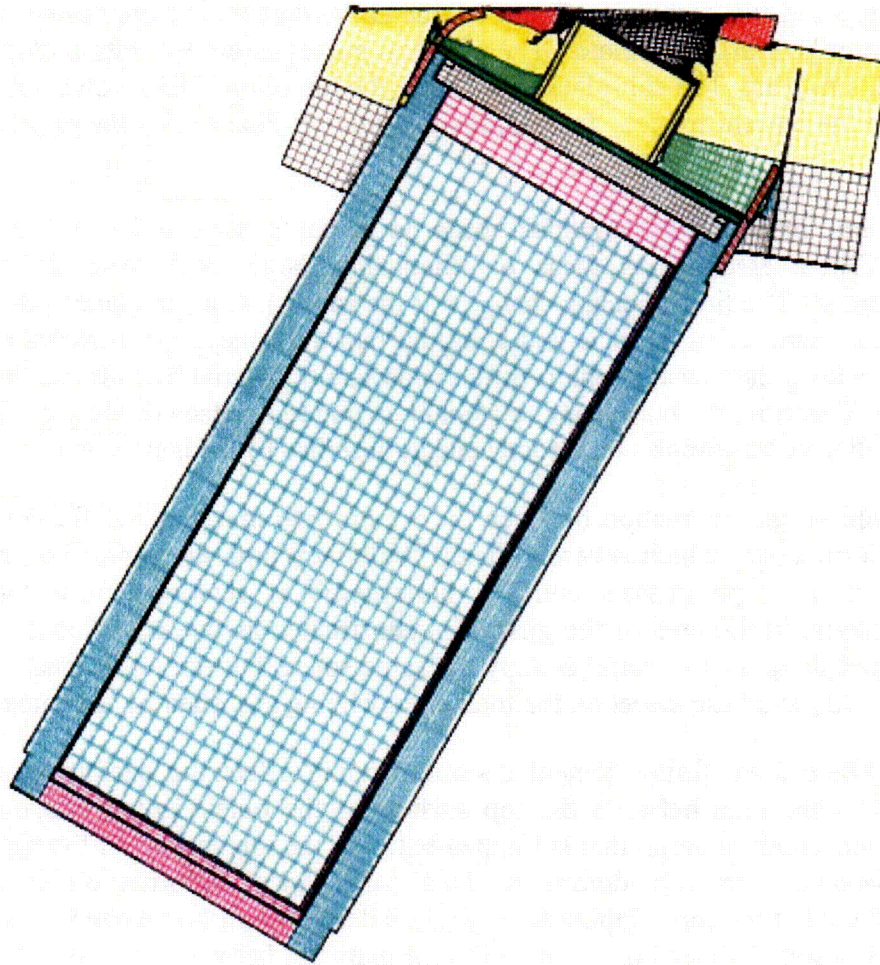


**Figure 20. HI-STAR impact limiter after 60 mph CG-over-corner impact onto a rigid target.**

The detailed model calculates a softer impact than the homogeneous model used in the initial calculations. This is a result of changes in the internal geometry of the impact limiter and the use of lower crush strength honeycomb materials in the detailed model. The jump to a peak acceleration of 55 Gs at forty milliseconds is due to the contact between the structural pipe and the rigid surface. As noted above, this is below the cask design level and resulted in no plastic deformation in the closure bolts or the cask body.

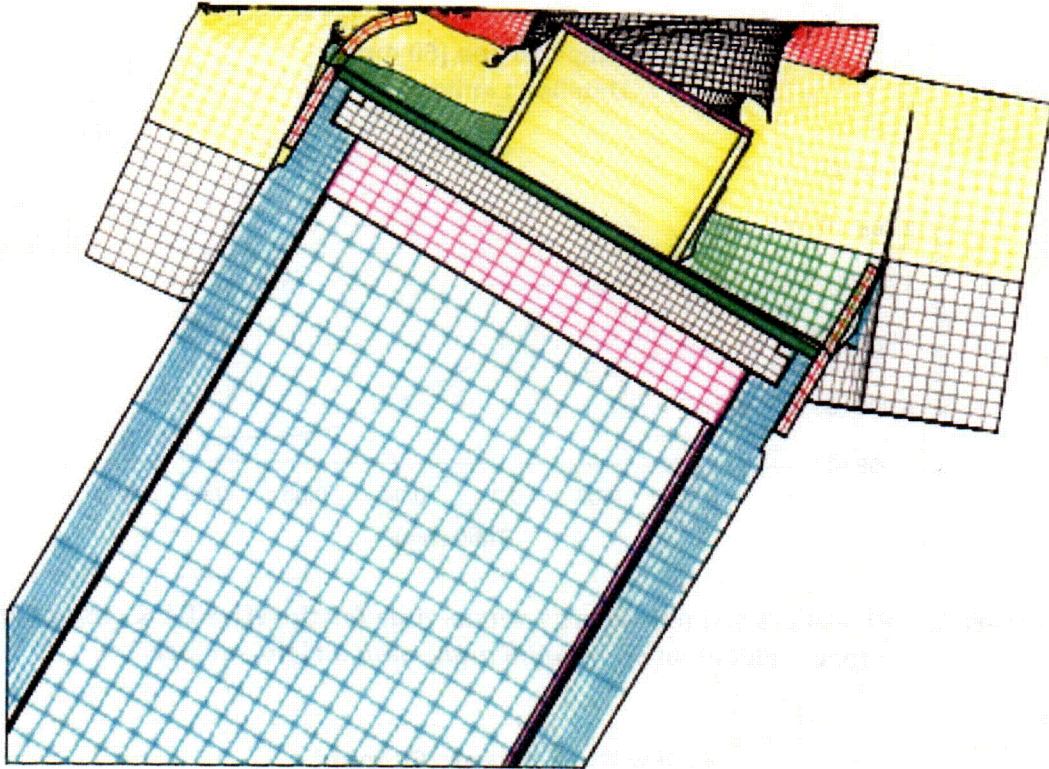


Figure 21. Detail of the damage depicted in Figure 20.

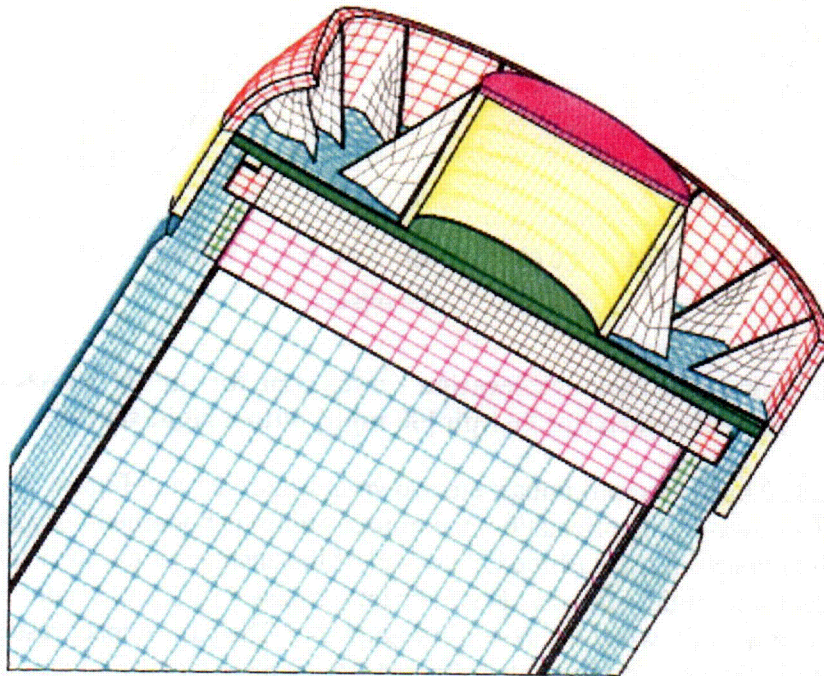
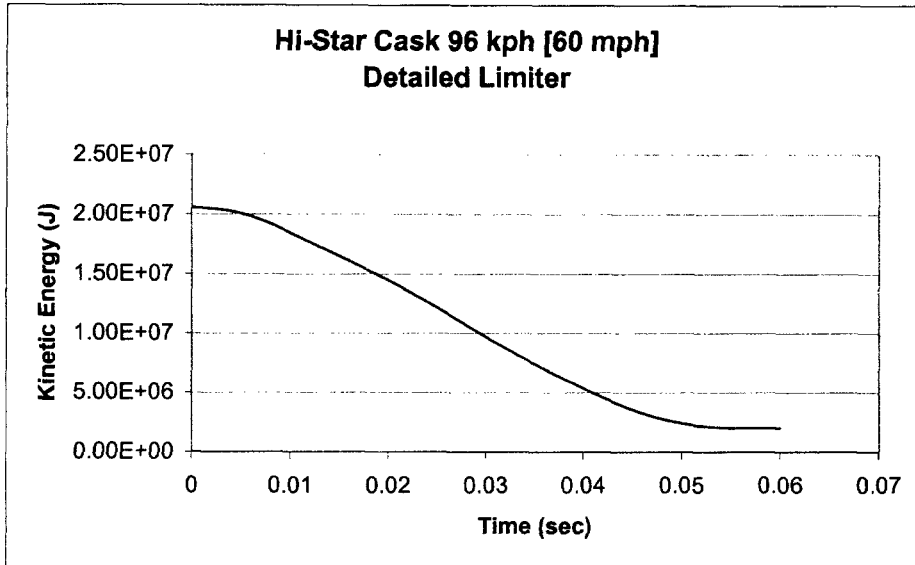
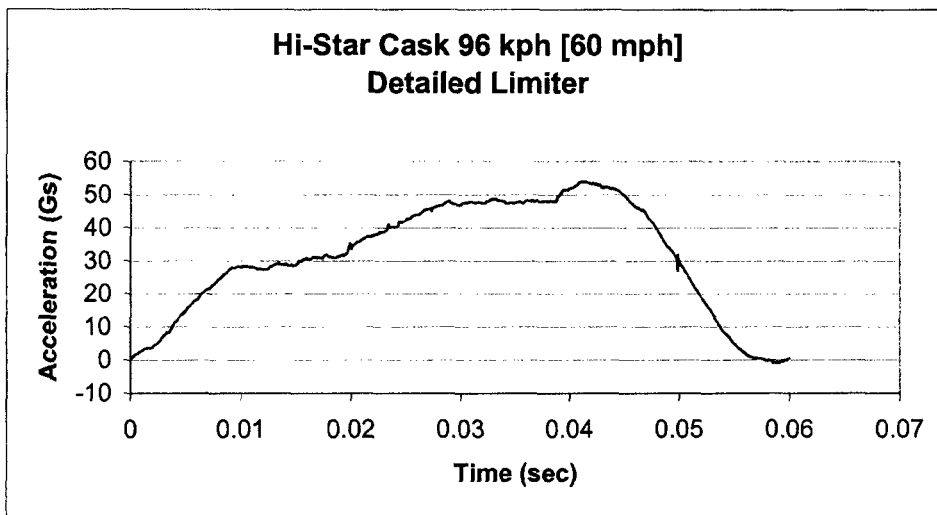


Figure 22. HI-STAR cask assembly after 96 kph [60 mph] CG-over-corner impact onto a rigid target, with foam material removed to show inner structure of impact limiter.



**Figure 23. Plot of cask kinetic energy versus time for the HI-STAR cask at an impact velocity of 96 kph [60 mph] onto a rigid surface.**



**Figure 24. Plot of the cask acceleration versus time for the HI-STAR cask at an impact velocity of 96 kph [60 mph] onto a rigid surface.**

The results of the 120 kph [75 mph] impact are shown in Figure 25 and Figure 26. At this velocity, for a cask in the CG-over-corner orientation, the impact limiter is bottomed-out against the corner of the cask body. The impact limiter absorbed almost all of the energy but the steel substructure and the cask side impacted the rigid surface. This impact produced a very small amount of plastic deformation in the cask wall, which is shown in Figure 27. The cask impact results in a peak value for the equivalent plastic strain on the order of about 4%, while a significant area experienced stains of about 1%. However, neither the cask body nor the bolts experienced strains high enough to indicate material failure. Therefore, it is expected that there will be no seal leakage.

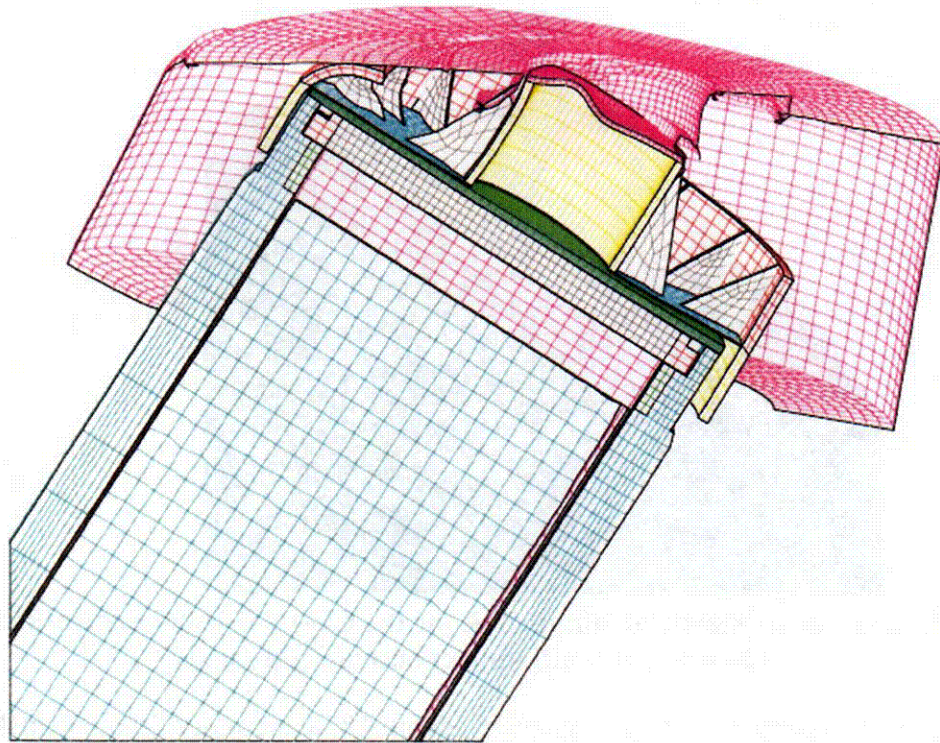


**Figure 25. HI-STAR impact limiter assembly after 120 kph [75 mph] CG-over-corner impact onto a rigid target.**

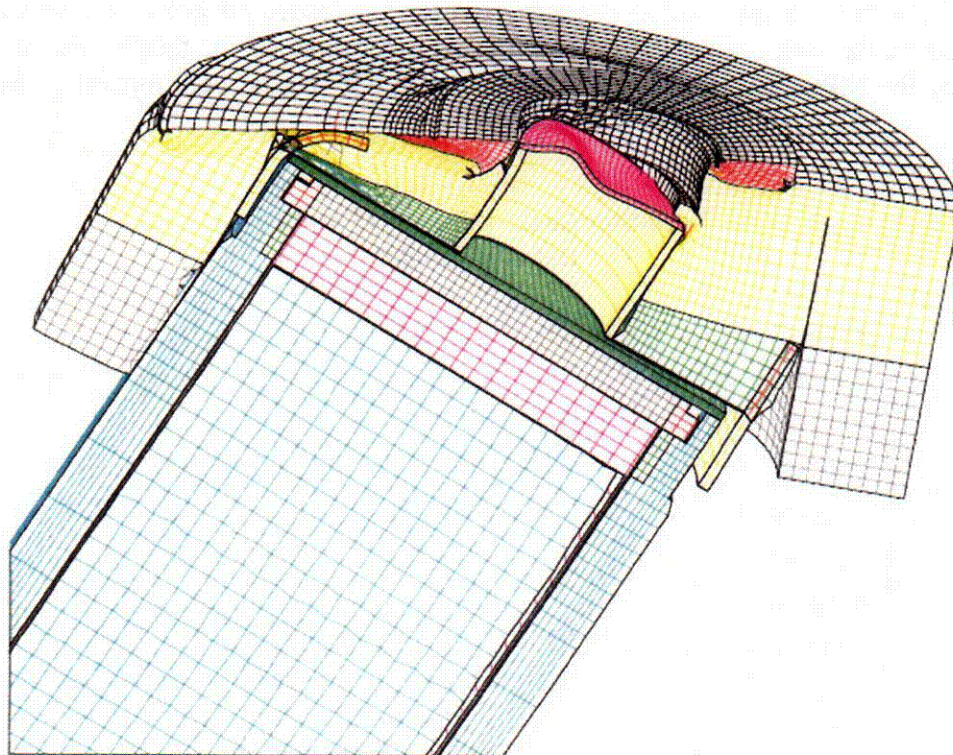


**Figure 26. HI-STAR impact limiter assembly after 120 kph [75 mph] CG-over-corner impact onto a rigid target, with honeycomb material removed to show inner structure of the impact limiter.**



**Figure 27. Equivalent Plastic Strain in cask for the CG-over-corner orientation after a 120 kph [75 mph] impact onto a rigid target.**

A plot of the kinetic energy with time is given in Figure 28, and a plot of the nominal acceleration versus time is presented in Figure 29. The peak acceleration of 103 Gs represents the maximum load experience by the cask. Although this is above the design level for the closure lid, the force of impact is transferred through the impact limiter and across the closure lid surface. During the early stage of the impact, very little of the loading is transferred to the closure lid bolts. However, during the rebounding phase the cask closure lid and the impact limiter separate and the closure lid and the bolts are loaded by the MPC. The rebounding load produces only elastic deformation in the closure lid bolts.

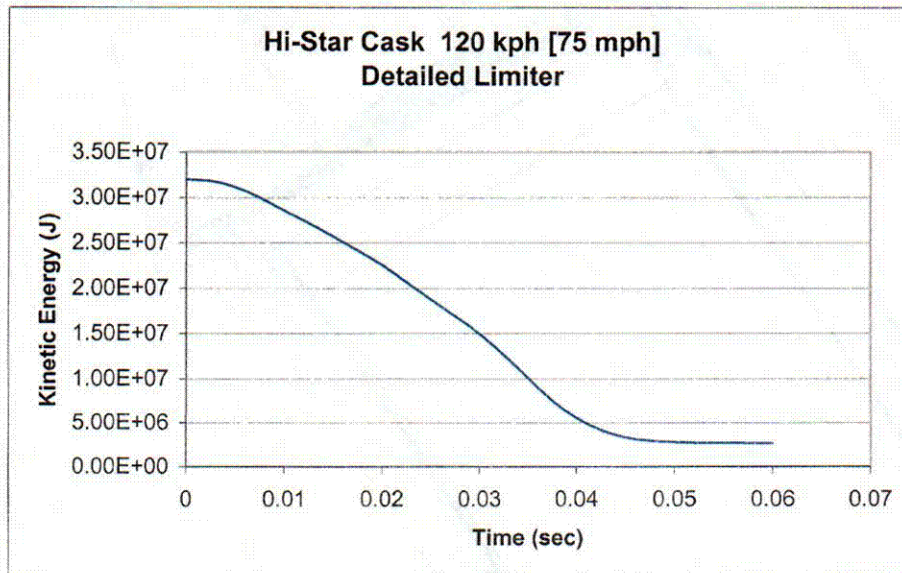


**Figure 28. Plot of cask kinetic energy versus time for the HI-STAR cask at an impact velocity of 120 kph [75 mph] onto a rigid surface.**

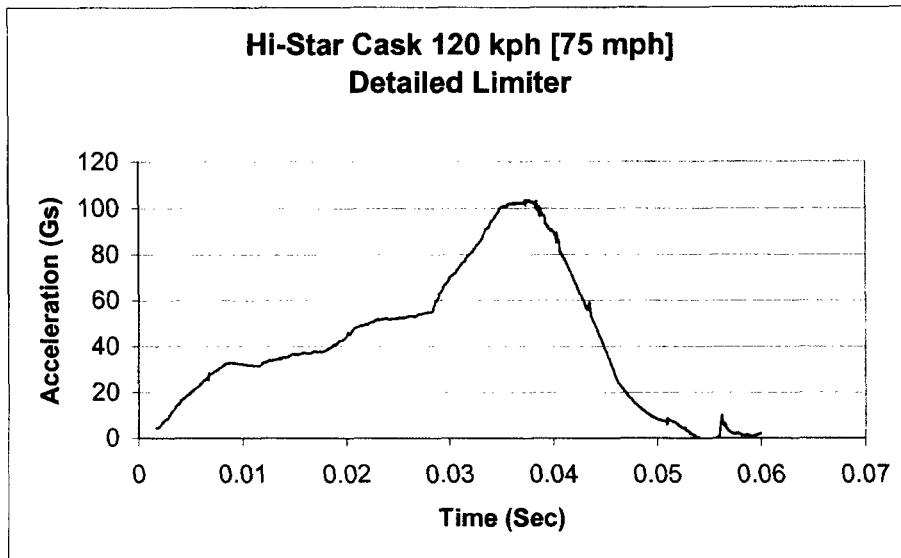


**Figure 29. Plot of the cask acceleration versus time for the HI-STAR cask at an impact velocity of 120 kph [75 mph] onto a rigid surface.**

2.4.5 Description of GA-4 truck cask [obtained from the *GA-4 Legal Weight Truck Spent Fuel Shipping Cask Safety Analysis Report for Packaging* (General Atomics, 1998)]

A schematic drawing of the GA-4 cask is presented in Figure 30. The cask is approximately 4.6 m [15 feet] long and has a square cross section, approximately 1.06 m [27 in] by 1.06 m [27 in]. The cask has a layered wall construction consisting of stainless steel-depleted uranium-stainless steel, with a total thickness of 114.3 mm [4.5 in]. The stainless steel material is ASME SA-182 Grade XM-19 and the depleted uranium is a cask material with less than 0.2% U235 by weight. The outer shell forms the containment boundary and is constructed from a 38.1 mm [1.5 in] thick stainless steel plate. The sandwiched section of Depleted Uranium (DU) is constructed from cast rectangular tube segments. Five overlapping DU segments are used along the length of the cask. The inner shell section is also made from stainless steel plate and forms the outer boundary of the fuel assembly support structure. The cask is sealed by a 279.4 mm [11 in] thick stainless steel closure lid, which is secured with twelve 25.4 mm [1 in] diameter closure bolts. The bolt material is ASME SB-637 alloy N07718.

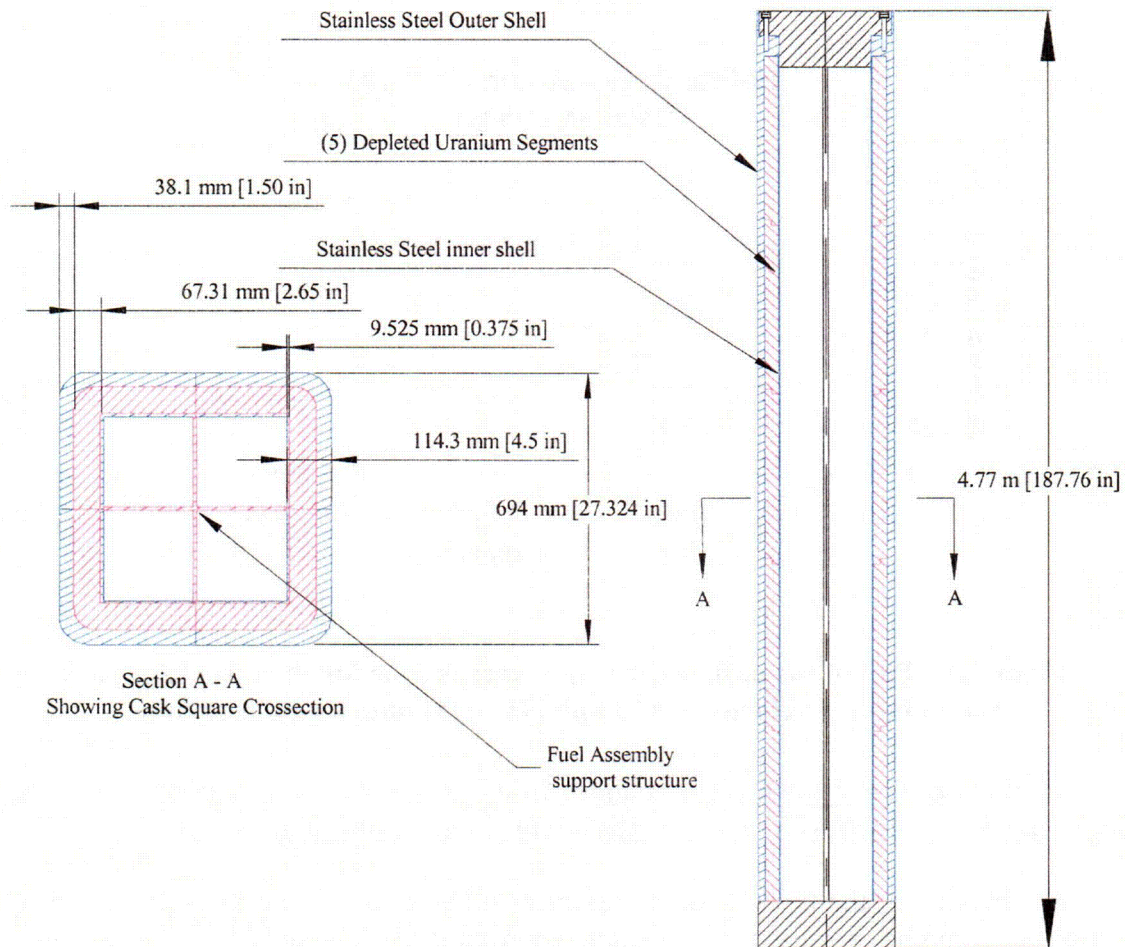


**Figure 30. Schematic drawing of GA-4 cask body.**

The GA-4 cask body is wrapped in a thin stainless steel structure used to form the neutron shield assembly (not shown in Figure 30). The assembly provides a cavity for the neutron absorbing material and it also provides a support structure near the ends of the cask for attaching the impact limiters (also not shown in Figure 30). The proposed impact orientation of the GA-4 cask is the “back-breaker” orientation, shown in Figure 31. This is an impact of the cask side against a small rigid surface (cylindrical) between the impact limiters. In this impact scenario, the impact limiters absorb no kinetic energy; their mass actually adds energy that must be absorbed by the cask body. In addition, the structural rigidity of the neutron shield assembly in the center of the cask is very small and will have a negligible effect on the response of the cask. Therefore, the neutron shield structure and the impact limiter structures will not be explicitly modeled in this finite element analysis.

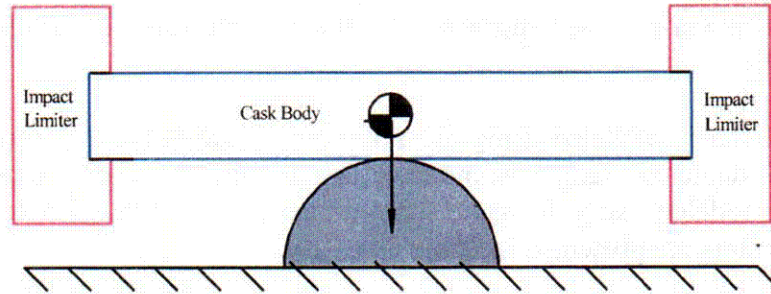


**Figure 31 Back-breaker cask orientation.**

#### 2.4.6 Finite element model

The finite element model developed for the GA-4 cask is shown in Figure 32. The model consists of the cask body, the contents, cask bottom, closure lid, and the impacting cylinder. The model contains 97,603 elements with a total of 127,465 nodes. A plane of symmetry is assumed along the center axis of the cask.

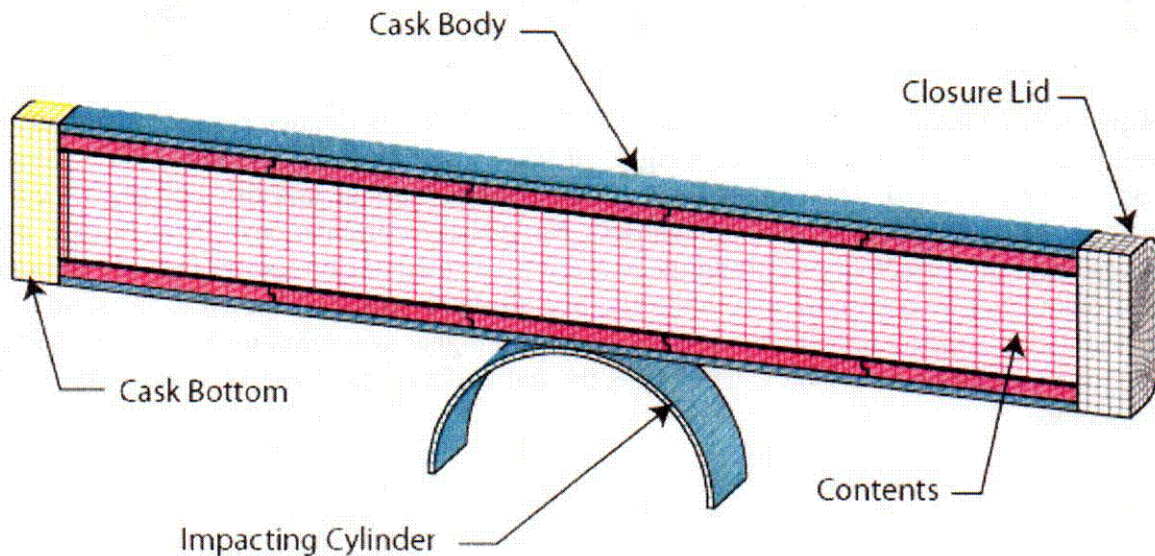


**Figure 32. Finite element model of GA-4 cask.**

The cask body is modeled as a composite structure consisting of the outer stainless steel shell, the DU segments and the inner stainless steel shell. The nominal manufacturing clearance between each of the wall components is included in the finite element model. A Coulomb friction model is used to model the interaction between the three wall components. Since the ends of the cask are not loaded during the back-breaker impact, the closure lid assembly is modeled as one solid block. There are no geometric details (such as a center plug and flange) and the retaining bolts are not modeled. The closure lid and cask bottom are attached to the cask body using "tied surfaces". As noted above, the neutron shield assembly and the impact limiters are not modeled explicitly. The mass of the impact limiters is added to the closure lid plate and

the bottom plate. The mass of the neutron shield structure and filler material is added to the mass of the cask contents.

The stainless material is modeled using the same power law-hardening model as described in Section 2.4.2. The depleted uranium is modeled using a bi-linear elastic plastic material model. The contents are modeled using the same foam model as in the HI-STAR cask. Values of the constitutive parameters are presented in Table 5.

**Table 5. GA-4 cask body constitutive model parameters.**

Component	Material Model	E GPa (ksi)	$\nu$	$\sigma_y$ or $\sigma_p$ GPa (ksi)	A or $E_p$ GPa (ksi)	N
Closure lid	Power-law Hardening	193.1 (28,000)	0.27	379.2 (55)	1.34 (193)	0.748190
Cask outer and inner shell	Power-law Hardening	193.1 (28,000)	0.27	379.5 (55)	1.34 (193)	0.748190
Depleted Uranium	Elastic-plastic	193.1 (28,000)	0.30	137.3 (20)	1.03 (150)	

The rigid, semi-cylindrical contact surface is 1.22 m [4 ft] in diameter and constructed of hexahedral elements. It is modeled as a rigid surface by setting all of the nodal displacement components equal to zero. The contact between the cylinder surface and the side of the cask is assumed to be frictionless. Figure 33 shows two possible orientations for a square cask contacting the rigid surface; it can hit on the corner of the square or on the flat face. Preliminary analyses of the GA-4 cask show that while the overall deformation of the cask are similar for either orientation, impacting the flat surface produces higher acceleration and greater plastic strains in the containment boundary. Therefore, the flat surface impact orientation is used in the GA-4 analyses.

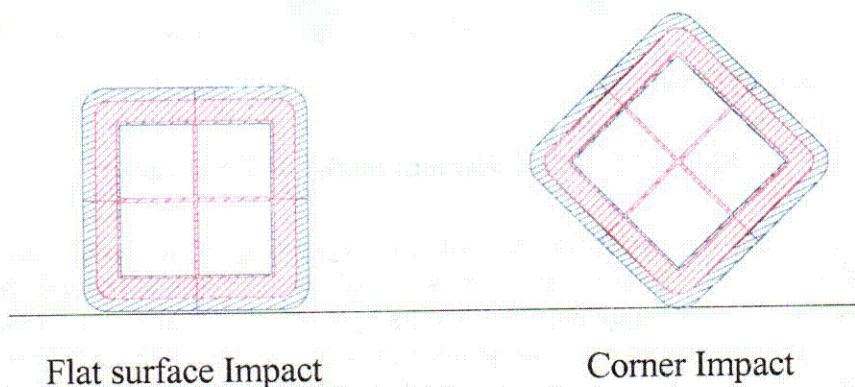


**Figure 33. GA-4 cask impact orientations.**

#### 2.4.7 GA-4 PRONTO-3D Finite Element Results

PRONTO-3D analyses were conducted for the GA-4 cask impacting a rigid semi-cylinder at 96 kph [60 mph] and 120 kph [75 mph]. The impact point was the flat surface of the cask face at the center of the cask body. The overall deformation of the cask body for a 96 kph [60 mph] impact is shown in Figure 34. The displacement of the cask ends is significant. They rotate about the cask center through an angle of approximately 10 degrees. However, all of the plastic deformation is localized in the center section of the cask and there is no plastic deformation at the ends of the cask. A gap is formed between the depleted uranium segments due to the bending of the cask body. The maximum gap is approximately 25.4 mm [1 in] and is opposite the point of impact. A section view, taken through the center of the cask is presented in Figure 35. This gives a detailed view of the local deformation of the inner shell, the depleted uranium, and the outer shell at the point of impact.

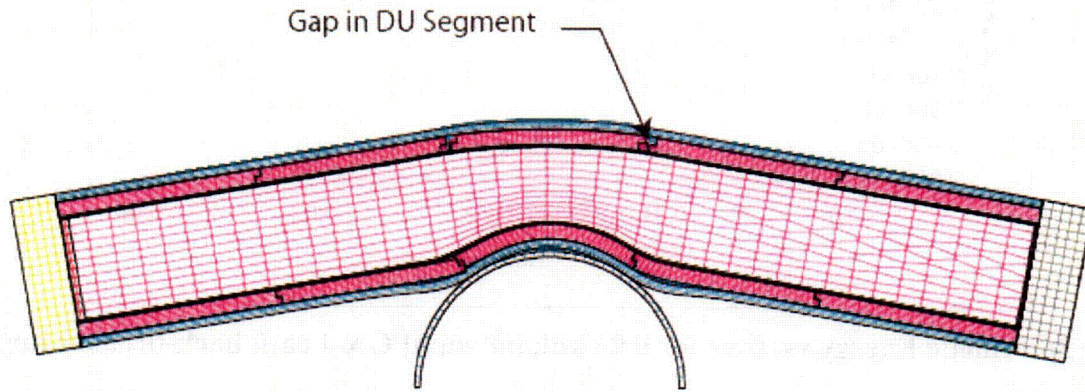


Figure 34. GA-4 cask after 96 kph [60 mph] back-breaker impact.

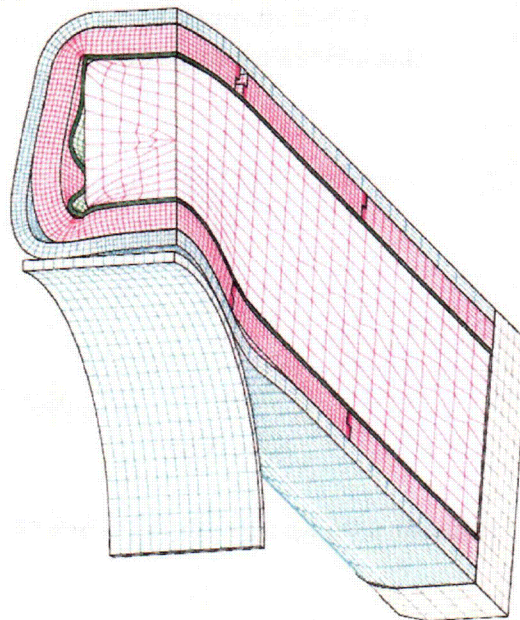


Figure 35. Section view of the GA-4 Cask after a 96 kph [60 mph] back-breaker impact.

A plot of the kinetic energy with time is given in Figure 36, and a plot of the nominal acceleration versus time is presented in Figure 37. The cask body is an efficient energy absorber. While the peak acceleration is about 130 g's, the acceleration curve is very flat with a sustained value of 105 Gs for the duration of the impact. After 27 milliseconds the cask rebounds slightly from the rigid target.

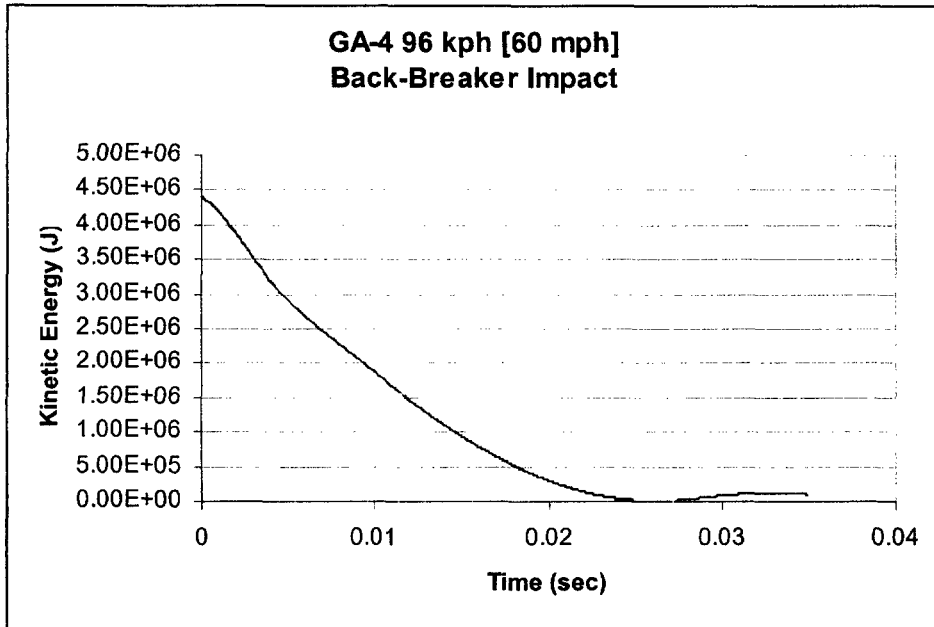


Figure 36. Kinetic Energy vs. time for a 96 kph [60 mph] GA-4 cask back-breaker impact.

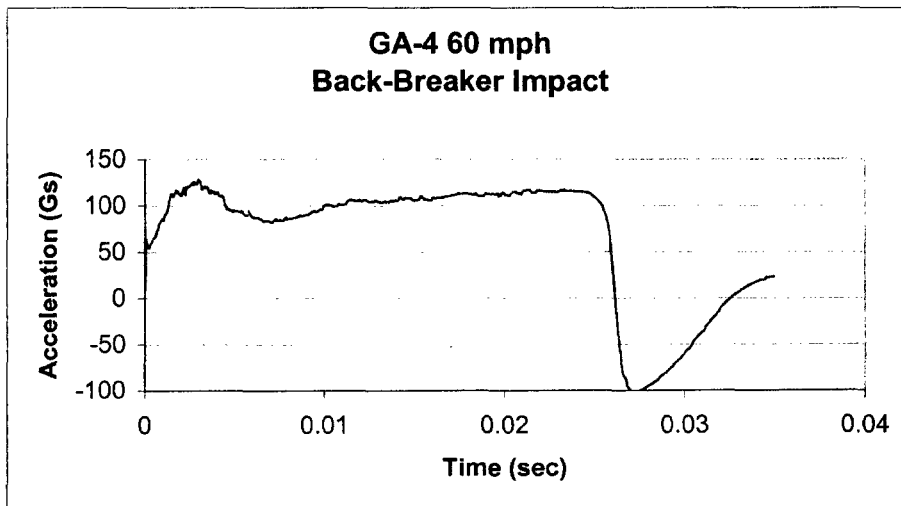


Figure 37. Acceleration vs time for a 96 kph [60 mph] GA-4 cask back-breaker impact.

Figure 38 shows the equivalent plastic strain in the outer shell, which forms the containment boundary. The maximum value of 32% occurs on the inside surface of the wall and is a compressive strain. The maximum tensile plastic strain in the outside wall has a magnitude of approximately 20%. These values are below the failure level of the material.



**Figure 38. Section view of the GA-4 Cask after a 96 kph [60 mph] back-break impact showing equivalent plastic strain in containment boundary.**

The equivalent plastic strain in the depleted uranium is presented in Figure 39. This shows compressive strains on the inside surface of the DU of approximately 50% and tensile strains on the outside surface of approximately 24%. Cast depleted uranium is a relatively brittle material with tensile strain of 6%-10% at failure; the model predicted the large strains because the current constitutive model does not contain a fracture failure criterion. Fracture of the DU material will probably occur well before a 25% tensile strain is reached. A failure model will be incorporated when the detailed analysis is done for the final test plan. However, to estimate the effect fractured DU would have on the response of the cask using the current material model, a second analysis was run in which the struck DU segments were each modeled as three pieces to capture the effect of fracturing. A model of a fractured segment showing the three pieces is illustrated in Figure 40.



**Figure 39. Section view of the GA-4 Cask after a 96 kph [60 mph] back-break impact showing equivalent plastic strain in the depleted uranium.**

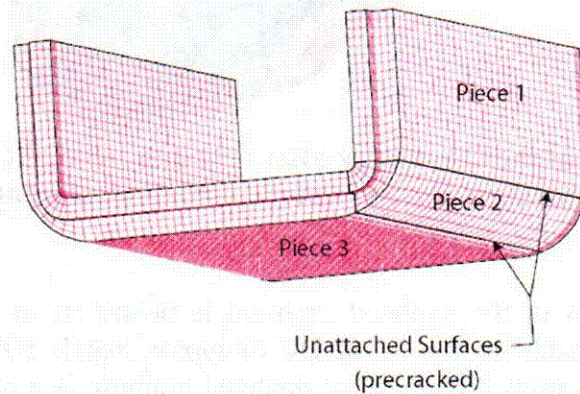


**Figure 40. Depleted Uranium segment modeled as three separate pieces to simulate the effect of fracturing.**

Figure 41 shows the result of an analysis for a 96 kph [60 mph] back-breaker impact in which the center three DU segments were modeled as fractured. The overall deflection is similar to the previous run without the fracturing. A section through the plane of impact is presented in Figure 42 to show the response of the middle fractured DU segment.

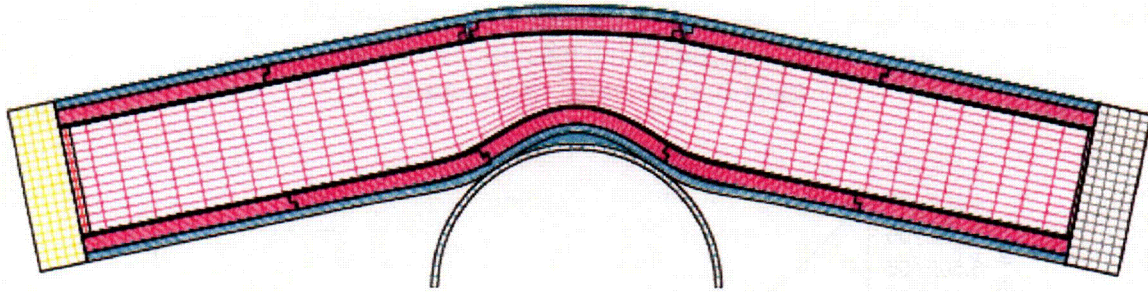


**Figure 41. GA-4 cask after 96 kph [60] mph back-breaker impact, modeled with fractured DU segments.**

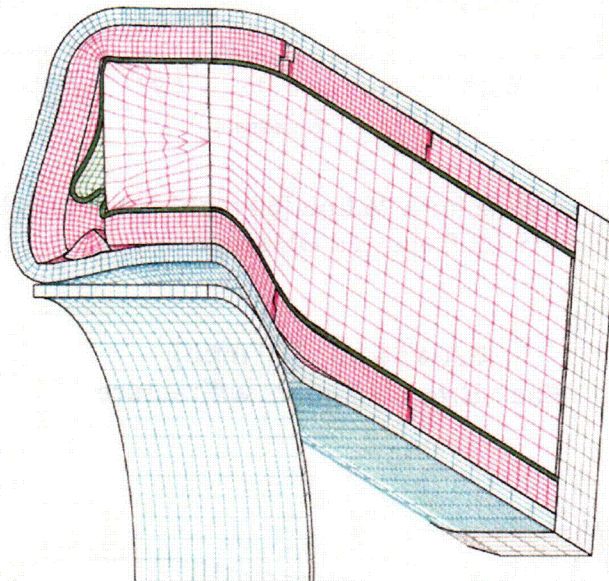


**Figure 42. Section view of GA-4 cask through the plane of impact, after 96 kph [60 mph] back-breaker impact, modeled with fractured DU segments.**

A plot of the kinetic energy and acceleration versus time are shown in Figure 43 and Figure 44. These curves are very similar to the model without the fractured DU. The fractured DU appears to have very little effect on the energy absorbing ability of the cask.

Figure 45 shows the equivalent plastic strain in the outer containment boundary. The maximum compressive and tensile strains are about 3% higher than they were in the analysis without the fractured DU segments. These values are also below the failure level for the material.

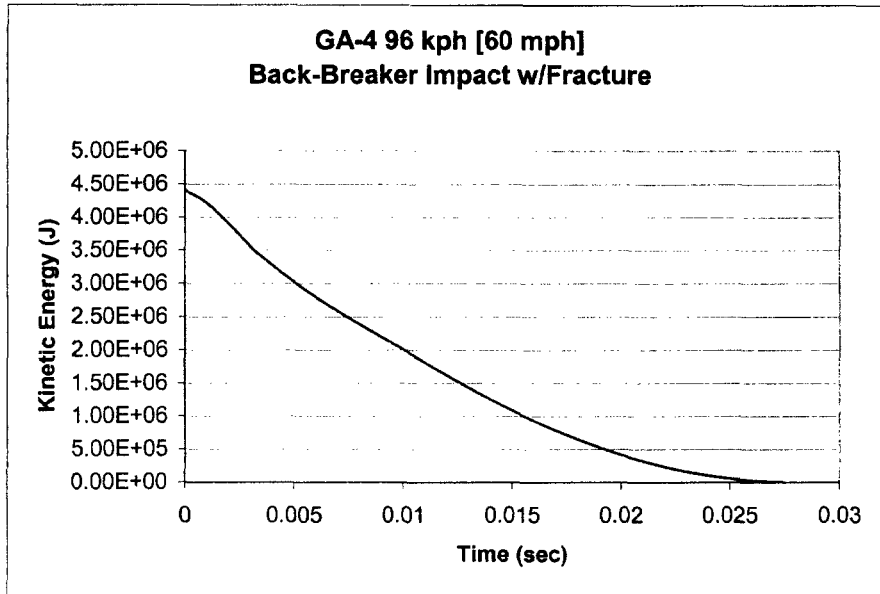


**Figure 43. Kinetic Energy vs. time for a 96 kph [60 mph] GA-4 cask back-breaker impact with fractured DU segments.**

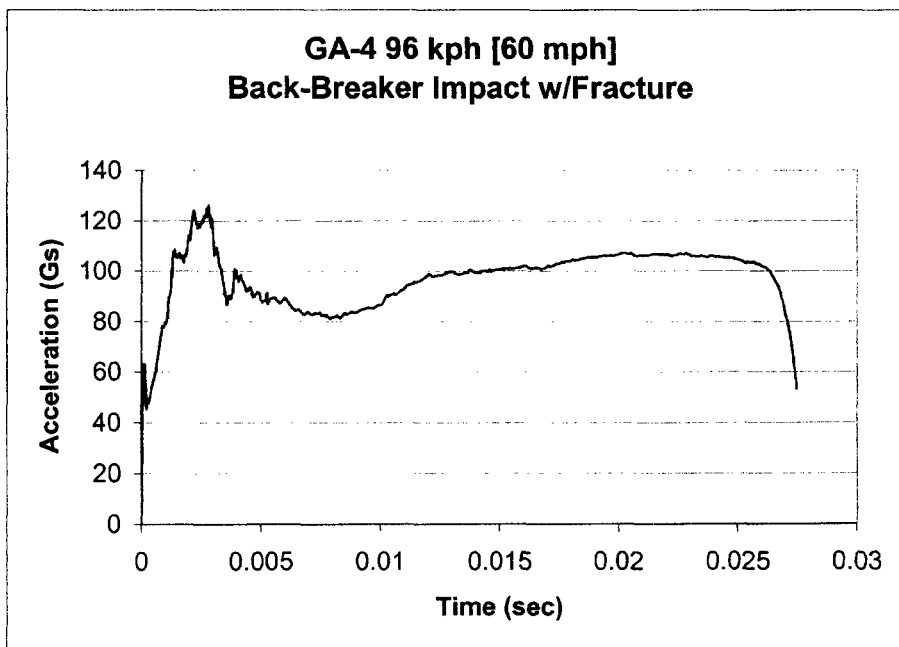


**Figure 44. Acceleration vs time for a 96 kph [60 mph] GA-4 cask back-breaker impact with fractured DU segments.**



**Figure 45. Section view of the GA-4 Cask after a 96 kph [60 mph] back-break impact showing equivalent plastic strain in containment boundary, modeled with fractured DU segments.**

The results of a 120 kph [75 mph] back-breaker impact are presented in Figure 46. The deformation of the cask is significantly larger than the 96 kph [60 mph] back-breaker impact. The cask ends rotate though and angle of approximately 20 degrees and the maximum gap in the DU segments is about 51 mm [2.5 in].

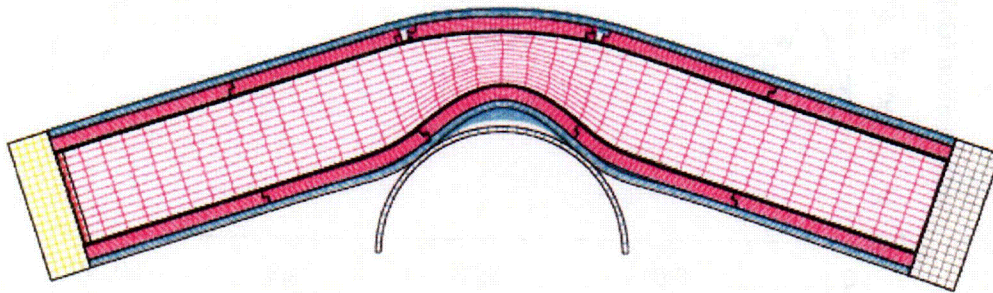


**Figure 46. GA-4 cask after a 120 kph [75 mph] back-breaker impact, modeled with fractured DU segments.**

Plots of the kinetic energy and acceleration versus time are shown in Figure 47 and Figure 48. These curves show a maximum acceleration of 145 g's and a sustained acceleration of 115 Gs. The acceleration curve is very flat and square, indicating that the cask body is an efficient energy absorber.

Figure 49 shows the equivalent plastic strain in the outer shell. The maximum strain in compression is about 50%, while the maximum strain in tension is about 35%. These values are quite high and are close to the material limit of 45% tensile strain. Strains in the closure region are very low, so no leakage is expected.

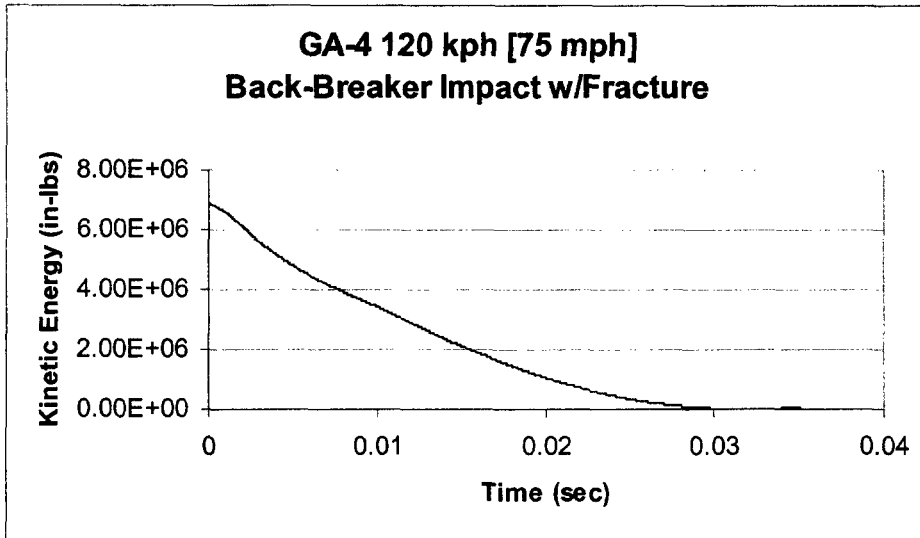


Figure 47. Kinetic Energy vs. time for a 120 kph [75 mph] GA-4 cask back-breaker impact with fractured DU segments.

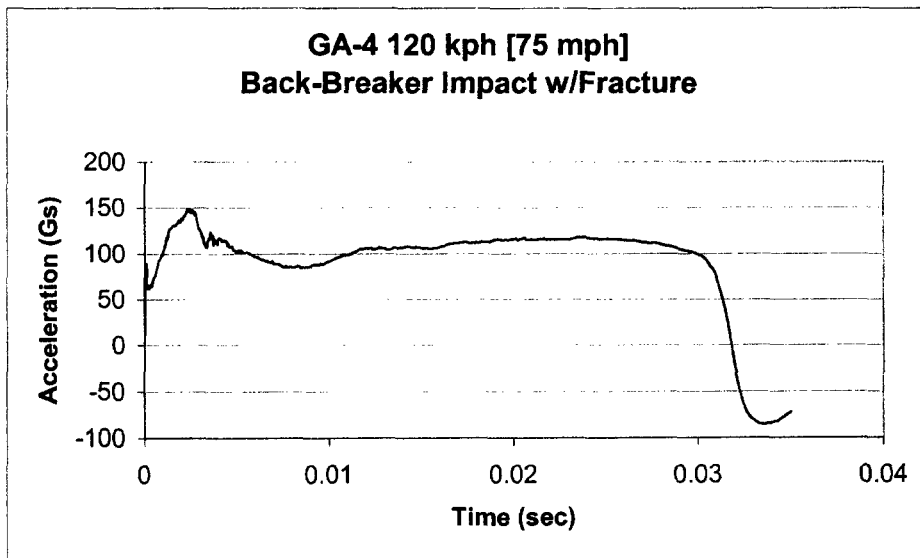
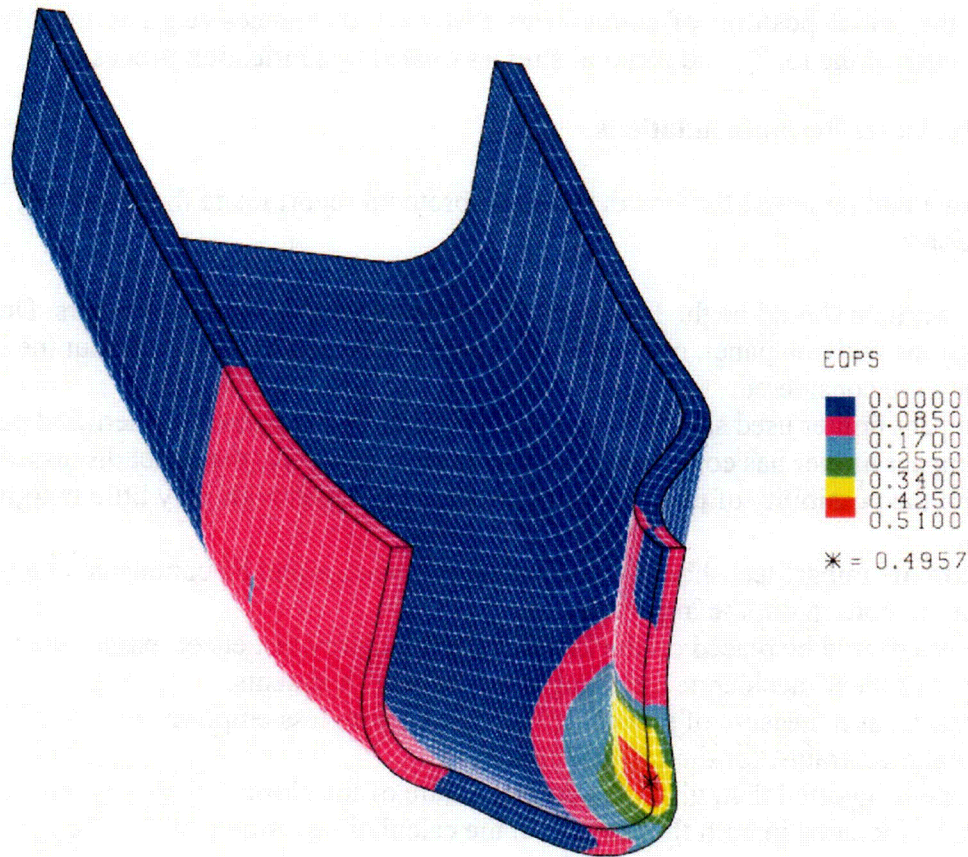


Figure 48. Acceleration vs. time for a 120 kph [75 mph] GA-4 cask back-breaker impact with fractured DU segments.



**Figure 49. Section view of the GA-4 Cask after a 120 kph [75 mph] back-break impact showing equivalent plastic strain in containment boundary, modeled with fractured DU segments.**

## 2.5 Limitations of Analyses

The finite element analyses discussed in the previous section are preliminary scoping calculations conducted to determine if using the HI-STAR 100 cask and the GA-4 cask as test articles can meet the objectives of the PPS, and to determine impact orientation and approximate impact velocity. They are not intended to be pre-test predictions of the cask response. During the preparation of the detailed test plan more rigorous finite element analyses will be performed. These analyses will model the anisotropic nature of the honeycomb impact limiter; the detail of the basket and surrogate fuel assemblies (a detailed analysis of the mock-up fuel assembly will not be included in the overall finite element model, but this component will be studied individually); the layered construction of the cask wall; and more detail within the closure. For the closure bolts the detailed finite element analysis will include more elements in the circular cross-section of the bolt (rather than treating it as a single square element), and the preload caused by the tightening torque.

When the detailed models are finished, they will be used to conduct uncertainty studies to determine the effect that parameters that are not well known have on the predicted result. Examples of parameters that may be investigated are: the tolerances between individual components, coefficient of friction between components; material properties (especially of the

honeycomb), the initial position of components that have clearances (e.g., is the MPC at the bottom of the cask or the top?); and residual stresses caused by fabrication processes.

## **2.6 Structural Panel Recommendations**

The expert panel that reviewed the first draft of this protocol report made the following recommendations:

1. The test article should be the Holtec HI-STAR 100 cask with impact limiters. During the discussions with the panel, options for using other casks and testing without the impact limiter were considered.
2. The impact limiter used should be the actual limiter that is part of the certified package. This impact limiter has considerable design margin of safety; the panel discussed and rejected the possibility of using a limiter that was designed with very little margin of safety.
3. The extreme impact test should focus on closure damage and be conducted at a sufficient velocity to bottom out the impact limiter.
4. Emphasis should be placed on the fact that the regulatory test encompasses the vast majority of “real” accidents, including most “severe” accidents.
5. Emphasize, as a measure of success, deformation, with less emphasis on decelerations/strains, for the extreme impact test.
6. The panel suggested that, given the critical nature of the closure modeling, bolt preload should be included in both the test and in the calculations using coupled analytical techniques.
7. The panel suggested that the contents be included in the model of the extreme impact, with quality post-test measurements of damage, including permanent deformation and leak testing of the MPC.
8. The panel suggested conducting a 9-meter CG-over-corner regulatory drop test prior to conducting the extreme impact test.

These recommendations have been incorporated into this document, or will be incorporated into the detailed test plans when they are prepared.

## **2.7 Impact Test Protocol**

Based upon the discussions and preliminary analyses above, the plan for the impact test portion of the Package Performance Study is to conduct a full-scale CG-over-corner drop of the Holtec HI-STAR 100 cask, including an impact limiter on the end of the cask being impacted, and an MPC-24 canister. The free drop impact velocity will be between 96 kph [60 mph] and 144 kph [90 mph] onto a flat, essentially rigid, horizontal target. The drop will be documented with real-time broadcast quality video, real-time regular video, high-speed video, and high-speed film. At a minimum, cameras will be located to provide orthogonal views of the impact.

Accelerometers will be mounted on the cask sidewall, the cask lid, and the MPC lid. These gages will provide information on the inertial loads experienced by the cask body overall and on the impact between the MPC and cask lid. Deformations of the impact limiter will be compared to the deformations predicted by pretest finite element calculations. Strain gage bolts and

displacement gages will be used to characterize the response of the cask closure. The output of these gages will also be compared with the pretest finite element predictions.

Strain gages in the closure weld region of the MPC will be used to determine if the pretest finite element analysis is accurately predicting the response of the canister in the weld region. The instrumentation leads from these gages will have to pass through the lid of the cask, making pressurization of the interior volume of the cask very difficult. Because the cask cannot be pressurized and because there is no direct way to calculate drop in pressure from the finite element analysis, the pressure between the MPC and the cask will not be monitored during the test.

In addition, a full-scale back-breaker test of the GA-4 cask will be conducted with a flat side of the nominally square cask impacting the target. The free drop impact velocity will be between 96 and 144 kph [60 and 90 mph] onto a semi-cylindrical rigid target that is welded to the top surface of the essentially rigid target used for the HI-STAR 100 cask test. The drop will be documented with real-time broadcast quality video, real-time regular video, high-speed video, and high-speed film. At a minimum, cameras will be located to provide orthogonal views of the impact.

Accelerometers will be mounted on each end of the cask and near the center of the cask on the top and side surfaces. Strain gages will be mounted on the upper surface of the cask (a hole will be cut through the neutron shield). The large deformations experienced by the cask will be easy to compare with the pre-test predictions (both the bending of the cask and the change in cross-section in the impact area). The leak tightness of the cask will be measured after the test. Because there is no anticipated deformation in the closure region, there will not be strain gage bolts or displacement gages for this test.

A detailed description of measures of success in the comparison between test and analysis results will be part of the Test Plan that will be prepared after these Test Protocols have been approved. The accuracy of the correlations will be given with each measurement that will be made. For example, a predicted elastic strain on the lid of the MPC may be  $420 \mu\epsilon \pm 50 \mu\epsilon$ ; a predicted peak acceleration on the cask wall may be  $8400 \text{ Gs} \pm 1000 \text{ Gs}$ ; a predicted force in a closure bolt may be  $890,000 \pm 89,000 \text{ N}$  [ $200,000 \text{ lb} \pm 20,000 \text{ lb}$ ], and a predicted crush distance in the impact limiter may be  $940 \pm 50 \text{ mm}$  [ $37 \text{ in} \pm 2 \text{ in}$ ]. In developing the correlations, the results of the uncertainty study and accuracy of measurement types will be considered. For the analysis and test results to be in good comparison, it is not necessary for all measurements to be within the uncertainty range.

When physically testing a package to the regulatory hypothetical accident conditions is conducted to support certification, measurement of the leak rate of the containment boundary is an important component. For the HI-STAR 100 cask, the containment boundary includes the closure seal and no credit is taken for the containment provided by the welded MPC. In risk analyses the protection provided by all barriers to release is considered. For the HI-STAR 100 cask, the barriers to release are the spent fuel itself, the welded MPC, and the cask body. The PPS will examine each of these barriers. The analyses performed as part of this report concentrated on the response of the cask body. The detailed test plan will include more detailed finite element analysis of the MPC. The response of the fuel is also being studied as part of the PPS.

Sensitivity of the finite element analysis results to the response of features that are too small to model will necessitate component tests for these features. Three candidates for component testing are the honeycomb impact limiter material, the closure bolts, and the surrogate fuel assembly. To develop an accurate finite element material model for the honeycomb impact limiter material requires the crush behavior in each of the three orthogonal directions of the material to be known. The way this behavior varies as a function of loading rate and sample size will be determined experimentally.

Bolt threads are expected to significantly affect the stress distribution in the bolt, which determines its response to impact loads. Modeling bolt threads in the finite element model of the rail cask would require a very large model. Component testing of the bolts can develop the data needed to allow the finite element model to correctly incorporate the effect of bolt threads. The effect of threads on bolt response will be examined experimentally in single bolt tests. These test results will be modeled, and then the modeling results will be used to adjust the cask finite element model to reflect the effect of bolt threads.

The complex structure of a fuel assembly also would require use of very small elements in the cask finite element model. Therefore, a fuel assembly not contained in a canister or a cask will be impacted onto an unyielding target. This will allow the collapse of the assembly to be recorded photographically. Modeling of these test results will then allow an approximate representation of an assembly to be developed that captures the response of a real assembly to impact loads. These tests will support both the determination of the cask response, because the fuel assembly provides loading to the cask, and the determination of fuel response, because it will show the distribution of forces within the fuel assembly and loading onto the individual fuel rods.

This page intentionally left blank

### **3.0 FIRE TESTS**

A coordinated program that will compare computer fire simulations to fire tests is planned to assure that the parameter values used in the CAFE fire model accurately predict the thermal performance of casks in large, long-duration fires. The behavior of casks in fires that last longer than the regulatory fire test will be assessed. The durations of fully engulfing optically dense fires that are required to cause seal failure or failure of spent fuel rods by burst rupture will be estimated. Instrumentation will be designed to assure that fire conditions are accurately measured. First, a calorimeter with dimensions similar to a spent fuel rail cask will be tested to confirm and enhance current fire modeling techniques. Next, an actual rail cask fire test will be performed to demonstrate both the accuracy of the fire predictions and the behavior of a cask when subjected to extreme fires. Finally, a real truck cask fire test will be performed to confirm the method used to predict the cask response to fires for a case where a calorimeter was not used to benchmark the heat fluxes to and from the cask.

As in the case of the impact tests of the rail and truck cask, there are a number of parameters needed for accurate predictions of the response of these casks under extreme thermal accident conditions. To obtain these needed parameters, it may be necessary to conduct some separate effects testing. Two examples of this need for testing are the thermal response of the rail and truck cask impact limiters and the margin-to-failure of the cask lid seal materials.

#### **3.1 Background**

For certification, packages for transporting large quantities of radioactive material (Type B packages) must be demonstrated to be capable of surviving in a well-defined hydrocarbon fire environment for 30 minutes. Risk studies use the fire exposure time that leads to the failure of package seals or the time when fuel rods burst to make an accurate assessment of accident severity. While the regulatory test provides assurance that a package provides a fire resistant shell for the package contents for 30 minutes under regulatory fire conditions, it does not indicate the margin a package has to failure when exposed to longer duration fires. The thermal studies that will be performed as part of the PPS will validate the ability to accurately calculate the time to cask and fuel rod failure for two different locations of a cask in an extreme fire:

- 1) with the cask positioned horizontally above the vapor dome (the central region of the fire immediately above the fuel pool where the air-fuel ratio does not support combustion) where the heat transfer to the cask is typically quite uniform because the cask is fully engulfed by the flame envelope, and
- 2) with the cask lying horizontally on or very near to the ground, submerged in the fire's vapor dome and in contact with the water layer that lies under the fuel pool.

Fire durations for these fire tests will be extended beyond the 30-minute requirement for the regulatory fire. Detailed computer modeling techniques will be used both to design these thermal tests and to predict by pretest calculations the expected thermal performance of the cask and its contents. For the purpose of this preliminary test protocol, the fire duration was chosen to be one hour. As demonstrated by the temperature histories shown later in this document, the temperature of the outer surface of the package started to approach the temperature of the fire. This simulation time was considered appropriate for the preliminary assessment of tests to be

conducted as well as to show the effect of package placement within the fire. It was not meant to be representative of any specific accident scenario. Nevertheless, the one-hour duration used for the calculations represents about 82% of all train fire accidents and 99% of all truck fire accidents (Fisher et al., 1987) and a fire of this duration should provide enough data for the benchmarking of the codes and/or techniques. The type of fuel being considered for the fire tests is JP-8 aviation fuel because

- it is readily available, and
- when burned, it produces flame temperatures typical of most hydrocarbon fuel fires (i.e., the heat of combustion for most hydrocarbons is nearly the same).

Comparison of these predictions to the actual thermal behavior of the cask during the test is expected to demonstrate the accuracy of fire models and increase confidence in extreme fire predictions.

### **3.2 Method**

Tests of a calorimeter the size of a rail cask, an actual rail cask, and an actual truck cask are planned as part of the PPS study. The calorimeter, an instrumented cylinder the size of a rail cask, will be designed to obtain accurate estimates of heat fluxes transmitted to/from objects within large pool fires and to develop data that can verify that computer codes can accurately predict such fire environments. The rail cask tests will demonstrate the behavior of casks under extreme fire conditions and provide information on the accuracy of predictions of cask performance. The truck cask test will confirm the method used to predict the cask response to fires for a case where a calorimeter was not used to benchmark the heat fluxes to and from the cask.

The calorimeter or the cask will be heated in a fully engulfing, optically dense, hydrocarbon fuel fire. Two calorimeter tests, two rail cask tests, and one truck cask test are proposed. For the calorimeter and rail cask one test will be performed with each test object suspended above the fire's vapor dome in the fire's flame envelope and one with each test object lying near enough to the ground so that the bottom surface of the cask has a significant loss of heat to the fuel pool and to the water layer that lies under the fuel pool. The truck cask will be tested in the regulatory position, 1-meter above the surface of the fuel. The test with the calorimeter suspended in the fire's flame envelope will measure the heat transferred to the calorimeter surface by a fully engulfing fire. The test with the calorimeter lying near the ground will determine:

- 1) the heat transfer to the calorimeter surface from the fire's vapor dome (the central region of the fire immediately above the fuel pool where the air-fuel ratio does not support combustion), and
- 2) the heat loss from the cask to the fuel pool and the water under that pool, which will simulate heat loss from the cask to the ground for accidents where the cask ends up lying on the ground in a fire.

The heat fluxes measured during these calorimeter fire tests will then be used to predict the thermal response of the rail cask, both when the cask is lying near the ground in contact with the water under the fuel pool, and when it is placed above the vapor dome of a fully engulfing fire.

The thermal performance of the rail cask during the two rail cask fire tests will be predicted by pretest finite element analysis (FEA) and computational fluids dynamics (CFD) calculations using computer codes already available at SNL. Among the codes to be used are the commercially available MSC PATRAN/Thermal (P/Thermal), the in-house Container Analysis Fire Environment (CAFE 3D) code, and the Sandia One-Dimensional Direct and Inverse Thermal (SODDIT) or equivalent code. CAFE 3D and P/Thermal are coupled to allow the simultaneous calculation of the fire environment and the modeling of heat transfer to, in, and from the cask by conduction, convection, and radiation. The CAFE-P/Thermal coupling allows more accurate simulations to be performed, bringing the computer modeling of fire scenarios closer to actual fire conditions. The one-dimensional inverse heat conduction code (e.g., SODDIT) will be used to estimate the surface heat flux of the test objects based on internal temperature measurements. By simulating the fire tests prior to performing them, the sensitivity of the simulation to the various fire parameters and the accuracy of the simulation can be evaluated by post-test comparison of the simulation to the actual test results.

The thermal performance of the truck cask will be predicted using the same set of codes. However, in this case there will not be any calorimeter test results to benchmark the heat fluxes experienced by the cask. Therefore, this test will demonstrate the ability to apply the methods used for the rail cask to other casks.

Success of the thermal program of this project will be measured by how accurately the predictions of the internal response (internal temperature histories and distributions) of the rail cask and the truck cask match the test results. A detailed description of the measures of success for both the calorimeter and the cask fire tests will be part of the detailed test plans.

### **3.3 Computer Simulations**

Computer simulations are commonly used to predict the response of objects to thermal environments. Nevertheless, computer models need to be benchmarked using test data before important decisions are made based on the results that are obtained from them. As part of this project, parameters used in the CAFE fire model will be corroborated and adjusted to generate realistic fire simulations that can be used for risk assessment studies.

#### **3.3.1 Simulation of Fires**

The thermal analyses that will support test design will be performed with the coupled CAFE-P/Thermal codes, which can simulate a scenario where a fire is unevenly heating the external surface of the cask and the heat absorbed by the cask surface is being transferred by conduction through the wall of the cask to the canister housed in the cask and to the fuel assemblies in the canister. The CAFE code (Suo-Anttila et al., 1999) has been developed to model all relevant fire physics for massive objects engulfed in large fires. It provides a realistic boundary-condition model for use in the design of radioactive material packages and in the assessment of the risks associated with fires during the transport of these packages. The CAFE code can be coupled with finite-element models of specific package designs. This coupled system can be used to determine the internal thermal response of packages engulfed in a fire to a range of fire environments. CAFE was designed to run rapidly so that it can be used on a typical desktop workstation.

### 3.3.2 Simulation of Packaging

The commercially available finite element software, MSC P/Thermal, will be used to model conduction through solid walls of the cask and convection and/or radiation from these walls to the cask atmosphere, the cask canister, and through the cask canister to its atmosphere and fuel assemblies.

### 3.3.3 Simulation of Fuel Bundles and Basket

An analysis to quantify the effect of the internal heat load to the temperature distribution within the package is planned. This will be performed once the cask under study has been accurately modeled without the internal heat load. The lumped mass method is being considered to model the fuel assemblies in the cask canister. That is, the fuel assemblies will be modeled by the P/Thermal code as a single homogenized solid mass that has material properties adjusted so that the thermal performance of this lumped mass agrees with the experimentally determined behavior (especially peak fuel rod temperatures) of real fuel assemblies (Thomas et al., 1999 and Burns et al., 1993). The lumped mass will contain a distributed internal heat source that simulates the decay heat load generated by the spent fuel in the fuel assemblies. This simulated decay heat load and the heat flux to this lumped mass from the cask canister will produce a temperature gradient across the lumped mass, which will be used to estimate the time when rods at different radial locations in the cask reach burst rupture temperatures. This will allow the timing of rod failure to be examined.

## **3.4 Preliminary Analyses**

A series of preliminary computer analyses were conducted to better understand the effect of package placement on the uniformity of the heat transfer from the fire to the cask surface. A finite-element model of the reference spent fuel rail cask, the Holtec HI-STAR 100 cask, was constructed in P/Thermal. The cask was represented by approximately 35,500 three-dimensional finite elements. This model is shown in Figure 50. Two cask boundary conditions were used in these preliminary analyses, an external boundary condition and an internal boundary condition. The external cask boundary condition was the heat flux from the fully engulfing fire to the cask exterior surfaces calculated by the CAFE code. For the purpose of this preliminary study, the interior surfaces of the cask were assumed to be perfectly insulated (no heat transfer through the wall). Note that there was no heat load applied to the internal surface of the cask (that is spent fuel decay heating was not modeled), because there would not be any heat generation inside the cask during the tests. The effect of the exclusion of the decay heat from the spent fuel rods will be lower temperatures throughout the cask at any given time. The reference spent fuel truck cask was modeled using the same assumptions mentioned above. The three-dimensional finite element model of the GA-4 truck cask consisted of approximately 88,000 elements and is shown in Figure 51. Note that the neutron shield is included for the thermal model, resulting in a round cross-section of the cask instead of the nearly square cross-section used in the impact analyses.

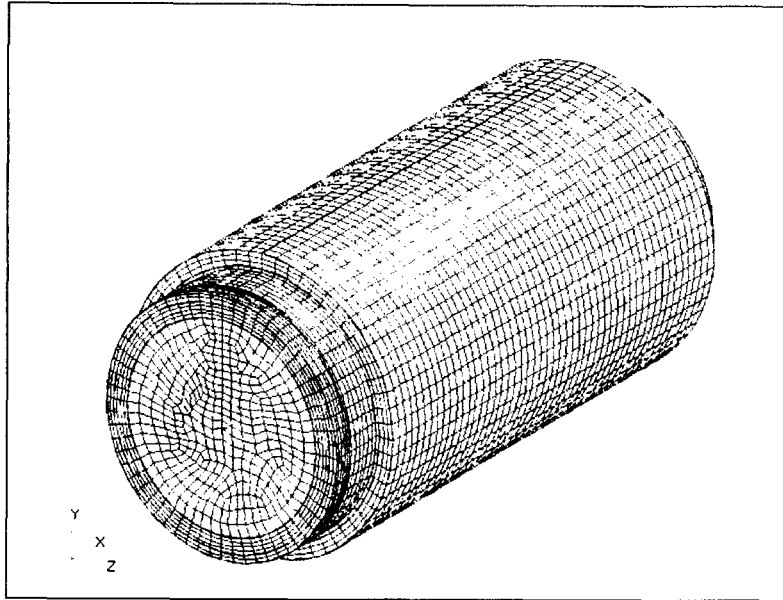


**Figure 50. Finite element model of the Holtec HI-STAR 100 rail cask.**

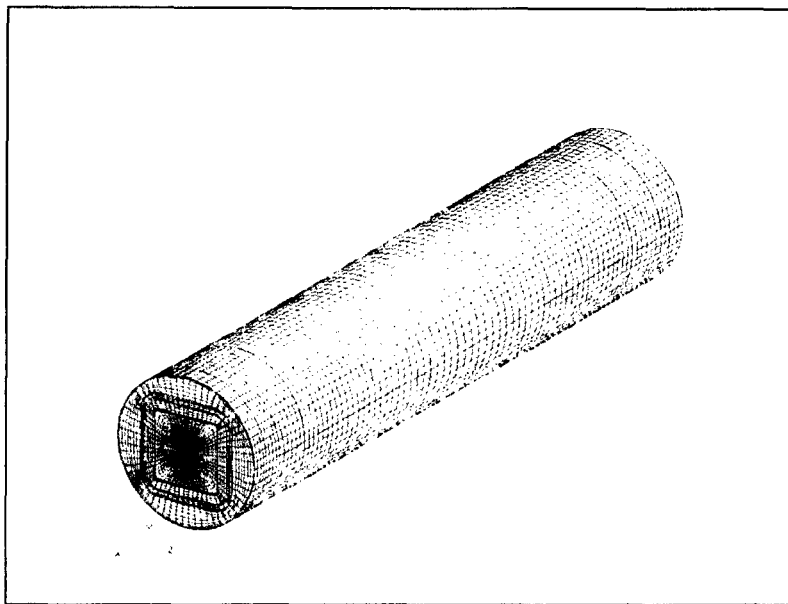


**Figure 51. Finite element model of the GA-4 truck cask.**

An analysis including the effect of the internal heat load to the temperature distribution within the package will be performed once the casks under study have been accurately modeled without the internal heat load. The material properties of the casks were obtained from the *HI-STAR Safety Analysis Report* (Holtec, 2000) and the *GA-4 Safety Analysis Report* (General Atomics, 1998). For the purpose of the preliminary analyses, the casks were assumed to have an initial uniform temperature of 38°C. An oval fuel pool surrounding the cask was simulated with CAFE. The edges of this pool were about 3 meters from the sides of the cask, to conform to the pool size

stipulated for the regulatory fire test. The CAFE fire model that was used for these preliminary simulations was composed of about 36,600 finite volume cells (grid points) with a computational domain of 19m x 24m x 19m for the rail cask and about 21,800 cells with a computational domain of 26m x 26m x 14m for the truck cask. The CAFE model was constructed with a variable grid size to allow the use of a finer mesh in the fire regions near the cask.

For this preliminary study, three cases were investigated for the rail cask to better understand the effect of the vapor dome on heat transfer from the fire to the cask and to estimate the height above the fuel pool surface at which the package should be placed so that it is outside of the vapor dome and receives a fairly uniform heat flux from the fire envelope. The height of the cask above the fuel pool surface was 1.3 m for Case 1, 0.3 m for Case 2, and 3.3 m for Case 3. For the truck cask, only a 1.0 m above the pool simulation was performed. Each fire simulation was run for one hour, and each assumed no wind (quiescent fire conditions) for the duration of the simulation.

Figure 52, Figure 54, and Figure 56 present the results of the CAFE fire calculations using the rail cask. In these figures, the cask is represented by the void area in the middle of the fire. Note that these figures were created without correcting for the variable cell size that was used in the simulations; therefore the relative sizes of the pool and test object are not accurately portrayed. The actual diameter of the cask is about 2.0 times larger and the length about 1.4 times longer than the dimensions shown in Figure 52 (a) and (b), the end and side views of the cask. If these end and side views were adjusted to reflect the actual size of the cask, the distance from the cask to the edge of the flame envelope would decrease and the temperature gradients through the envelope would increase. This graphics display problem will be corrected in future calculations.

#### 3.4.1 Case 1: Rail Cask 1.3 Meters Above the Fuel Pool Surface, No Wind

This case approximates the fire conditions specified in 10CFR71.73. The results from this case are presented in Figure 52 and Figure 53. Figure 52 presents typical fire conditions; Figure 53 presents one-hour temperature histories.

Figure 52 (a) and (b) show that when the cask is positioned 1.3 m above the fuel pool surface, the fire vapor dome (the brown to reddish portions of the fire envelope in these figures) partially surrounds the cask. Figure 52 (c) presents the mole fraction of (unburned) fuel in the fire and clearly shows the presence of large amounts of unburned fuel vapor at the bottom and the sides of the cask. There is some unburned fuel high above the cask in the middle of the fire because even in this region, there is no oxygen to support combustion. Together, Figure 52 (a) through (c) show that for this case the vapor dome surrounds the cask on three sides but is greatly thinned on the top of the cask. Consistent with these observations, Figure 52 (d) shows that cask surface temperatures are lowest on the bottom of the cask, somewhat higher on the sides of the cask, and highest on the top of the cask. Note that the temperature color scale for Figure 52 (a) through (c) is different from the color scale in Figure 52 (d).

Temperature histories for the hottest internal node and several external nodes are presented in Figure 53 at two locations along the length of the cask: at the middle of the cask and at the lid end of the cask. In the figure legends, East refers to the positive z-axis direction in Figure 52 (d); thus east is the right side of the cask, west is the left side of the cask, and in and out refer to the inside and

outside of the cask wall at the indicated position. As shown in Figure 53 (a), for the middle of the cask, the temperature history at the top of the cask (“C\_top\_out”) lies significantly above the temperature history at the sides (“C\_east\_out” and “C\_west\_out”). The temperature histories at the sides are nearly identical and lie significantly above the temperature history at the bottom location (“C\_bottom\_out”). The internal top temperature (“C\_top\_in”) is significantly lower than any of the outer temperatures due to the thermal insulating effect of the 5-inch thick neutron shielding material and the 9-inch thick steel wall.

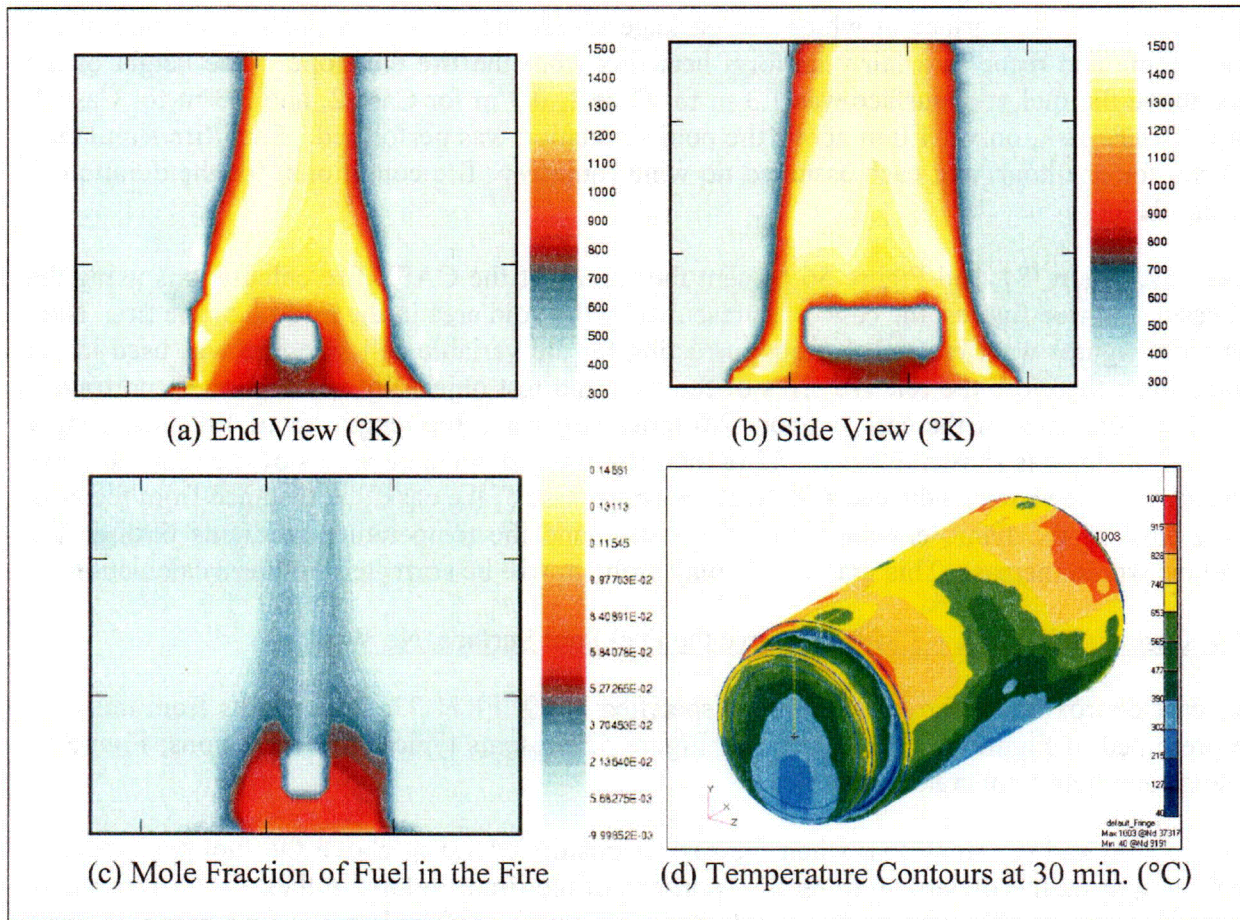
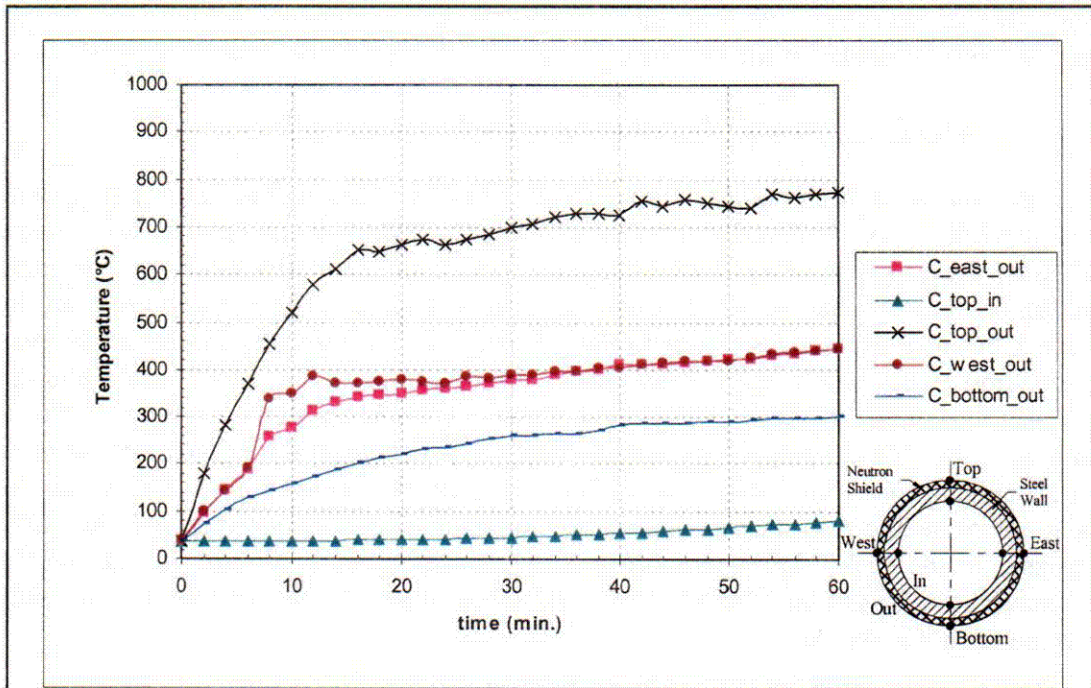
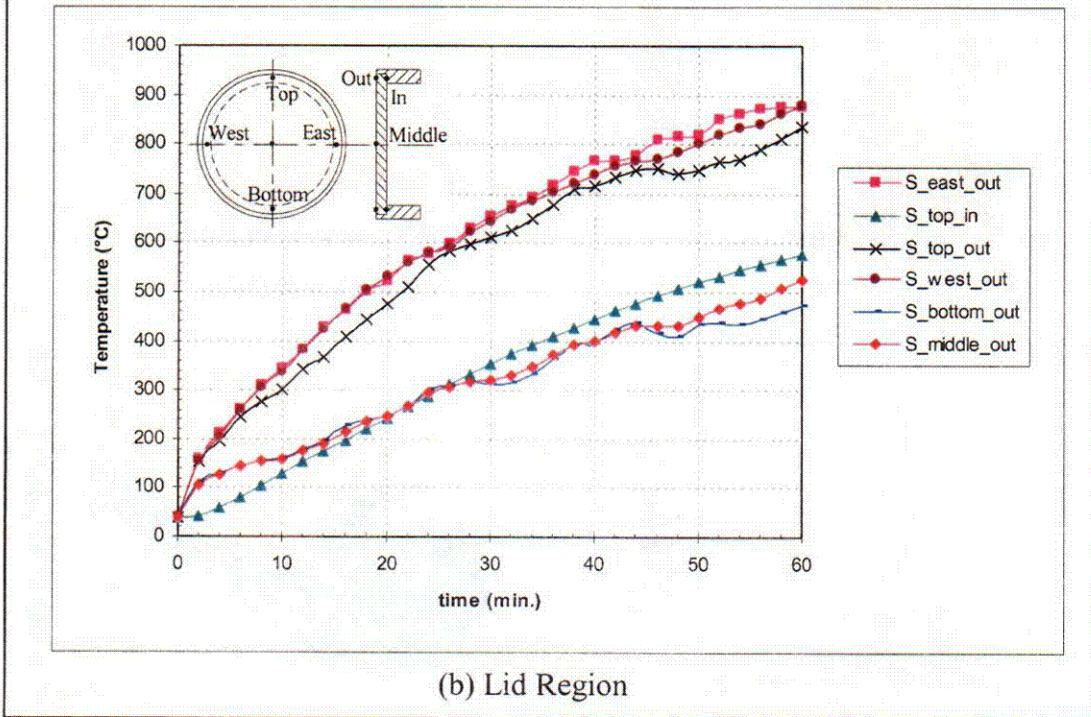


**Figure 52. CAFE results for Case 1 (1.3 m above fuel pool surface).**

As shown in Figure 53 (b), for the lid region, only the outside temperatures at the top (“S\_top\_out”) and the sides (“S\_east\_out” and “S\_west\_out”) were hotter than the internal top location (“S\_top\_in”) at all times. On the other hand, the outside temperatures at the bottom (“S\_bottom\_out”) and middle (“S\_middle\_out”) location were hotter than the inside temperature at the top location (“S\_top\_in”) for about 23 minutes into the simulation and then the inside top temperature becomes hotter than the two outside temperatures. This is because on the outer surface, the bottom of the cask stays colder than the top while the top inside location is receiving heat by conduction from the hot “S\_top\_out” location faster than the bottom the cask (i.e., the “S\_top\_in” location is much closer to the hot “S\_top\_out” locations than the “S\_bottom\_out” location). The temperature difference between “top\_in” and “top\_out” in Figure 53 (b) is less



(a) Middle of the Cask ( $x = L/2$ )



(b) Lid Region

Figure 53. Temperature History for Case 1 (1.3 m above fuel pool surface).

than seen in Figure 53 (a) because heat is being diffused through steel only in the lid region. Furthermore, this is the reason why the internal surface temperature of the lid is about 500°C hotter than the internal surface at the middle of the cask at the end of the one-hour simulation.

### 3.4.2 Case 2: Rail Cask 0.3 Meters Above the Fuel Pool Surface, No Wind

For Case 2, the cask is positioned 0.3 m above the fuel pool surface, and all other parameters are the same as in Case 1. As Figure 54 (a) through (c) show, although the cask is now somewhat less engulfed by the vapor dome (e.g., because the vapor dome is smaller for Case 2, it encloses less of the top of the cask than it did for Case 1), the temperatures at the cask bottom are lower than in Case 1 because the cask is closer to the ground. For example, as Figure 55 shows, the outer surface temperature at the cask bottom in the middle of the cask is 120°C at the end of one hour for Case 2, which is substantially lower than the cask bottom temperature (300°C) calculated at one hour for Case 1. On the other hand, temperatures at the top and the sides of the cask are higher than those found for Case 1. The net result of positioning the cask closer to the ground is to increase the temperature gradients around the cask circumference, and thus the thermal stresses in the cask. The waviness in some of the curves in Figure 55 may be due to numerical instabilities within the CAFE. This will be examined closely, and the findings will be reflected in the detailed test plan.

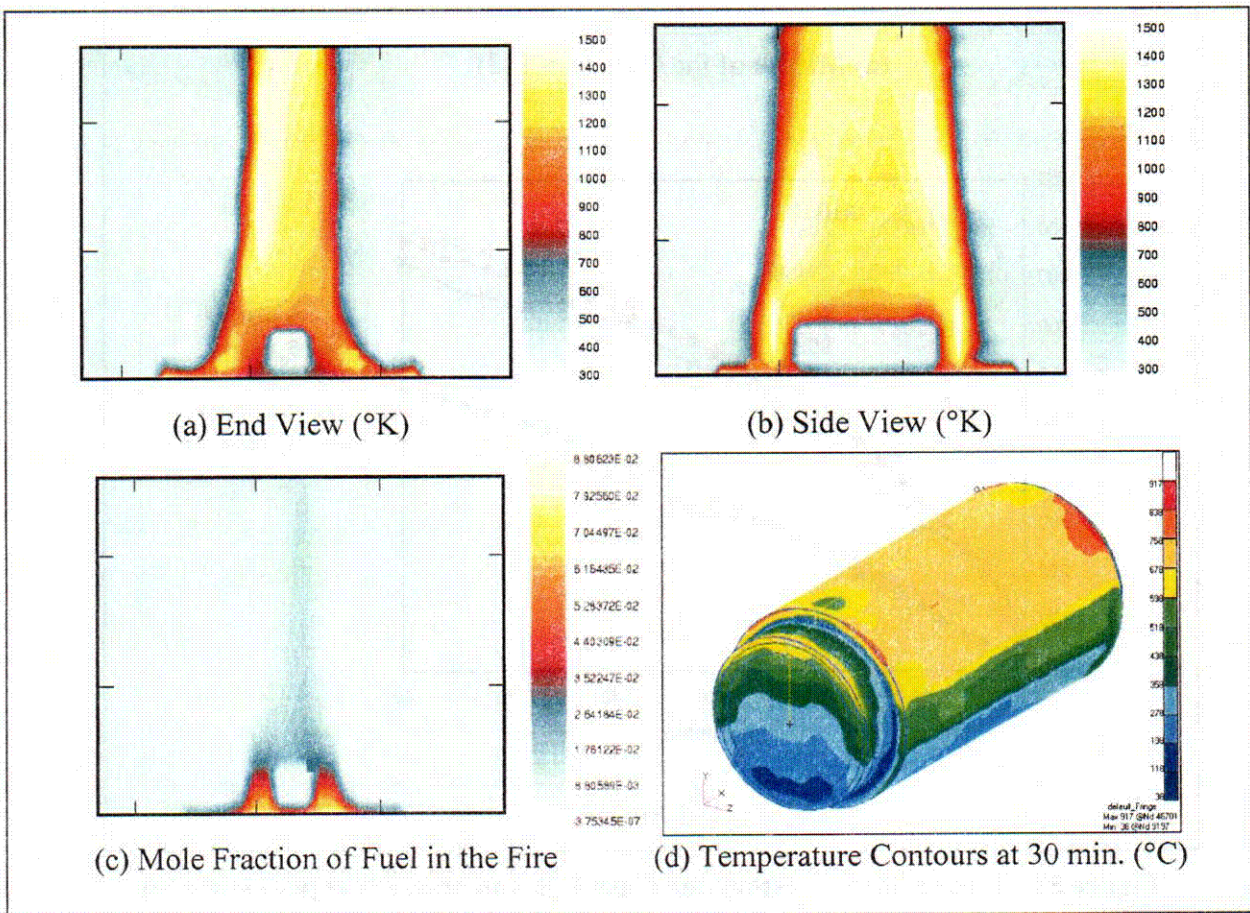
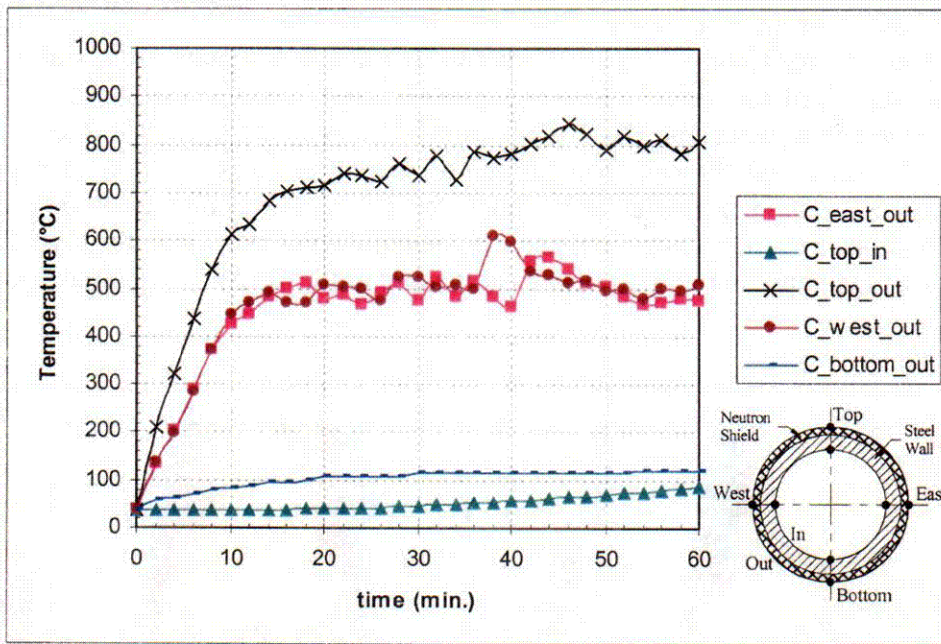
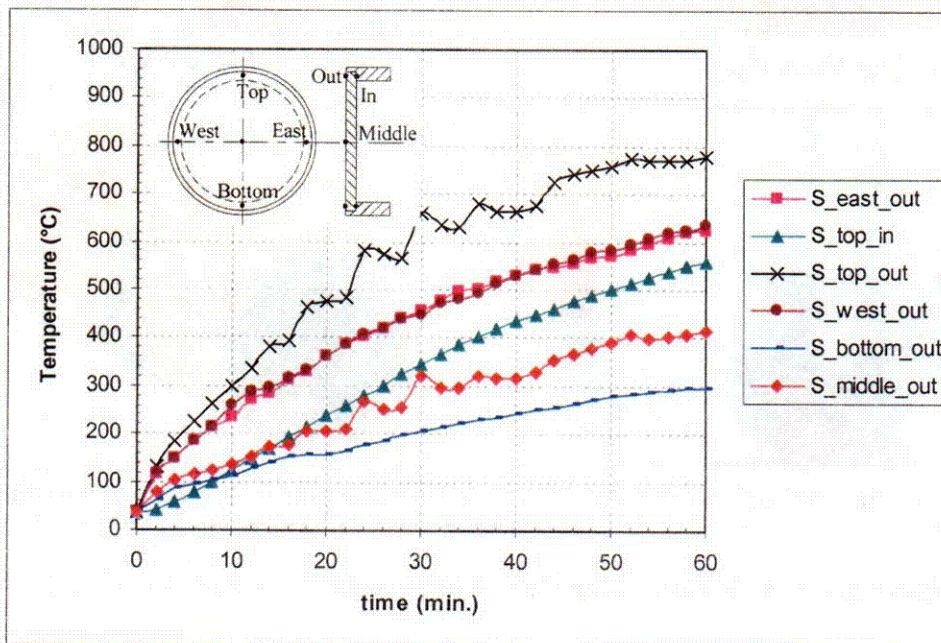


Figure 54. CAFE results for Case 2 (0.3 m above fuel pool surface).



(a) Middle of the Cask ( $x = L/2$ )



(b) Lid Region

Figure 55. Temperature History for Case 2 (0.3 m above fuel pool surface).

### 3.4.3 Case 3: Rail Cask 3.3 Meters Above the Fuel Pool Surface, No Wind

In Case 3, the cask has been positioned 3.3 m above the fuel pool surface with all other parameters the same as for Case 1. Figure 56 shows that the cask is now mostly above the fuel vapor dome and that all of the cask surface, except its bottom, is now exposed to regions of the flame envelope where vigorous combustion is occurring. Comparing Figure 57 (a) to Figure 55 (a) and Figure 53 (a) shows that the cask top surface temperatures for Case 3 are very similar to those for Case 2 and slightly higher than those for Case 1, but that cask bottom surface temperatures for Case 3 exceed those for Case 1 by about 250°C and those for Case 2 by about 430°C. Note that the temperature around the cask is more uniform for Case 3 than it is for Cases 1 and 2.

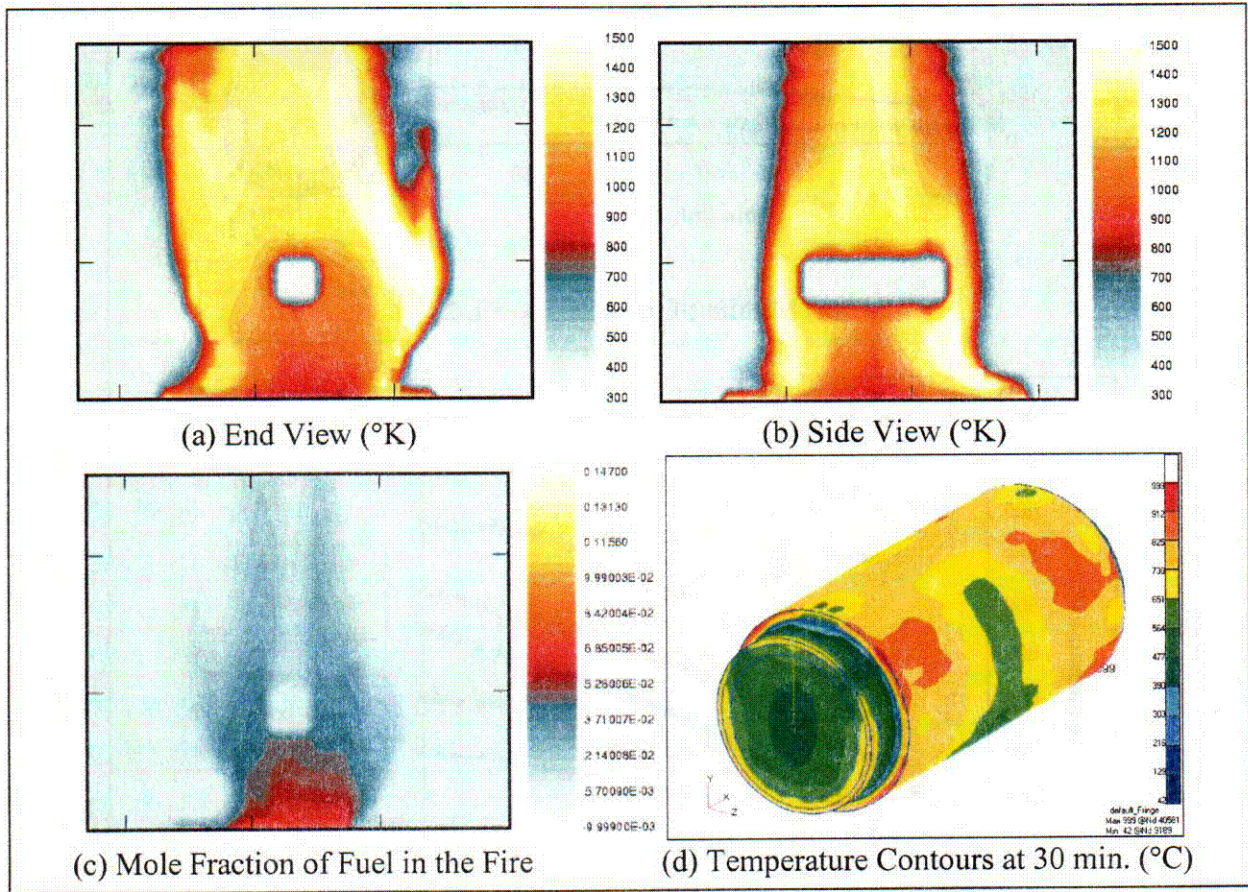
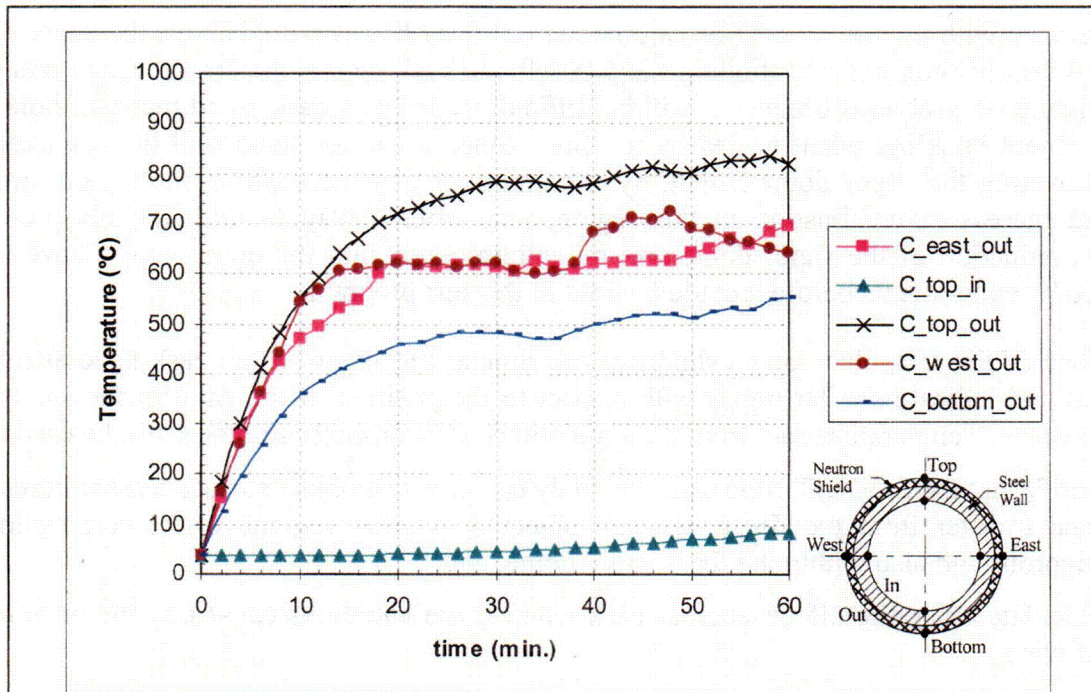
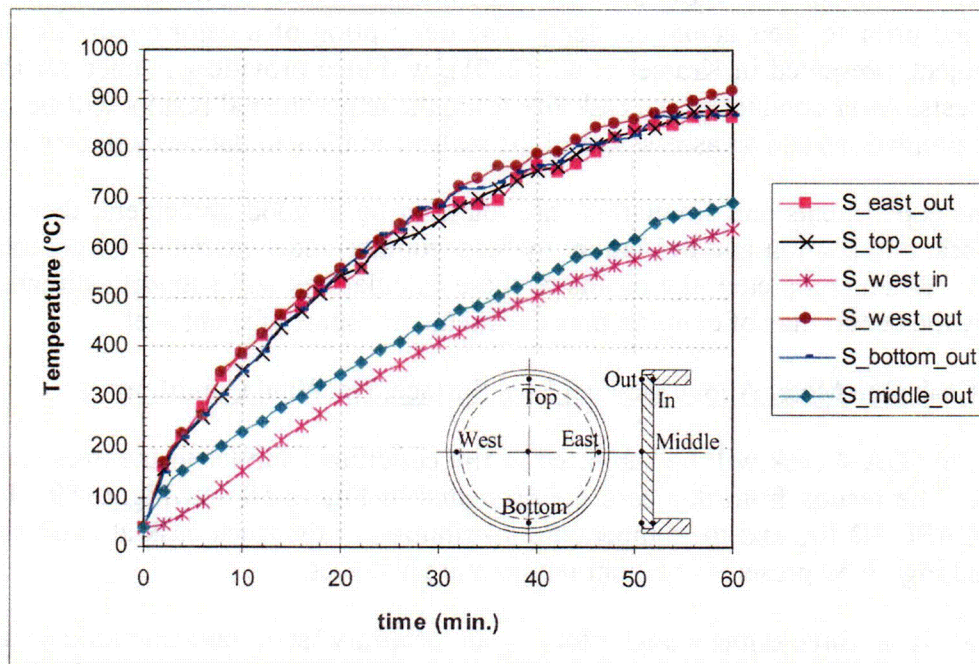


Figure 56. CAFE results for Case 3 (3.3 m above fuel pool surface).



(a) Middle of the Cask ( $x = L/2$ )



(b) Lid Region

Figure 57. Temperature History for Case 3 (3.3 m above fuel pool surface).

An experiment with the test object (the calorimeter or the cask) positioned above the vapor dome is planned for this program. Positioning a 225,000-lb rail cask several meters above the fuel pool surface may pose problems because it will be difficult to design a cask stand that will hold this weight without buckling when heated by the fire. Since a shorter stand will be less likely to buckle, lowering the vapor dome height, by entraining air into the vapor dome region through pipes and increasing combustion in this region, may offer a way to mitigate this problem. However, reduction of the vapor dome size by entraining air into the dome would have to be confirmed by experiments before it could be used in this test program.

Simulations of fire tests that use a cylindrical calorimeter the size of a rail cask have also been conducted and indicate similar trends with respect to the position of the calorimeter relative to the vapor dome. Temperature data from the simulations of calorimeter fire tests will be used to:

- (1) verify that the SODDIT code can accurately estimate test object surface temperatures and heat transfer from the fire to the test object in the fire regions where combustion is vigorous and also within the fire's vapor dome, and,
- (2) calculate other fire effects such as cask temperature variations caused by the occurrence of wind.

After the calorimeter fire tests have been performed, the cask fire calculations presented above will be rerun with the CAFE input data modified to reflect the results of these calorimeter tests. The refined CAFE model will allow the cask experiments to both be better designed and also better simulated prior to their actual conduct. The description of a calorimeter fire test for at truck-sized object, presented in Kramer et al., (2001), will also provide guidance for the design of these fire tests. After conduct of the cask fire tests, the experimental results will be compared to the pretest simulations and an assessment of the realism of the simulations will be conducted.

Given that the experiments and simulations are found to be in good agreement, then improved estimates of seal degradation and rod failure by burst rupture under extreme fire conditions will be performed. When completed, the results of these calculations will support estimation of the risks posed by the occurrence of extreme fires during the transport of spent fuel.

#### 3.4.4 Truck Cask One Meter Above the Fuel Pool Surface, No Wind Condition

For this case, the GA-4 cask will be subjected to fire conditions similar to the ones specified in 10CFR71.73. The results from this case are presented in Figure 58 and Figure 59. Figure 58 presents the CAFE 3D fire and the temperature distribution of the truck cask at one-half hour of simulation and Figure 59 presents one-hour temperature histories.

Figure 58 (a) is a three-dimensional plot of an arbitrary soot concentration mapped by temperature. In this figure, a small section of the cask (the green region on the lower front section of the fire) seems to be exposed to the environment outside the fire when in reality it is exposed to a different soot concentration within the fire. However, this plot provides a near-real representation of the fire, which helps when used to design experiments or to obtain an overall idea about the fire that is being simulated. Similar to what was shown in previous sections for the rail cask simulations, Figure 58 (b) shows that cask surface temperatures are lowest on the

bottom of the cask, somewhat higher on the sides, and highest on the top. Note that the temperature color scale for Figure 58 (a) is different from the color scale in Figure 58 (b).

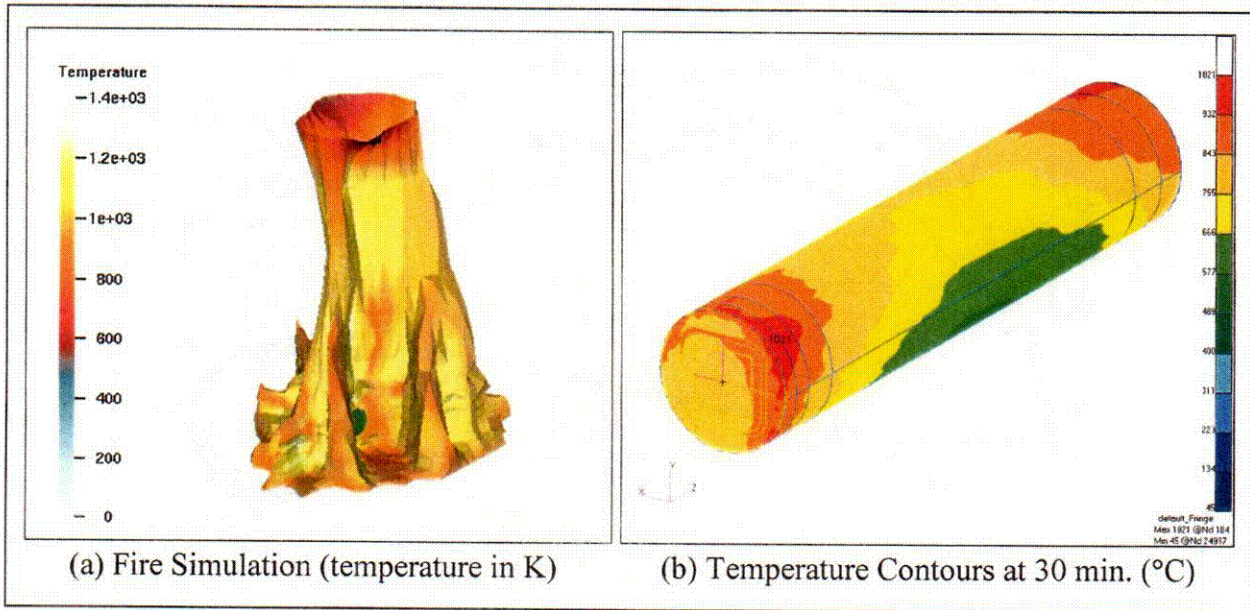
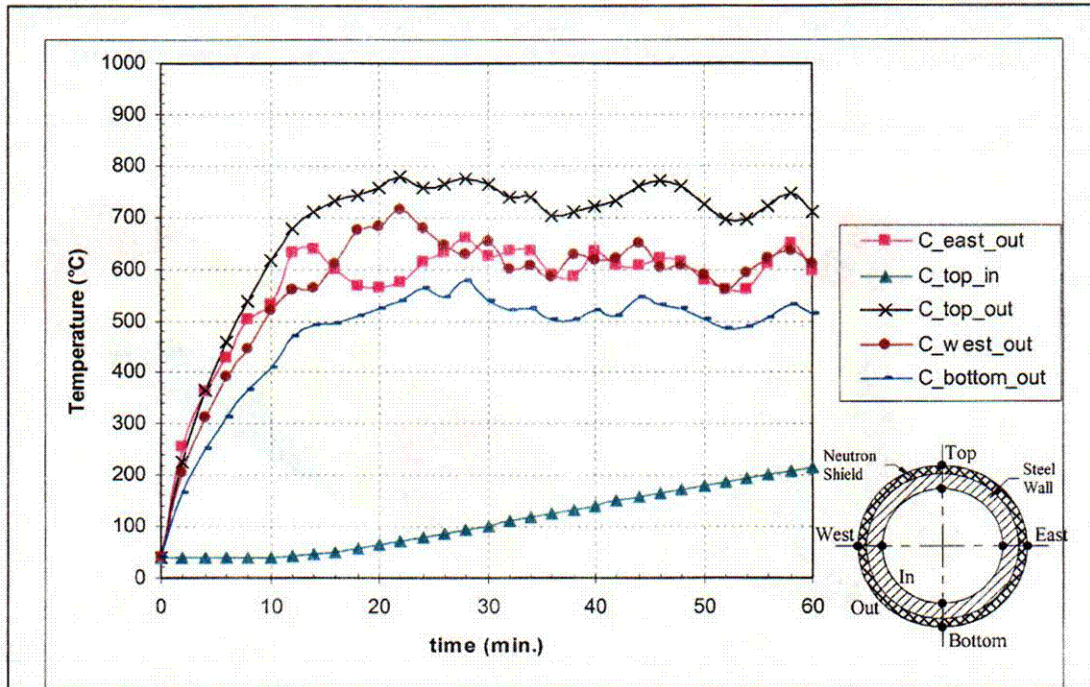


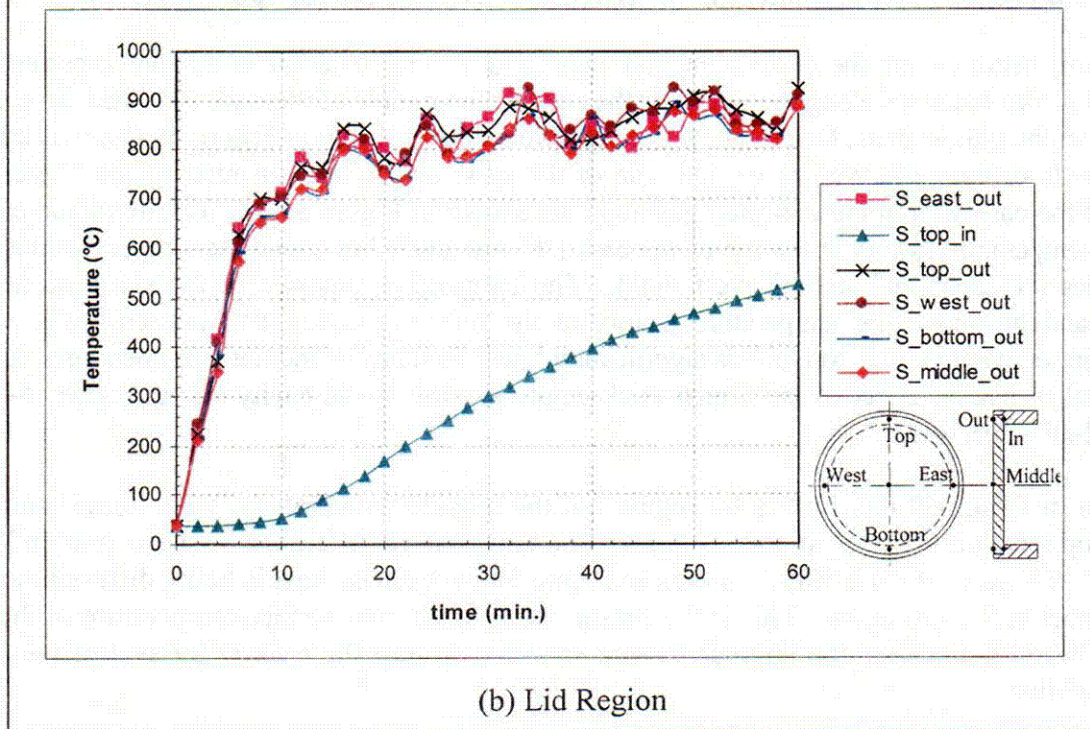
**Figure 58. CAFE results for the truck cask (1 m above fuel pool surface).**

Temperature histories for the hottest internal node and several external nodes are presented in Figure 59 at two locations along the length of the cask: at the middle of the cask and at the lid end of the cask. In the plot legends, East refers to the negative x-axis direction in Figure 58 (b); thus east is the right side of the cask, west is the left side of the cask, and in and out refer to the inside and outside of the cask wall at the indicated position. As shown in Figure 59 (a), for the middle of the cask, the temperature history at the top of the cask (“C\_top\_out”) lies above the temperature history at the sides (“C\_east\_out” and “C\_west\_out”). The temperature histories at the sides are nearly identical and lie above the temperature history at the bottom location (“C\_bottom\_out”). The internal top temperature (“C\_top\_in”) is significantly lower than any of the outer temperatures due to the thermal insulating effect of the 6-inch thick empty neutron shield cavity and the nearly 5-inch thick steel-DU-steel wall.

As shown in Figure 59 (b), for the lid region, all the outside temperatures were hotter than the internal top location (“S\_top\_in”) at all times. The temperature difference between “top\_in” and “top\_out” in Figure 59 (b) is less than seen in Figure 59 (a) because heat is being diffused mostly through steel in the lid region. This is the reason why the internal surface temperature of the lid is about 300°C hotter than the internal surface at the middle of the cask at the end of the one-hour simulation.



(a) Middle of the Cask ( $x = L/2$ )



(b) Lid Region

Figure 59. Temperature History for the Truck Cask (1 m above fuel pool surface).

### **3.5 Fire Instrumentation**

In fire tests, the main purpose of the instrumentation is to determine how the surrounding fire affects the test object. This is a fundamental difference from structural tests, such as a drop test, where the major focus is on understanding and predicting the response of the package itself. Because of this difference, instrumentation is not only on and in the package, but it is also distributed throughout the fire and the surrounding environment. Key parameters often measured in fires and in and near the package are temperature, heat flux, and gas flow velocities. Additional parameters such as package surface emissivity and fuel evaporation rates are also measured.

Thermal computer codes that model packages and their internal contents have been refined to permit accurate prediction of package temperatures if the surrounding fire boundary conditions are known. In contrast, the prediction of the surrounding fire environment involves the study of thermal radiation in a participating medium (soot), understanding the complicated turbulent flow field induced by the fire, and determining the important chemical reactions that occur in the turbulent well-mixed region of the fire when oxygen availability is limited. Advances in computer speed permit many of these complex fire features to be captured in computer models (e.g., see Suo-Antilla et al., 1999), but instrumented fire tests are still essential to understand and adjust the accuracy of these fire models.

Many effects have been observed in large pool fires. For example, a relatively cool vapor dome exists immediately above the burning pool where there is insufficient oxygen to permit combustion (Gritzo et al., 1998). Others (Nicolette and Larson, 1990, Gritzo and Nicolette, 1993) have observed that massive objects cool the gasborne soot particles near the object, leading to a reduction of the thermal radiation incident on the object. Kramer et al. (2001) observed that even light winds affect the fully engulfing nature of large fires. The design of instrumentation used for the PPS study will include features that allow evaluation of these and other effects, as well as the response of the test object to the fire.

#### 3.5.1 Types of Fire Instrumentation

Fire instrumentation has evolved over 30 years of large-scale fire testing. Many devices have been tried and the advantages and limitations of each evaluated. As formal test plans are prepared, instrumentation will be selected that allows (within the available budget) fire and test object parameters to be measured.

For routine testing, instrumentation must be simple and rugged if it is to survive multiple fire tests. Metal-sheathed, mineral-insulated thermocouples have been shown through extensive experience to have the characteristics necessary to measure temperatures, both in the fire and in the test object. Typically, Type K (chromel-alumel) thermocouples are used because they exhibit a good measurable response over the entire range of fire temperatures. However, the use of thermocouples in fire tests presents some problems. For example, how to position or attach the thermocouple to the test object so that surface temperatures are accurately measured, and how to insulate and cool the thermocouple leads that must be routed through the fire zone. If the leads are not properly protected, thermocouple-shunting error causes erratic readings as the mineral insulation loses its insulating properties at elevated temperatures. While it is possible to

estimate fire temperatures with sheathed thermocouples directly exposed to the fire, experience has shown that such measurements yield temperatures that are 50° to 100°C above temperatures measured by other techniques.

To improve estimates of fire temperatures over those made with a bare thermocouple, the directional flame thermometer (DFT), first described by Burgess (1986), has often been used. This simple device consists of a cylinder with thin metal ends that looks like a food can found in grocery stores. The thin metal ends have a view of a hemisphere of fire, and quickly approach the fire temperature when engulfed by the fire. Thermocouples are attached to the inside surface of the thin metal ends to provide the temperature reading, and the cylinder interior is filled with an insulating material which prevents the thermocouple from responding to the temperature of the sides of the cylinder. These devices have been used successfully in fires for more than 15 years and also have been used to estimate local fire heat fluxes (Koski et al., 1998; Kramer et al., 2001). In addition, errors introduced by their use have been carefully evaluated (Blanchat et al., 2000). For the PPS study, a grid network of these devices will be used to estimate the fire conditions in the flame envelope of the test fire.

A second measurement technique that relies solely on thermocouples is inverse heat conduction. This technique gets its name from the “backwards” nature of the problem solution. In conduction heat transfer problems, the response of an object to surrounding boundary conditions is usually calculated. In inverse problems, the response of an object is used to estimate the boundary conditions that caused the response. For the PPS experiments, thermocouples will be mounted on the interior of the test object, and the Sandia One-Dimensional Direct and Inverse Thermal (SODDIT) code (Blackwell et al., 1987) or similar will be used to estimate surface heat transfer and surface temperatures. A major advantage of this technique is that it can estimate point-by-point surface heat transfer from the fire to the test object. Care must be taken to mount the thermocouples in locations where the heat conduction is primarily in one direction (Lopez, et. al., 2000). This eliminates complex geometries where two- or three-dimensional heat conduction occurs, such as near the ends of transportation casks or in finned areas.

Other techniques for measuring surface heat transfer (heat flux) include heat flux gages and radiometers. Heat flux gages usually consist of several thermocouples in series (a thermopile) in a fixed geometry that yields a direct measurement of the heat transfer through the gage. The advantage of such gages is that they can be calibrated easily and accurately. The disadvantage is that making the heat flux gage an integral part of the test object is often difficult. For example, to measure surface heat flux, heat flux gages are mounted directly on the outer surface of the test object, and measure the heat transfer through the gage, not through the cask surface. Differences in gage conductivity and surface emissivity make the heat transfer through the gage different than the heat transfer through the cask surface. Use of heat flux gages will be further evaluated as detailed test plans are prepared for the PPS.

Two principal types of radiometers have been used for fire testing: the Gardon gage and the Schmidt-Boelter radiometer. For the Gardon gage, radial heat transfer from the center to the edge of a cooled disk, located behind an infrared transparent window, is calibrated with a blackbody radiative source. For the Schmidt-Boelter gage, a cooled thermopile behind an infrared transparent window is calibrated with a blackbody radiative source. Use of radiometers offers the following advantages: radiometers measure incident rather than absorbed energy,

respond relatively rapidly to fire transients, and can be calibrated against known standards. Disadvantages include the fact that fires are not a true blackbody emitter of energy, making radiometer calibrations suspect, and the fact that surface emittance must be estimated before the energy absorbed at the cask surface can be calculated. In addition these devices are expensive, special-order items that must be protected, cooled, and kept above the dew point of the combustion gases to function properly. Gardon gages have the additional disadvantage that convection past the gage surface can in some circumstances destroy the radial heat transfer symmetry, making the reading unreliable. Limited use of Schmidt-Boelter gages could enhance the PPS study, permitting estimates of cask surface emittance during fires to be made. Such estimates are difficult because soot attaches to the surface of the cask at low temperatures and “burns off” as temperature increases; this significantly affects the radiometer measurements. In addition, radiometers could give estimates of the magnitude and frequency of heat flux fluctuations near the surface of the test object.

Bidirectional flow probes (McCaffrey and Heskestad, 1976; DiNenno et al., 1988) are often used to estimate gas flows within the fire zone. Pressure differences across a small, hollow cylinder that is blocked at the center are measured and calibrated to estimate flow in one direction (up and down or left and right) depending on the cylinder orientation. Advantages are that these gages are rugged and well proven in fire testing. Disadvantages include the fact that the properties of the hot gas flow (density, composition, etc.) are not known, so properties of hot air are substituted based on a thermocouple reading near the probe. This makes the accuracy of the flow velocity measurement difficult to determine precisely. Placement of these probes near the test object can be useful in determining asymmetries in flow around the cask, and also wind effects on heat transfer to the cask. Probes of this type are readily available, and will be included in PPS test plans.

Several weather stations will be positioned outside the fire zone, and wind direction and velocity at various elevations recorded throughout each test. Off-the-shelf, well-calibrated units for this purpose are available, and will be included in the PPS thermal test plans.

### **3.6 Fire Tests Protocol**

To have a thermal program that can help answer some of the questions that are of interest to the NRC and stakeholders in relation to extreme fire environments, two calorimeter fire tests, two rail cask fire tests, and one truck cask fire test will be performed as described above in Sections 3.1 and 3.2. These tests are expected to provide information that will allow the verification of the extreme accident fire modeling in NUREG/CR-6672, increase public confidence by demonstrating the robustness of transportation casks in general, and demonstrate the ability of the analysis techniques used to predict the test results to also predict the thermal response of spent fuel casks to hypothetical extreme accident fire environments.

Based on the results from the preliminary analyses that were discussed above, the following tasks will be performed to develop the needed thermal results:

- 1) **A more detailed computer modeling of the fire and calorimeter including uncertainty analysis** — A more accurate fire mesh in CAFE 3D is necessary to better represent the fire environment surrounding the calorimeter. The results from this detailed modeling will be used to make decisions about the duration of the planned fire tests, the

height of the test object above the fuel pool surface, and the positions and types of instruments that will be used to gather the test data. All of this information will be discussed more thoroughly in the detailed test plan. An uncertainty analysis of the modeling will be performed in order to envelop the predicted response of the calorimeter to these tests. This will allow for a better and fairer assessment of the error of the predictions by the computer model.

- 2) **Calorimeter tests including uncertainty analysis of the measurements** — Two full-scale fire tests of a calorimeter the size of a rail transport cask are recommended to collect the data (e.g., heat flux, temperature distributions, and temperature histories) necessary to better predict the fire performance of the rail cask. The two suggested tests will position the calorimeter:
  - a) first above the vapor dome, and
  - b) near or on the ground. The test fire durations will be at least an hour and the fuel pool will extend three meters from the sides of the calorimeter.

The interior surface of the calorimeter will be insulated to minimize the internal thermal radiation, which could lead to misleading temperature measurements. The emissivity of the exterior surface of the calorimeter would be measured before and after each test as it cannot be measured during the test and it may vary from test to test. The unobtainable variation of the surface emissivity during the fire introduces an unknown component to the analysis. An uncertainty analysis of the measured parameters will be performed to have a better understanding of the collected values and perform a fair assessment of the error of the values predicted by the simulations.

- 3) **Refinement of computer models and modeling of the full-scale cask** — Using the data acquired from the full-scale calorimeter tests, the CAFE fire model will be refined and then used to analyze the full-scale rail cask fire tests.
- 4) **Full-scale rail transport cask fire tests** — Two fire tests of the full-scale rail cask selected by the NRC will be conducted and the test data will be reduced, analyzed, and presented to the public. These two tests will have the same test configuration and duration as the two calorimeter tests. One test will be performed with the neutron shield, and the second without it as it is difficult to estimate the deterioration of the neutron shielding material and the effect that may introduce after the first fire. The emissivity of the exterior surface of the cask will be measured before and after each test because it cannot be measured during the test and it may vary from test to test. The unobtainable variation of the surface emissivity during the fire introduces an unknown component to the analysis.

The full-scale rail cask tests will provide information on the accuracy of predictions of cask thermal performance, as well as to demonstrate the behavior of casks under extreme fire conditions. Because these tests will exceed the regulatory limits, containment is not going to be verified after the fire tests. In contrast to regulatory testing where containment is one of the measures of success, these tests will be used to evaluate the predicted internal response of the package. Nevertheless, the temperature in the seal region will be measured during the test to allow for other studies and conclusions to be made.

After the fire is out, the cool down temperature data will be collected as the internal temperatures are expected to peak at a later time. However, the cool down data is not intended to be used as part of the measure of success of the predictions.

- 5) **Full-scale truck transport cask fire test** — A fire test of the full-scale GA-4 truck cask will be conducted and the test data will be reduced, analyzed, and presented to the public. The test will be performed with the cask positioned one meter above the surface of the fuel pool. The cask will be bent after the impact test, therefore the orientation will need to be determined. In addition, it is very likely that the neutron absorbing material will be lost following the impact test, thus it is assumed it will not be present for the fire test. The test will be conducted in a similar manner as the rail cask tests.

### 3.7 Thermal Expert Panel Recommendations

The discussion of the thermal expert panel led to the following recommendations:

- 1) Conduct a PIRT (Phenomena Identification and Ranking Table) to evaluate how well the current fire model captures identified scenarios and obtain suggestions on modifications of the model.
- 2) Perform an uncertainty analysis of the readings from the installed instrumentation (e.g., thermocouples) to quantify the installation errors.
- 3) Conduct a few inside fire tests with controlled wind conditions using a smaller calorimeter to help benchmark the CAFE model. (Note: Existing data generated at SNL for other projects could also be used.
- 4) Conduct three additional thick-walled calorimeter tests (using the 2-in. calorimeter described in previous sections) at the regulatory elevation of 1m above the fuel pool with low-, mid-, and high-wind conditions.
- 5) Perform a benchmark exercise for the finite element model of the rail package prior to the predictions of its thermal response when exposed to the fire. This will isolate the uncertainties of the finite element modeling (cask) from CAFE (fire) modeling. This could be accomplished by:
  - i. applying a well known heat load (e.g., from a electric heater band) at a given location,
  - ii. recording the response of the package, and
  - iii. adjusting the finite element model to match these results.

The adjustment may be necessary due to the uncertainties of the thermophysical properties of the package components.

- 6) Revisit the PIRT for complex features of the packages (i.e., how to properly model the thermal response of the internals, including the fuel rods, the basket, and void spaces inside of the cask).

## 4.0 SUMMARY OF TEST PROTOCOLS

Two sets of tests have been described:

- impact of a rail cask at about 96 kph [60 mph] in a center-of-gravity over corner orientation onto an unyielding flat surface and of a truck cask onto a rigid semi-cylinder between its impact limiters and
- fully engulfing fire tests of a calorimeter the size of a rail cask, a rail cask, and a truck cask.

A high-speed full-scale rail spent fuel cask impact test and a high-speed full-scale truck spent fuel cask impact test are planned as part of the PPS. The results of these tests will be compared to detailed pretest predictions of these results developed by finite element analysis. Less detailed finite element analyses were performed to develop the preliminary design of the impact tests that are described in this report. This preliminary impact test protocol recommends that:

- a full-scale Holtec HI-STAR 100 rail cask should be subjected to an extreme impact onto a flat unyielding surface,
- during the impact test, the lid end of the cask should be equipped with an impact limiter and the cask should contain a Multi-Purpose Canister, specifically the MPC-24 canister, that in turn contains one real fuel assembly packed with surrogate fuel and 23 dummy assemblies,
- the impact should be onto the end of the cask that is equipped with the impact limiter
- the test impact orientation should be center-of-gravity over corner, and
- the cask impact velocity onto the unyielding surface should be between 96 and 144 kph [60 and 90 mph],  
and:
- a full-scale General Atomics GA-4 truck cask should be subjected to an extreme “back-breaker” impact onto a rigid semi-cylinder,
- during the impact test, both ends of the cask should be equipped with impact limiters and the cask should contain one real fuel assembly packed with surrogate fuel and 3 dummy assemblies,
- the impact should be onto one of the flat sides of the cask midway between the impact limiters, and
- the cask impact velocity should be between 96 and 144 kph [60 and 90 mph].

For the HI-STAR cask impact, deformations of the impact limiter will be compared to the finite element predictions of these deformations. The output of strain gage bolts and displacement gages will be used to characterize the closure response, which will be compared to the finite element predictions of the closure response. Strain gages in the closure weld region of the canister will be used to determine if the finite element analysis is accurately predicting the response of the weld region. Accelerometers will be mounted on the cask sidewall, the cask lid, and the canister lid to provide information on the inertial loads experienced by the cask body overall, and on the impact between the canister and cask lid.

For the GA-4 cask impact, deformations of the cask body will be compared to the finite element predictions of these deformations. Accelerometers on the two ends of the cask and at the centerline will be used to characterize the contact force between the semi-cylinder and the cask, and will be compared to the finite element prediction of these forces. Strain gages on the upper side of the cask will provide an additional means of measuring the amount of bending experienced by the cask during the test. In this test there will be no internal instrumentation. This will allow the leak-tightness of the cask to be measured after the test. This measurement result will be compared to the pre-test leak test result, and will be used to verify the finite element prediction that there will be no deformation to the closure region.

The finite element analysis results may depend significantly on the response of cask features that are too small to model. This will necessitate component tests to determine how these features effect the global response of the cask.

Fully engulfing fire tests of an instrumented cylindrical calorimeter the size of a full-scale rail cask, a full-scale rail cask, and a full-scale truck cask are planned as part of the PPS study. The calorimeter will be designed and instrumented to obtain estimates of heat transfer within large pool fires and to verify that computer codes can accurately predict such fire environments. The rail and truck cask tests will provide information about the accuracy of predictions of cask thermal performance, and also will demonstrate the behavior of the cask under extreme fire conditions. Test fire durations will most likely be longer than the 30-minute duration of the regulatory fire test. Test instrumentation will be selected to assure that fire conditions are accurately measured.

The rail and truck cask collision tests will develop data that will be used in the Package Performance Study (PPS) to validate finite element code predictions of collision damage to Type B spent fuel casks. The fully engulfing fire tests of a calorimeter the size of a rail cask, a rail cask, and a truck cask will develop data about the heat fluxes from an engulfing hydrocarbon fuel fire to Type B spent fuel casks lying on the ground and from that cask to the ground.

Development of this data will substantially improve the technical basis that underlies the estimation of the risks posed by extreme accidents that might occur during the shipment of spent fuel in Type B packages.

## 5.0 REFERENCES

- American Society of Testing and Materials, *Standard Test Method for Conducting Drop-Weight Test to Determine Nil-Ductility Transition Temperature of Ferritic Steels*, ASTM Test E 208 – 95a (Reapproved 2000).
- J. Bai et al., Effect of Hydrides on Ductile-Brittle Transition in Stress-Relieved, Recrystallized and  $\beta$ -Treated Zircaloy-4, *Proceed. ANS/ENS Topical Meeting on Light Water Reactor Fuel Performance*, Avignon, France, April 1991, p. 233-241.
- C. Bernaudat, Mechanical Behavior Modeling of Fractured Nuclear Pellets, *Nuclear Engineering and Design*, **156**, 373-381 (1995).
- B. F. Blackwell, R. W. Douglass, and H. Wolf, *A User's Manual for the Sandia One-Dimensional Direct and Inverse Thermal (SODDIT) Code*, SAND85-2478, Sandia National Laboratories, May 1987.
- T. K. Blanchat, L. L. Humphries, W. Gill, *Sandia Heat Flux Gauge Thermal Response and Uncertainty Models*, SAND2000-1111, Sandia National Laboratories, May 2000.
- M. H. Burgess, Heat Transfer Boundary Conditions in Pool Fires, in *Proceedings of the Symposium on the Packaging and Transportation of Radioactive Materials*, 1986.
- S. P. Burns, R. E. Canaan, D. E. Klein, A Numerical Analysis of Spent Nuclear Fuel Thermal Characteristics, in *Proc. 1993 High Level Radioactive Waste Management Conference*, vol. 2, pp. 1778-1784.
- K. S. Chan and Y. Lee, A Fracture Mechanics-Based Model for Assessing the Mechanical Failure of Nuclear Rods Due to Rock Fall, *Nuclear Engineering and Design*, **201**, 209-226 (2000).
- Commission of the European Communities, *Qualification Experiments of the Release Behavior of LSA Materials in Accident Conditions with Mechanical Impact*, Commission of the European Communities, CEC Project 4.1020/D/96-012, September 1998.
- P. J. DiNunno, Ed., *SFPE Handbook of Fire Protection Engineering*, National Fire Protection Association, Boston, MA, 1988, p. 1-132.
- L. E. Fischer, et al., *Shipping Container Response to Severe Highway and Railway Accident Conditions*, NUREG/CR-4829, Lawrence Livermore National Laboratory, Livermore, CA, February 1987, Tables 5.1 and 5.2.
- General Atomics., *GA-4 Legal Weight Truck Spent Fuel Shipping Cask Safety Analysis Report for Packaging (SARP)*, Revision G, COC 9226, General Atomics Report No. 910469/G, General Atomics, San Diego, CA, 1998 (available from NRC document room).
- L. A. Gritzko, and V. F. Nicolette, Coupled Thermal Response of Objects and Participating Media in Fires and Large Combustion Systems, in *Heat Transfer in Fire and Combustion Systems*, HTD-250, ASME, 1993.
- L. A. Gritzko, J. L. Moya, and D. Murray, *Fire Characterization and Object Thermal Response for a Large Flat Plate Adjacent to a Large JP-4 Fuel Fire*, SAND97-0047. Sandia National Laboratories, Albuquerque, New Mexico, January 1997.
- L. A. Gritzko, W. Gill, V. F. Nicolette, Estimates of the Extent and Character of the Oxygen-Starved Interior in Large Pool Fires, *Very Large-Scale Fires*, ASTM STP 1336, N. R. Keltner, N. J. Alvares, and S. J. Grayson, Eds., American Society for Testing and Materials, 1998.
- R. F. Hazelton, *Characteristics of Fuel Crud and its Impact on Storage, Handling and Shipment of Spent Fuel*, PNL-6273, Pacific Northwest National Laboratory, Richland, WA, September 1987.

- Holtec Inc., *Safety Analysis Report for the Holtec International Storage, Transport, And Repository Cask System (HI-STAR 100 Cask System)*, Revision 9, COC 9261, Holtec International Report No. HI-951251, Holtec Inc., Marlton, NJ, 2000 (available from NRC document room).
- W. Jahrei, R. Manzel, and E. Ortlieb, Einflu des Wasserstoffgehaltes und der Bestrahlung auf das Mechanische Verhalten von Brennelementstrukturteilen aus Zircaloy, *Jahrestagung Kerntechnik 1993*, Cologne, Germany, May 25-27, 1993, p.303-306.
- M. Kawaguchi et al., Deposition of Model Crud on Boiling Zircaloy Surfaces at High Temperature, *Nuclear Technology*, **62**, 253 (1993).
- J. A. Koski, S. D. Wix, and D.E. Beene, Jr., Experimental Measurement of a Shipboard Fire Environment with Simulated Radioactive Materials Packages, in *Very Large-Scale Fires, ASTM STP 1336*, N. R. Keltner, N. J. Alvares, and S. J. Grayson, Eds., American Society for Testing and Materials, 1998.
- M. A. Kramer, M. Greiner, J. A. Koski, C. Lopez, and A. J. Suo-Antilla, Measurements of Heat Transfer to a Massive Cylindrical Object Engulfed in a Regulatory Pool Fires, in *Proc. 2001 Heat Transfer Conference*, ASME, 2001.
- C. Lopez, J. A. Koski, and A. Razani, 2000, Estimates of Error Introduced when One-Dimensional Heat Transfer Techniques are Applied to Multidimensional Problems, Paper NHTC2000-12037, in *Proc. 2000 National Heat Transfer Conference*, ASME, Pittsburgh, Aug. 20-22, 2000.
- L. Mdler, W. Koch, F. Lange, and K. Husemann, In-situ Aerodynamic Size Classification of Aerosols in the Size Range between 0.1 and 100 µm for Dustiness Tests and Powder Characterization, *J. Aerosol Science*, 30:451 (1999).
- L. Mdler, *Release of Fine Particles by Transient Application of Mechanical Forces*, Thesis (in German), University of Freiberg, 1999.
- B. J. McCaffrey and G. Heskestad, A Robust Bidirectional Low-Velocity Probe for Flame and Fire Application, *Combustion and Flame* **26**, p. 125-127, 1976.
- V. F. Nicolette and D. W. Larson, The Influence of Large, Cold Objects on Engulfing Fire Environments, in *Proceedings of the AIAA/ASME Thermophysics and Heat Transfer Conference*, Seattle, WA, June 18-20, 1990.
- O. Nolte, *Feinstaeube aus Fragmentierungsprozessen sproeder Materialien (Production of fine dust during fragmentation of brittle material)*, Diploma-Thesis (in German), Technical University of Clausthal, 2000.
- Y. Otani, *Aerosol Science Technol.* **10**, 463 (1989).
- T. L. Sanders, et al., *A Method for Determining the Spent-Fuel Contribution to Transport Cask Containment Requirements*, Appendix III, Spent Fuel Response to Transport Environments, SAND90-2406, Sandia National Laboratories, Albuquerque, NM, November 1992(a), p. IV-12.
- T. L. Sanders, et al., *A Method for Determining the Spent-Fuel Contribution to Transport Cask Containment Requirements*, Table I-3, Manufactured Physical Properties of LWR Fuel Rods, SAND90-2406, Sandia National Laboratories, Albuquerque, NM, November 1992(b).
- T. L. Sanders, et al., *A Method for Determining the Spent-Fuel Contribution to Transport Cask Containment Requirements*, Section I.3.2, Post-Irradiation Fuel Pellet Condition. Manufactured Physical Properties of LWR Fuel Rods, SAND90-2406, Sandia National Laboratories, Albuquerque, NM, November 1992(c).
- R. P. Sandoval et al., *Estimate of CRUD Contribution to Shipping Cask Containment Requirements*, SAND88-1358, Sandia National Laboratories, Albuquerque, NM, January 1991(a), Figures I-10 through I-12.
- R. P. Sandoval et al., *Estimate of CRUD Contribution to Shipping Cask Containment Requirements*, SAND88-1358, Sandia National Laboratories, Albuquerque, NM, January 1991(b), p. I-8.

- R. P. Sandoval et al., *Estimate of CRUD Contribution to Shipping Cask Containment Requirements*, SAND88-1358, Sandia National Laboratories, Albuquerque, NM, January 1991(c), pps. 14 and I-23.
- J. L. Sprung et al., *Reexamination of Spent Fuel Shipment Risk Estimates*, NUREG/CR-6672, U.S. Nuclear Regulatory Commission, Washington, DC, March 2000 (available at <http://ttd.sandia.gov/nrc/modal.htm>), Section 7.3.3, Particles, and 7.3.6, CRUD.
- J. L. Sprung, D. J. Ammerman, J. A. Koski, and R. F. Weiner, *Spent Nuclear Fuel Transportation Package Performance Study Issues Report*, NUREG/CR-6768, U.S. Nuclear Regulatory Commission, Washington, DC, June 2002.
- A. J. Suo-Anttila, J. A. Koski, and L. A. Gritzko, CAFE: A Computer Tool for Accurate Simulation of the Regulatory Pool Fire Environment for Type B Packages, in *Proc. 1999 ASME Pressure Vessels and Piping Conference*, vol. 390, pp 101-109.
- G. R. Thomas and R. W. Carlson, *Evaluation of the Use of Homogenized Fuel Assemblies in the Thermal Analysis of Spent Fuel Storage Casks*, UCRL-ID-134567, Lawrence Livermore National Laboratory, July 1999.
- U.S. Nuclear Regulatory Commission, *Final Environmental Statement on the Transportation of Radioactive Material by Air and Other Modes*, NUREG-0170, U.S. Nuclear Regulatory Commission, Washington, D.C., December 1977.

## **APPENDIX A:**

### **Frequency of Accidents and Metrics for PPS Test Parameters – An Example**

#### **Background**

The NRC staff has a number of decisions to make regarding the test parameters for the Package Performance Study. Examples of these decisions include selection of the speed for the impact tests of the rail and truck casks and the duration of the thermal tests. The staff has committed to take public comments on the Test Protocols report into consideration in developing the specifications for the detailed test plans that will guide the PPS tests. In addition to the public comments, the staff will also take into consideration a number of technical metrics in developing the detailed test plans. To illustrate this decision process, the speed of the rail cask impact will be taken as an example of how the NRC staff will consider technical metrics. The process sketched here will also be followed in making decisions for other important test parameters.

This appendix describes three of the metrics that may be considered by the staff in determining appropriate test parameters. The first metric is associated with the probability of the actual occurrence of the test parameters. The staff will examine the available data related to the occurrence of rail accidents under specific conditions, such as cask orientation on impact, the rigidity of the target, and the frequency of occurrence. The staff would determine a speed that would represent a beyond-design-basis accident, but would not select a higher speed that has essentially no realistic probability of occurring.

The second metric is associated with the PPS objectives of analysis code validation. The capabilities of the analysis model and code would not be challenged by studying elastic (non-permanent) deformation of the cask. Plastic (permanent) deformation must be achieved to verify the ability of the model and code to predict impact damage to the cask. Elastic deformation of the cask body can not be visually verified; after the test the cask has returned to its original dimensions.

The third metric involves public confidence. The metric can be achieved through a combination and consideration of both the first metric involving probability and realism in the test scenarios and second metric involving model and code validation. The test parameters must be realistic and limiting to envelope the various transportation hazards a spent fuel package may encounter during transport. The test parameters must also be selected and clearly identified so that post-test analysis can determine and validate the predictive capability of the modeling and codes to the parameters tested.

This Test Protocols report describes at a conceptual level the proposed tests that the NRC staff believes balance the objectives of the PPS to increase public confidence in the robustness and inherent safety of transportation casks and to obtain experimental information that validates analysis codes and provides data on the response of transportation casks to extreme and realistic accident conditions. Thus, the data and analysis provided by PPS would be used to confirm the adequacy of risk models employed by previous transportation risk studies (e.g., NUREG/CR-

6672). The proposed tests are consistent with the information and views collected during the scoping phase of the PPS, including several public meetings, as documented in the PPS issues report (NUREG/CR-6768).

The public confidence objectives of the PPS are also supported by the proposal for a full-scale Holtec HI-STAR rail cask impact test at a reasonable speed (e.g., within the range of 96 and 144 kph [60 to 90 mph]), with an associated pre-test analysis that successfully predicts the test outcome. (The prediction will include size and location of any deformation.) Use of full-scale cask bodies eliminates the need to address scaling issues associated with sub-sized model fabrication and analysis. The use of a reasonably high speed eliminates the need to convert cask test impact speed to realistic accident scenarios. Although such translations have been used to equate the 10 CFR Part 71 regulatory drop (48 kilometers per hour [30 mph] onto an unyielding surface) to higher speed vehicle impact accidents, explaining these calculations in clear, unambiguous terms is often difficult. The NRC staff believes that an accurate pre-test prediction by analysis for the proposed test should provide convincing evidence of our abilities to analyze casks for a variety of conditions without the need for further confirmatory physical tests of other cask models.

The technical objective of the PPS, to confirm the adequacy of the computational methods, is also supported by the proposed tests. A high-speed impact is necessary to fully engage the impact limiter and transmit sufficient force into the cask lid region to result in some plastic deformation. Cask response to the regulatory drop test is well understood and characterized by elastic structural response. However, spent fuel transportation risk assessments, such as those that may be conducted as follow-on activities to PPS, necessarily consider plastic deformation in the lid that could result in potential release pathways. Although the staff does not believe that the PPS proposed tests are of sufficient speed to cause a breach of the canister, measurable deformation of the cask closure is necessary in order to confirm adequacy of modeling methods. Testing onto an unyielding surface supports this objective by providing a controlled experimental design and reducing the number of variables to analyze.

In addition to considering public confidence and technical objectives, the NRC also believes it important to consider risk insights that might be gained from the proposed tests, to support NRC goals of regulatory effectiveness and efficiency. Conducting tests that represent transport accidents that are so highly improbable that they are unlikely to occur, would not be consistent with how risks are assessed at other facilities regulated by NRC (e.g., nuclear power plants, repositories) and would provide little additional information to support NRC's risk informed regulations.

### **Probabilistic Metric: Frequency of the Occurrence of Specific Conditions in Transportation Accidents**

To add perspective to the tests in the protocols, the likelihood of transportation accident sequences that are comparable to the tests in the protocol are compared to the likelihood of event sequences that must be considered in the NRC's licensing regulation for the disposal of high-level waste at Yucca Mountain, 10 CFR Part 63. The probability range of *event sequences* (i.e.,

a series of actions and/or occurrences that could potentially lead to radiation exposure, including one or more initiating events and associated combinations of system component failures) that must be considered in pre- and post-closure repository risk assessments are specified in 10 CFR Sections 63.111 and 63.114. Specifically, the post-closure performance assessment must consider only events that have greater than one chance in 10,000 of occurring over 10,000 years (or  $10^{-8}$  per year); and the pre-closure safety analysis must consider events sequences that have at least one chance in 10,000 of occurring before permanent closure (e.g., before ~100 years), referred to as Category 2 event sequences (or  $10^{-6}$  per year).

By multiplying the transportation statistics for the accident rate per distance traveled for rail transportation ( $2.8 \times 10^{-7}$  per railcar km [ $4.5 \times 10^{-7}$  per mile]), the average rail distance from reactor locations to a repository (3600 km [2237 miles]), and estimates for the number of annual spent fuel shipments (150 rail shipments at 3 casks each), a rough estimate of the expected number of annual transportation accidents can be calculated to be 0.45 per year. Of these accidents, only a small fraction could challenge NRC certified casks. To obtain an event sequence probability that parallels the PPS test protocol proposal, this value must be multiplied by the fraction of all accidents that are derailment accidents (0.82), the fraction of all impacts that occur in a center-of-gravity-over-corner orientation (0.722), the fraction of route wayside surfaces that are hard rock (0.0006), and the fraction of all derailment accidents equivalent to a 96 kph [60 mph] or greater impact onto hard rock (0.01). At DOE-assumed repository shipment rates, the annual probability of an accident comparable to the PPS protocol's proposal of a 96 kph [60 mph] impact into an unyielding surface is estimated to be  $1.6 \times 10^{-6}$ . Note that concurrent transport operations associated with the Private Fuel Storage project, if licensed, could add to this probability (PFS is currently projected at 50 shipments of 4 casks each per year). The upper end of the range in the PPS protocol's proposed impact test, 144 kph [90 mph], is estimated to be about 100 times more infrequent than the 96 kph [60 mph] lower end of the proposal; therefore yielding an annual event sequence occurrence probability of  $1.6 \times 10^{-8}$ .

From the forgoing, the annual probabilities associated with the PPS test protocol impact test range –  $10^{-6}$  per year for a 96 kph [60 mph] test down to  $10^{-8}$  per year for a 144 kph [90 mph] test – compare favorably to the probabilities considered in Part 63 safety or performance assessments –  $10^{-6}$  per year for pre-closure or  $10^{-8}$  per year for post-closure. In this connection, transportation risk assessments, such as NUREG/CR-6672, traditionally consider a range of accidents that encompasses these and even more extreme, or lower probability of occurrence, transportation accidents.

When comparing between regulatory programs for transportation and facility licensing, important distinctions must be made: (1) unlike a geologic repository, transportation accidents can occur in close proximity to members of the public (e.g., accidents in urban areas with little or no standoff distance) and/or place greater populations at risk, (2) transportation accidents could result in greater economic and dose consequence as compared to a repository; and (3) although the transportation accident risk is small and it takes a very extreme and rare accident to cause a release, the rare accident sequences that could cause release contribute a greater fraction to the summed transportation risk. The NRC staff, therefore, considers the likelihood of accidents represented by the PPS Test Protocol's proposal to be appropriate.

## **Mechanistic Metric**

To validate the available analysis code to calculate the response of a rail cask to extreme accident conditions, it is appropriate/necessary to challenge the predictive capabilities of the code by performing tests, which result in plastic deformation. The proposed PPS tests are intended to cause plastic deformation of the casks in the lid region. The analysis codes will be exercised to obtain predictions of the location and sizes of the deformations that will occur from an impact at the selected speed. Computer code development and modeling has simulated the physical effects of a drop test on a transportation cask including impact limiters, in differing orientations and at differing speeds. All analyses involved examining the effects at different speeds of drop tests of casks onto an unyielding surface. [An unyielding surface was selected to simplify the analysis, rather than considering the wide variety of surface conditions that could potentially be encountered and the complexities of the plastic deformation of the impact surface (e.g., soil) as well as the cask. In addition to simplifying the analysis by eliminating the need to select an impact surface and analyze it, the PPS tests are intended to validate the capability of the code to predict the behavior of the cask, not the impact surface.] The predictions from these preliminary analyses, using simplifying assumption about components such as the impact limiters, can be categorized as follows:

- For the Holtec HI-STAR design at impact speeds above 96 kph [60 mph] into an unyielding surface, the transportation cask lid or body begins to plastically deform.
- For the Holtec HI-STAR design at impact speeds below 96 kph [60 mph] into an unyielding surface, the impact energy is completely absorbed by the impact limiters, with no effect on the transportation cask. Testing performed at speeds below 96 kph [60 mph] will effectively test only the impact limiter, since there is no predicted damage to the cask.
- For the Holtec HI-STAR cask, at impact speeds above 120 kph [75 mph], plastic deformation continues to increase and the metallic closure seal begins to leak.

Transportation casks have some level of margin beyond certification requirements; they are expected to maintain integrity even during extreme accident conditions. It should be noted that the speed at which plastic deformation of the cask is predicted to initiate (96 kph [60 mph]) exceeds the regulatory design basis and is within extreme accident conditions. Speeds in excess of 96 kph [60 mph] were analyzed to thoroughly understand the physical response of the cask to varying conditions.

## **Impact Speed Metric**

While the above probabilistic consideration of the rail accident statistics shows that the speed range of 96 to 144 kph [60 to 90 mph] for the rail cask test corresponds to a frequency range of between  $1.6 \times 10^{-6}$  and  $1.6 \times 10^{-8}$  as an event sequence frequency, the NRC staff has decided that the mechanistic metric described above will be the criteria used to select the impact speed for the rail cask test. There are a number of reasons for this decision:

- An objective of PPS is to validate the capability of the available computer code to accurately predict the response of transportation casks to extreme accident conditions. To do this in a credible, unambiguous manner requires some plastic deformation of the cask as described above.
- Another objective is to demonstrate the robustness and inherent safety of certified casks under extreme accident conditions.
- As was done with nuclear power reactors, it is important to understand the margin to failure that which transportation casks have beyond their design basis. The NRC research office has recently completed a series of nuclear power plant containment tests to validate analysis codes for beyond-design-basis accident conditions under overpressure and beyond design basis earthquakes.
- Test results which produce measurable and predicted cask performance will enhance public confidence in analysis capabilities and demonstrate the objective of having an understanding of the cask response which is not solely based upon computer modeling as would be the case for elastic deformations.

For the rail cask test, the staff has considered the reasons cited above and has proposed a 120 kph [75 mph] impact speed whose effects are illustrated in Section 2 of this report.

## **APPENDIX B:**

### **Peer Review Panel Members**

#### **Structural Panel**

Dr. Robert Nickell  
Applied Sciences & Technology  
Poway, California

Dr. Bernhard Droste  
Bundesanstalt für Materialforschung und -Prüfung  
Berlin, Germany

Dr. Robert Kassawara  
Electric Power Research Institute  
Palo Alto, California

Dr. Richard Suave  
Kinetrics, Inc. (associated with Ontario Hydro)  
Toronto, Canada

Mr. Steven Heffelfinger  
Sandia National Laboratories  
Albuquerque, New Mexico

#### **Thermal Panel**

Professor Miles Greiner  
University of Nevada, Reno  
Reno, Nevada

Mr. Jack Hovingh  
Lawrence Livermore National Laboratory  
Livermore, California

Dr. Ronald Alpert  
Factory Mutual Research Corp.  
Norwood, Massachusetts

Dr. Walter Gill  
Sandia National Laboratories  
Albuquerque, New Mexico

A transcript of the expert panel meetings is available from the NRC.

NRC FORM 335 (2-89) NRCM 1102, 3201, 3202	U.S. NUCLEAR REGULATORY COMMISSION	1. REPORT NUMBER (Assigned by NRC, Add Vol., Supp., Rev., and Addendum Numbers, If any.)
<b>BIBLIOGRAPHIC DATA SHEET</b>		NUREG-1768
2. TITLE AND SUBTITLE  United States Nuclear Regulatory Commission Package Performance Study Test Protocols  Draft Report for Comment		3. DATE REPORT PUBLISHED
		MONTH                      YEAR
		February                      2003
		4. FIN OR GRANT NUMBER
5. AUTHOR(S)  NRC Staff	6. TYPE OF REPORT	
		7. PERIOD COVERED (Inclusive Dates)
		December 2001 - January 2003
8. PERFORMING ORGANIZATION - NAME AND ADDRESS (If NRC, provide Division, Office or Region, U.S. Nuclear Regulatory Commission, and mailing address; if contractor, provide name and mailing address.)		
Division of Engineering Technology Office of Nuclear Regulatory Research U.S. Nuclear Regulatory Commission Washington, DC 20555-0001		
9. SPONSORING ORGANIZATION - NAME AND ADDRESS (If NRC, type "Same as above"; if contractor, provide NRC Division, Office or Region, U.S. Nuclear Regulatory Commission, and mailing address.)		
Same as above		
10. SUPPLEMENTARY NOTES		
None		
11. ABSTRACT (200 words or less)		
<p>This test protocols report presents the NRC staff's preliminary plans for an experimental phase of the Package Performance Study (PPS), which is examining the response of transportation casks to extreme transportation accident conditions. The staff proposes to conduct tests of full-scale rail and full-scale truck casks including a high-speed impact with an unyielding surface followed by an extreme fire test. The NRC has a contract in place with Sandia National Laboratories (SNL) to conduct the impact and fire tests and to carry out a series of analyses to support the test program. These tests support the PPS objectives of enhancing public confidence in the inherent safety of spent nuclear fuel cask design, validating the capability of the cask models and analysis codes to accurately capture cask and fuel response to extreme mechanical and thermal environments, and providing data to refine dose risk estimates.</p> <p>The objective of publishing this report is to continue the process of enhanced public involvement in the development of this program and to satisfy a specific commitment the NRC made to make these preliminary test plans available and to request comments on them</p>		
12. KEY WORDS/DESCRIPTORS (List words or phrases that will assist researchers in locating the report.)		13. AVAILABILITY STATEMENT
Transportation Casks Impact Tests Thermal Tests Spent Nuclear Fuel		unlimited
		14. SECURITY CLASSIFICATION
		(This Page)
		unclassified
		(This Report)
		unclassified
		15. NUMBER OF PAGES
		16. PRICE



Federal Recycling Program

**NUREG-1768  
DRAFT**

**UNITED STATES NUCLEAR REGULATORY COMMISSION  
PACKAGE PERFORMANCE STUDY TEST PROTOCOLS**

**FEBRUARY 2003**

**UNITED STATES  
NUCLEAR REGULATORY COMMISSION  
WASHINGTON, DC 20555-0001**

---

**OFFICIAL BUSINESS  
PENALTY FOR PRIVATE USE, \$300**